Understanding the growth of *Corynebacterium glutamicum*

Dissertation

zur Erlangung des Doktorgrades der Naturwissenschaften

(Dr. rer. nat.)

an der Fakultät für Biologie der

Ludwig-Maximilians-Universität zu München

vorgelegt von

Fabian Mark Meyer

aus München

München, Januar 2024

Eidesstattliche Versicherung

Ich erkläre hiermit an Eides statt, dass ich die vorliegende Dissertation mit dem Titel:

Understanding the growth of *Corynebacterium glutamicum*

selbständig verfasst, mich außer der angegebenen keiner weiteren Hilfsmittel bedient und alle Erkenntnisse, die aus dem Schrifttum ganz oder annähernd übernommen sind, als solche kenntlich gemacht und nach ihrer Herkunft unter Bezeichnung der Fundstelle einzeln nachgewiesen habe.

Ich erkläre des Weiteren, dass die hier vorgelegte Dissertation nicht in gleicher oder in ähnlicher Form bei einer anderen Stelle zur Erlangung eines akademischen Grades eingereicht wurde.

Kiel, 04.05.2024   Fabian Mark Meyer

There is more to the picture than meets the eyes.

Neil Young

Index

Abbreviations

aa	amino acid
AG	arabiniogalactan
Ara*f*	arabinofuranose
B. subtilis	*Bacillus subtilis*
C. glutamicum	*Corynebacterium glutamicum*
CMN	(*Corynebacteria*, *Mycobacteria*, *Nocardia*)-group
D-Glu	D-glutamic acid
DP	decaprenolphosphate
DPA	decaprenylphosphoryl arabinose
DPM	decaprenylphosphoryl mannose
DPR	decaprenylphosphoryl ribose
DPX	intermediate epimer between DPR and DPA
E. coli	*Escherichia coli*
Gal*f~*	galactan chain
GlcNAc	N-acetylglucosamine
GRAS	generally regarded as safe for humans
HMW-PBPs	high molecular weight-PBPs
L-Ala	L-alanine
LAM	lipoarabinomannan
LM	lipomannan
LMW-PBPs	low molecular weight-PBPs
M. tuberculosis	*Mycobacterium tuberculosis*
MA	mycolic acids
Man*p*	mannopyranose
mDpm	meso-diaminopimelic acid
MDR	multiple drug resistant strains of *M. tuberculosis*
MM	myco-membrane
MOP-protein	multidrug/oligo-saccharidyl-lipid/polysaccharide-superfamily protein
MSG	mono-sodium glutamate
MurNac	N-acetylmuramic acid
PBPs	penicillin binding proteins
PG	peptidoglycan
PI	phosphatidyl-myo-inositol
PIM	phosphatidyl-myo-inositol mannosides
Rha*p*	rhamnopyranose
RNAP	DNA-dependent RNA polymerase
SEDS-protein	shape, elongation, division, and sporulation superfamily protein
SMC	structural maintenance of the chromosome
spp.	species
STPKs	Ser/Thr kinases
TG	transglycosylases
TMM/TDM	trehalose mono- & dimycolates,
TP	transpeptidases
UDP-GlcNAc	uridine-diphospho-N-acetylglucosamine
UDP-MurNAc	uridine-diphospho-N-acetylmuramine
Van-FL	fluorescently labeled vancomycin
XDR	extensively drug resistant strains of *M. tuberculosis*

Publications and contributions relevant for this work

First and shared first author publications:

Meyer, F. M.*, Repnik, U., Karnaukhova, E., Schubert, K., & Bramkamp, M. (2023). Effects of benzothiazinone and ethambutol on the integrity of the corynebacterial cell envelope. *The Cell Surface*, 100116.

All biological experiments, except TEM and SEM preparation and analysis. Automated data analysis and visualization method of fluorescence micrographs, and data curation. Major part of the figure design. Writing the original draft and reviewing and editing the manuscript.

Messelink J.J.*, **Meyer F.***, Bramkamp M., Broedersz C.P. (2021) Single-cell growth inference of *Corynebacterium glutamicum* reveals asymptotically linear growth. *Elife*, 10:e70106. doi: 10.7554/eLife.70106. https://doi.org/10.7554/elife.70106

All biological experiments, development of an automated data analysis and visualization method for time-lapse fluorescence micrographs. In parts design of the figures. Writing of the original draft and reviewing and editing the manuscript.

Schubert K.*, Sieger B.*, **Meyer F.***, Giacomelli G., Böhm K., Rieblinger A., Lindenthal L., Sachs N., Wanner G., Bramkamp M. (2017) The antituberculosis drug ethambutol selectively bocks apical growth in CMN group bacteria. *MBio*, 8(1):e02213-16. https://doi.org/10.1128/mbio.02213-16

Contribution to the biological experiments, development of automated data analysis, visualization method for static fluorescence micrographs. In parts design of the figures. and data curation. Reviewing and editing of the draft.

Co-author publications:

Peng, F., Giacomelli, G., **Meyer, F. M.**, Linder, M., Haak, M., Rueckert-Reed, C., Weiß, M., Kalinowski, J. & Bramkamp, M. (2023). Deletion of SMC renders FtsK essential in *Corynebacterium glutamicum*. *bioRxiv*, 2023-10.

Timpe-lapse microscopy and data analysis and visualization. Reviewing and editing of the draft.

Böhm K., **Meyer F.**, Rhomberg A., Kalinowsk J., Donovan C. & Bramkamp M. (2017) Novel Chromosome Organization Pattern in Actinomycetales — Overlapping Replication Cycles Combined with Diploidy. *MBio,* 8(3), e00511-17. https://doi.org/10.1128/mbio.00511-17

Fluorescence microscopy and data analysis and visualization. Reviewing and editing of the draft.

III

Zusammenfassung

Aus zellbiologischer Sicht besteht große Ähnlichkeit zwischen dem harmlosen Bodenbakterium *Corynebacterium glutamicum* und *Mycobacterium tuberculosis*, dem Auslöser der Lungenkrankheit Tuberkulose. Das Längenwachstum einzelner Zellen erfolgt ausschließlich von den Polen her. Dies unterscheidet sich von der Mehrheit der bekannten Bakterien. Ein weiteres Merkmal der sogenannten CMN (*Corynebacteria, Mycobacteria, Nocardia*)-Gruppe besteht in dem Aufbau der Zellwand. Diese ist charakterisiert durch eine äußere, hydrophobe Mycomembran (MM), die kovalent über eine Schicht aus Arabinogalaktan (AG) an das Murein (PG) der Zellwand gebunden ist.

In der vorliegenden Arbeit wurden verschiedene Aspekte des Wachstums und der Teilung von *C. glutamicum* charakterisiert. Die räumlich-/ zeitliche Organisation einzelner Zellen und deren Bestandteile standen dabei im Fokus. Die Analysen erfolgten mit Hilfe biochemischer, mikroskopischer und datenverarbeitungstechnischer- Methoden. Die Entwicklung einer Bild-Analyse Umgebung fand Anwendung in mehreren Publikationen.

Mit Hilfe einer Mikrofluidik-Kammer wurden mikroskopische Zeitreihen-Aufnahmen von wachsenden *C. glutamicum* Mikrokolonien erstellt. Einzelnen Zellen aus den jeweiligen Teilbildern wurden mittels einer eigens dafür entwickelten Software vermessen und in einen genealogischen Kontext gesetzt. Die so erhaltenen Daten wurden von dem Co-Autor der Studie mit einer neu entwickelten Inferenz-Methode analysiert. Daraus ergab sich eine Charakterisierung der Wachstumsdynamik einzelner Zellen. Der ,asymptotisch linear' genannte Modus beschreibt eine anfängliche Beschleunigung der Elongations-geschwindigkeit, die dann in eine Sättigung übergeht. Die Erklärung hierfür liegt in Organisation der Wachstumszonen und der Reifung des neuen Zellpols nach der Teilung. Weiter konnte anhand der Daten gezeigt werden, dass eine strikte Teilungssymmetrie bei apikal wachsenden Bakterien für eine normale Längenverteilung der Zellen innerhalb einer Population überflüssig ist.

In einem weiteren Teil-Projekt wurden die zellulären Effekte von zwei Antibiotika verglichen. Hierbei handelt es sich um das lange etablierte Ethambutol (EMB) und die experimentelle Substanz Benzothiazinon 043 (BTZ).

EMB wird seit längerem für Behandlung von Tuberkulose angewendet, BTZ hingegen wird momentan zu diesem Zweck klinisch evaluieret. Beide Stoffe wirken an unterschiedlichen Stellen des Stoffwechselweges zum Aufbau der AG-Schicht. Mit speziellen Färbetechniken, Fluoreszenzmikroskopie und Bild-Analyse konnte gezeigt werden, dass durch nicht letale Konzentrationen beider Substanzen das apikale Wachstum in einzelnen Zellen zum Erliegen kommt. Dies geht einher mit einer Änderung der Morphologie, behandelte Zellen erscheinen kürzer und breiter. Neben dieser Gemeinsamkeit zeigten die Antibiotika auch einen unterschiedlichen Effekt. Im Fall von EMB konnte nach entsprechender Färbung eine Diskontinuität der MM an den Zellpolen beobachtet werden. Nach der Zugabe von BTZ trat hier keine Veränderung im Vergleich zur Kontrolle auf. Der entsprechende Befund konnte mittels elektronenmikroskopischer Aufnahmen bestätigt werden. Hierbei zeigte sich auch, dass die Organisation der einzelnen Schichten der Zellwand durch beide Stoffe stark beeinflusst wird. Die Integrität der MM spielt für die Zelle eine schützende Rolle. Dies zeigte sich anhand von kombinierten Verdünnungsreihen. Zusammen mit EMB zeigten β-Lactam Antibiotika eine synergistische Wirkung. Im Gegensatz dazu wurde bei der Kombination mit BTZ nur eine additive Wirkung festgestellt.

Mittels einer programmierten Analyse von statischen, fluoreszenzmikroskopischen Aufnahmen, konnte zur Entdeckung der diploiden Chromosomenorganisation von *C. glutamicum* beigetragen werden. Durch die Extraktion von Fluoreszenzprofielen einzelner Zellen und anschließender Sortierung konnte die dynamische Lokalisation von ParB über den Zellzyklus dargestellt werden. Diese zeigt ein spiegelsymmetrisches Muster, bei dem jeweils ein Fokus vom Zellpol zur Mitte migriert, abhängig von der Länge der Zelle. Die bekannte wirkweise des ParABS-Systems und der apikale Wachstumsmodus untermauern die Entdeckung.

Des Weiteren konnte im Rahmen dieser Arbeit die zellzyklusabhängige Lokalisation der DNS-Pumpe FtsK durch datenverarbeitungstechnische Bildanalyseverfahren dargestellt werden. Mit Hilfe eines Transposon Mutagenese Experiment wurde zunächst ermittelt, dass sich *ftsK* im Kontext der Abwesenheit des DNS-Topologie organisierenden Proteins SMC als essenziell darstellt. Die längere Verweilzeit des markierten FtsZ Derivats in

mutierten Zellen wurde als Folge erhöhter Entropie auf den Fortschritt des Zellzyklus bewertet und mit Hilfe von Einzelmolekülanalyse (single particle tracking, SPT) bestätigt.

Zusammenfassend wurden eine Reihe neuer Erkenntnisse über das Wachstum und die Teilung von *C. glutamicum* gewonnen. Dabei kamen auch neu entwickelte Methoden zum Einsatz, welche einen weiteren Einsatz erlauben. Wichtige Aspekte zur Regulation der Zelllänge wurden erstmals für das apikale Wachstums dargestellt. Die zellbiologische Charakterisierung von EMB und BTZ trägt zum Verständnis der Wirkweise beider Antibiotika bei. Abschließend gelang mit den Beiträgen zur Entdeckung der diploiden Chromosomenorganisation von *C. glutamicum* und der Beschreibung des Einflusses der Chromatidstruktur auf den Fortschritt des Zellzyklus ein tieferer Einblick in das dynamische Werden der Zellstruktur.

Abstract

From a cell biological standpoint, there is a great similarity between the harmless soil bacterium *Corynebacterium glutamicum* and *Mycobacterium tuberculosis*, the causative agent of the lung disease tuberculosis. Longitudinal growth of individual cells occurs exclusively from the poles, differing from the majority of known bacteria. Another characteristic of the so-called CMN (*Corynebacteria, Mycobacteria, Nocardia*) group is the structure of the cell wall. It is characterized by an outer hydrophobic mycomembrane (MM) and a layer of arabinogalactan (AG) covalently bound to the peptidoglycan (PG) of the cell wall.

In the present work, various aspects of *C. glutamicum* growth and division were characterized. The spatio-temporal organization of individual cells and their components were the focus. Analyses were performed using biochemical, microscopic, and data processing methods. A developed image analysis environment found application in several publications.

By using a microfluidic chamber, microscopic time-lapse images from growing *C. glutamicum* microcolonies were obtained. Individual cells from each timeframe were measured and placed in a genealogical context using custom software developed during the thesis. The resulting data were analyzed by the co-author of the study by using a newly developed inference method. This resulted in a characterization of the growth dynamics of individual cells. The mode called 'asymptotic-linear' describes an initial acceleration of the elongation velocity, which then changes into plateau. The explanation for this lies in organization of growth zones and maturation of the new cell pole after division. Further, the data showed that strict division symmetry in apically growing bacteria is unnecessary for a normal length distribution of cells within a population.

In another sub-project, the cellular effects of two antibiotics were compared. These are the well-established anti-tuberculosis drug ethambutol (EMB) and the experimental compound benzothiazinone 043 (BTZ). Both substances act at different points in the metabolic pathway building up the AG layer. By using special staining techniques, fluorescence microscopy and image analysis, it was shown that sublethal concentrations

of both substances cause apical growth in individual cells to cease. This is accompanied by a change in morphology. Treated cells appear shorter and broader. In addition to this commonality, the antibiotics also showed a different effect. In the case of EMB, discontinuity of MM at the cell poles was observed after appropriate staining. Upon the addition of BTZ, no change occurred here compared to the control. The corresponding finding was confirmed by electron microscopy. This also showed that the organization of the individual layers of the cell wall is strongly influenced by both substances. The integrity of the MM plays a protective role for the cell. This was shown by combined dilution series. Together with EMB, β-lactam antibiotics showed a synergistic effect. In contrast, when combined with BTZ, only an additive effect was observed.

Furthermore, the analysis of static fluorescence microscopic images, described in this thesis contributed to the discovery of the diploid chromosome organization of *C. glutamicum*. By extracting fluorescence profiles of single cells and subsequent sorting, the dynamic localization of ParB over the cell cycle could be visualized. This shows an opposing pattern of foci, migrating from the cell poles to the center, depending on the length of the cell. The known mode of action of the ParABS system and the apical growth mode support the discovery of diploidy.

Finally, the cell cycle-dependent localization of the DNA pump FtsK was demonstrated by using image analysis. With the help of a transposon mutagenesis experiment it was first determined that *ftsK* gets essential in the context of the absence of the DNA topology organizing protein SMC. The longer dwell-time of the labeled FtsZ derivative in mutant cells was found to be a consequence of increased entropy on cell cycle progression and was further confirmed by single particle tracking (SPT).

In summary, several new insights into the growth and division of *C. glutamicum* were gained. Newly developed methods were extensively used and allow for further application. Important aspects of the regulation of cell length were presented for the first time for apical growth. The cell biological characterization of EMB and BTZ contributes to the understanding of the mode of action of both antibiotics. Finally, the contributions to the discovery of the diploid chromosome organization of *C. glutamicum* and the description of the influence of chromatid structure on the progress of the cell cycle, a deeper insight into the dynamic development of this cell structure was gained.

1 Introduction

1.1 Importance of *Corynebacterium glutamicum*

1.1.1 Biotechnological relevance

By the mid-1950s, an increasing demand for L-glutamate as a flavoring agent set the Asian food market for innovative production methods. The Japanese pharma company Kyowa Hakko started a screening program for the isolation of L-glutamate producing microorganisms (Kinoshita et al., 1957). The resulting discovery and characterization of *Micrococcus glutamicus*, later renamed to *Corynebacterium glutamicum*, was the global starting point of industrial amino-acid fermentation (Abe et al., 1967; Kinoshita, Nakayama, & Akita, 1958). Nowadays, the accompanying research on the physiological, metabolic, and genetic properties has contributed to a detailed picture of the central metabolism in *C. glutamicum*.

Uniting a variety of useful assets, *C. glutamicum* has established as one of the most important organisms in the field of white biotechnology (J. Y. Lee et al., 2016). *C. glutamicum* is generally regarded as safe for humans (GRAS). It grows to high cell densities, uses a broad spectrum of carbon sources, and strong secondary metabolism properties make it an ideal platform for fermentative production (Hartbrich et al., 1996; Kawaguchi et al., 2009; J. Y. Lee et al., 2016; Nakamura et al., 2003; Wendisch, Bott, & Eikmanns, 2006).

After the first successful commercial production of L-glutamate, the economic potential of a fermentative industry was broadly recognized and further developed. Within a few years, based on the L-glutamate producing strain, random mutagenesis and selection methods were used to create a potent production strain for L-lysine (Kinoshita, Nakayama, & Kitada, 1958). In the 1970s, strains for the production of L-tyrosine, L-phenylalanine and L-tryptophane were engineered (Hagino & Nakayama, 1973, 1974, 1975). More strains for the industrial production of different amino acids and strategies for yield optimization were developed in the 1990s (Ikeda & Katsumata, 1992; Mizukami et al., 1994).

In the beginning of the millennium, DNA microarrays and high-throughput methods helped to reveal global transcriptional regulatory networks of *C. glutamicum* (Loos et al., 2001). In 2003, the whole genome sequence was published by two independent groups

(Ikeda & Nakagawa, 2003; Kalinowski et al., 2003). By then, DNA recombination technologies and growing insights into vector systems and the metabolic flux allowed for the heterologous expression of organic acids, alcohols, biopolymers, and proteins (B. Lee et al., 2015; J. Lee, 2014; M. J. Lee & Kim, 2018; Liu et al., 2007; Siebert & Wendisch, 2015).

Along with general developments in the field of molecular biology, the product portfolio of *C. glutamicum* has dramatically increased. Systems- and synthetic biology approaches are harnessed to optimize the yield of certain products (Ravasi et al., 2012; Wendisch, Bott, Kalinowski, et al., 2006). Recent developments aim at the metabolic engineering of aromatic compounds, amines and non-proteogenic ω-amino acids (Grigoriou et al., 2020; Heider & Wendisch, 2015; Kallscheuer & Marienhagen, 2018; Wendisch, 2020). The ongoing improvements of sequencing technologies enabled for TN5 transposon mutagenesis analyses (Suzuki et al., 2006). This technique provides a global view on the importance of single genes under a certain condition. Consequently, with various CRISPR/Cas9-applications, a broad access to the genome is granted (Cho et al., 2017; Cleto et al., 2016).

Still, to this day, the main products produced by *C. glutamicum* are L-amino acids (Lee et al., 2016). Predominantly they find use as feed supplement for livestock industries. The feed-supplements L-lysine and D-/L-methionine are used to increase the protein yield in animals and represent the highest production volumes. Besides only niche usage in pharmacy and cosmetic industry, the food industry is the second biggest market for fermentative produced amino acids. Here, the salt of L-glutamic acid, mono-sodium glutamate (MSG) plays an important role as flavor enhancer and ubiquitous ingredient in convenience-food. A further example of amino acids in food industry is the dipeptide Asp-Phe, better known as the artificial sweetener aspartame. The COVID-19 pandemic has shown an increase in the demand of packaged food and pharmaceuticals. Regarding only glutamic acid, the global market value is expected to rise from 9.8 bn$ in 2020 up to 16.6 bn$ in 2030 (Alliedmarketresearch, 2023).

The prominent role of *C. glutamicum* in the industry has caused many related projects in academic research. Today, the growing set of methods for manipulating *C. glutamicum* includes various types of plasmids, such as *E. coli - C. glutamicum* shuttle expression

vectors (Bakkes et al., 2020). Different kinds of inducible and constitutive promoters are available next to a broad variety of selection markers. The plasmid-based, ectopic expression of gene products provides an accessible approach for affinity-tag protein purification and basic microscopic localization studies of fluorescent proteins (Nešvera & Pátek, 2011). For the chromosomal integration of genes, cloning vectors based on the relaxase Mob of the *E. coli* conjugation system were developed (Schäfer et al., 1994). Via homologous recombination, tagged or altered variants of target genes can be integrated into the native genomic locus. This either enables microscopic localization studies of gene products at native concentrations, or the selective disruption of a gene or gene parts.

1.1.2 Taxonomic subsumption

Right after the discovery of *C. glutamicum*, the genus was misinterpreted (Kinoshita, Nakayama, & Akita, 1958). Seventy years ago, all reported *Corynebacteria* were classified as pathogens, among them *C. diphtheriae* and *C. pseudotuberculosis*. Peer-group suggestions eventually led to a renaming from *Micrococcus glutamicus* to *Corynebacterium glutamicum* by its discoverers (Abe et al., 1967). With improvements in taxonomic analysis methods, various, formerly mis-classified species and strains were renamed to *C. glutamicum* or used as synonyms. Among them, representatives of *Brevibacteria*, *Microbacteria*, *Micrococci*, or *Arthrobacter* (Liebl et al., 1991; Oberreuter et al., 2002). Several clinically relevant species were revealed as close taxonomic relatives of *C. glutamicum*. By using classical approaches, and later confirmed by 16S rRNA/rDNA sequencing, a distinct clade was detected that includes the genera *Mycobacterium*, *Corynebacterium* and *Nocardia* (Barksdale, 1970; Danhaive et al., 1982; Stackebrandt et al., 1997). The common denominator of this, so called CMN-group, is found in the molecular organization of the cell-envelope. The robust, diderm type of envelope consists of a peptidoglycan (PG) layer on top of the plasma membrane that carries an arabinogalactan (AG) scaffold for an outfacing hydrophobic, mycomembrane (MM). This is specific for the high-GC Gram-positive bacteria. Compared to the type of cell wall which represents the low-GC Gram-positive bacteria, e.g., *Staphylococcus aureus, Streptococcus pneumoniae,* or *Bacillus subtilis*, it appears substantially different. Here, the cell wall is formed only by a thick, single mesh of PG (Fig. 1).

For CMN-bacteria, the outfacing bilayer of surface-bound MAs and free trehalose mono- and dimycolates (TMM/TDM) serves as physical barrier against the aqueous environment (Marrakchi et al., 2014). The viscosity of the MM is rendered by the chain length of the MA-residues. This trait is used as a taxonomic marker within the CMN-group (M. D. Collins et al., 1982). With a length of 90 C-atoms, the MA-residues cause a waxy and uneven surface on growing colonies of *Mycobacterium* spp.. Single bacteria stain acid-fast. In *C. glutamicum*, shorter MA-residues with a length of about 40 C-atoms lead to colonies that exhibit a smooth and moist surface, while acid-fast staining shows a negative result (Lamanna, 1946).

The MM protects the cell inside from water-soluble chemicals. This plays a central role in the persistent infection of human macrophages by *Mycobacterium tuberculosis* (Rankine-Wilson et al., 2021). The associated consumptive illness has coevolved towards a steady burden for global health (WHO, 2021). Until today, no broadly applicable measure has been found to reliably contain or cure this disease. The emergence of multiple (MDR) and extensively drug resistant (XDR) strains of *M. tuberculosis* marks the present challenge in the field. Besides that, other notorious diseases caused by the infection of CMN-members had shown to be more prone to medical intervention. Today, the respiratory system disease diphtheria, caused by the toxin producing *C. diphtheriae*, is controlled by vaccination and antibiotics (Young & Mood, 1945). Also, the threatening potential of the Hansen's disease, caused by *Mycobacterium leprae*, nowadays is limited by an effective treatment (Bechelli & Guinto, 1970). Nonetheless, a large variety of inflammatory ailments are still related to representatives from the superordinate CMN-group. With *C. ulcerans*, *C. equi*, *M. heamophilum* and *Nocardia farcinica* only to name a few, zoonotic and opportunistic CMN-type pathogens provide a potential threat, especially for immunocompromised patients (Lipsky et al., 1982). Among other beneficial traits, the harmlessness of *C. glutamicum* qualifies for the role as a model for various pathogens. Besides providing a good proxy for the effectiveness of antibiotics, basic genetic CMN-elements can be studied at a minimum-security level.
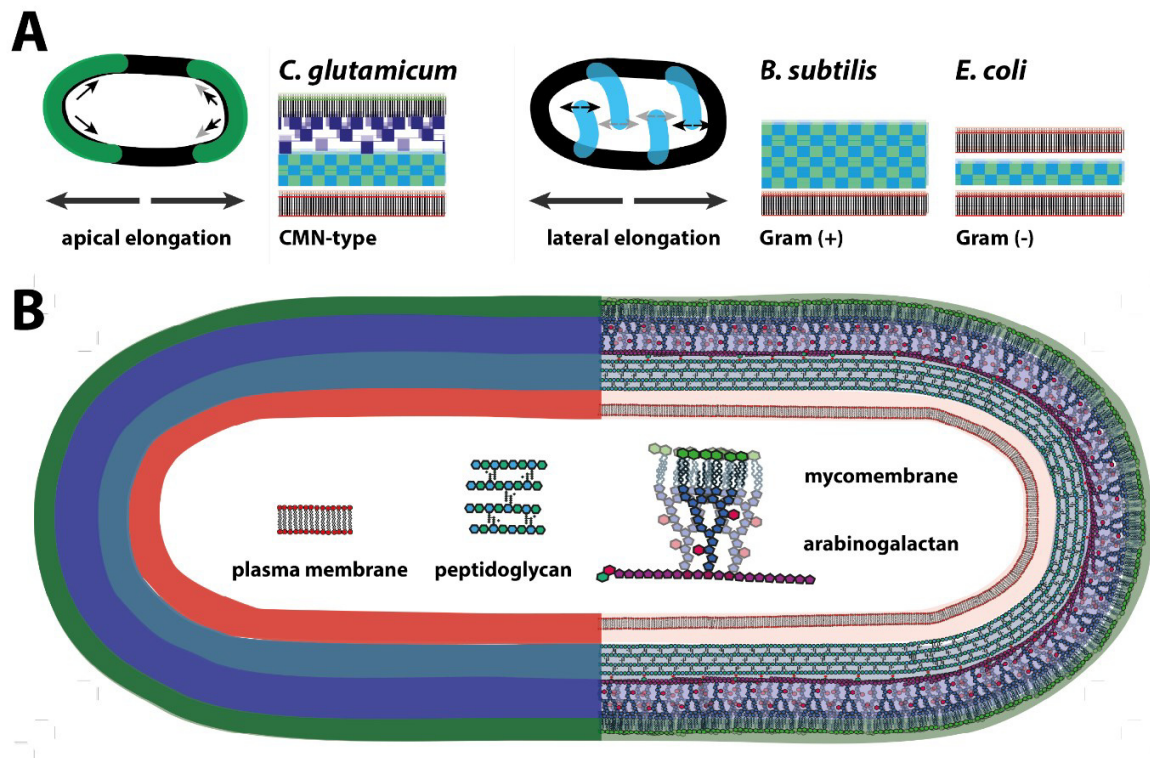
Figure 1: Cell wall models of the prokaryotic model organisms *C. glutamicum*, *B. subtilis* and *E. coli*. (A) The mode of single cell elongation differs in bacteria. The rod-shaped morphology is commonly maintained by, either the incorporation of PG through moving patches along the sidewall, as it is the case for *B. subtilis* and *E. coli*, or by an apical, i.e. strict polar, elongation, as it is characteristic for *C. glutamicum* and *M. tuberculosis.* Gram-negative bacteria are characterized by an inner and outer cell membrane (red). Gram-positive bacteria are more rigid due to a thick layer of peptidoglycan (PG, blue/green). All three model species represent a unique type of envelope that is connected to certain features. The CMN-type cell wall occurs more rigid than in Gram-negatives, but includes an extracellular layer of arabinogalactan (AG, violet) and a mycomembrane (MM, green) made of mycolic acids. **(B)** The apical synthesis of the CMN-type of cell wall is connected to a unique structure. Like in all other bacteria, the plasma membrane defines the innermost layer of the containment. The PG appears thicker compared to Gram negative cells, due to a positive result upon respective staining. Distinct layers of arabinogalactan (AG) and mycolic acids form a supportive surface for the arrangement of a hydrophobic mycomembrane (MM) as the outermost layer.

1.2 The corynebacterial cell wall

The envelope of the Actinobacterium *Corynebacterium glutamicum* consists of several distinct layers. Apically elongating peptidoglycan (PG) gets covalently decorated by a consecutive composite of arabinogalactan (AG) and mycolic acids (MA) (Fig. 2). The multilayered envelope bears physical features that are distinct form the common model organism *E. coli* or *B. subtilis* (Alderwick et al., 2015; Daffé, 2005; Daffe et al., 1990; Houssin et al., 2020) (Fig. 1).
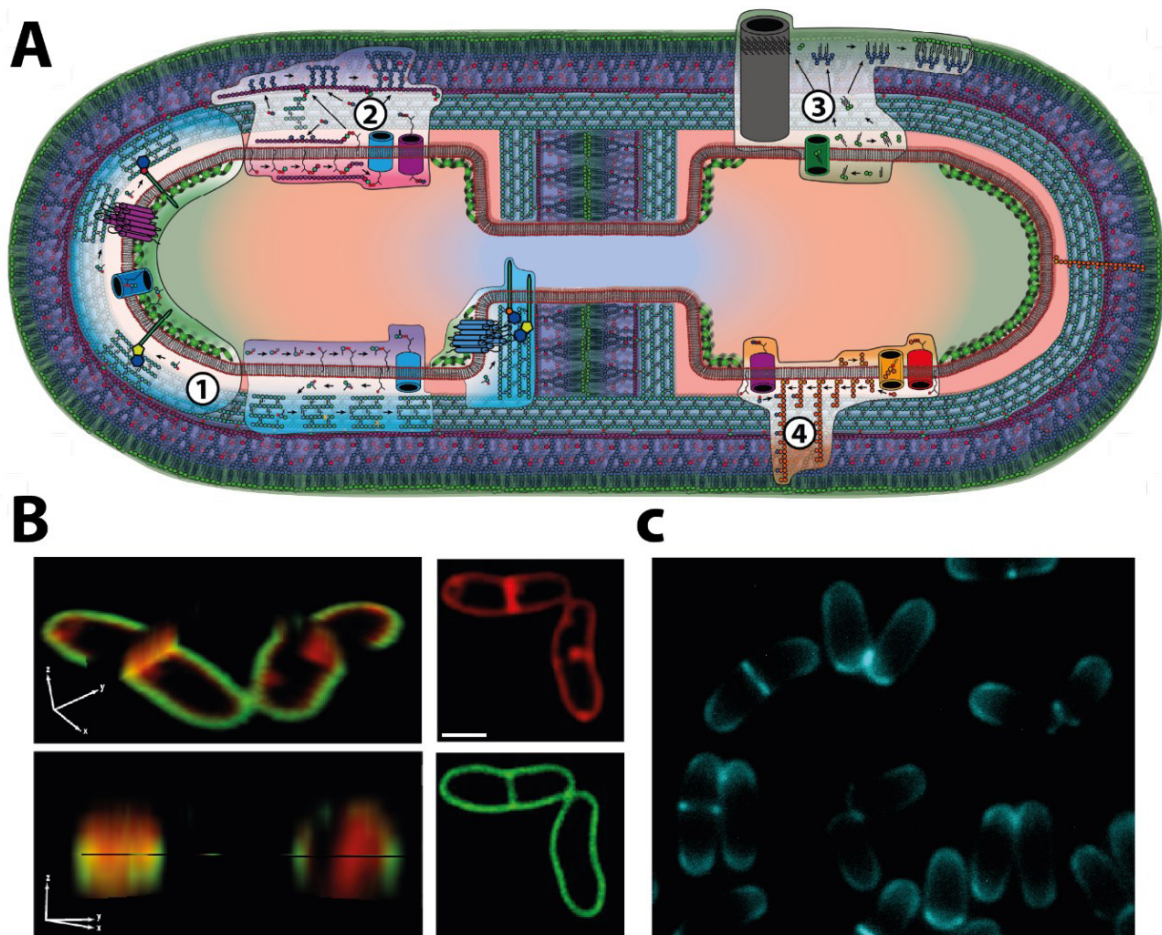
Figure 2: Mechanism of PG synthesis in *C. glutamicum*. (A) Representation of important steps during the cell wall synthesis of *C. glutamicum*. The sequential assembly of peptidoglycan (PG, ①, blue), arabinogalactan (AG, ②, violet), and the mycomembrane (MM, ③, green) define the sacculus, while lipoglycans serve as structural trait (④, orange). **(B)** 3D-fluorescence micrograph of a v-shaped pair of *C. glutamicum* cells. The green signal is exclusively obtained from a metabolic labeling of the MM, while the red signal derives from the plasma membrane and the MM, due to a staining with NileRed. The forming division septum shows the consecutive arrangement of both layers. **(C)** The fluorescence micrographs of nascent PG unveil the apical mode of growth for *C. glutamicum* cells.

The particular cell wall architecture is unique for a narrow clade among the genus of Actinobacteria, named CMN (*Corynebacterium*, *Mycobacterium*, *Nocardia*)-group (Barksdale, 1970; Jankute et al., 2015). Structurally different from the Gram-positive and Gram-negative type of cell wall, it shares functional features of both (Cummins & Harris, 1958). The hydrophobic character of the MM is comparable to the outer membrane of diderm Gram-negative bacteria (Claus & Roth, 1964) (Fig. 2B). While the rigidity of the cell wall is attributed to a thick layer of PG, which is a common trait among Gram-positive bacteria (Vadillo-Rodriguez et al., 2009) (Fig. 1A). The mode of longitudinal growth of single cells also differs from the commonly used model organisms *E. coli* or *B. subtilis* (Den Blaauwen et al., 2008; Shi et al., 2018). While both model species grow in length by the incorporation of new material at the side walls, *C. glutamicum* exclusively grows from the cell poles (Fig. 2C) (Daniel & Errington, 2003). The outfacing mycolic acids serve as the inner leaflet of the characteristic, hydrophobic mycomembrane (MM) (Dover et al., 2004). The exposed MA are structurally completed by a mobile phase of trehalose mono (TMM)- and -di-mycolates (TDM). Consequently, the spatial and temporal organization of the cell envelope sets the base for phenotypic characteristics, such as the club-shaped morphology or the occasionally asymmetric cell division or the rapid v-snapping (Umeda & Amako, 1983; Zhou et al., 2019).

Besides serving as a loadbearing structure for maintaining turgor, the cell wall appears as a well-structured arrangement, populated by numerous functional proteins complexes (Puech et al., 2001). These include active and passive transporters, sensory Ser/Thr kinases (STPKs), cytoplasmatic cell wall precursor enzymes and cell wall assembly complexes (Brecik et al., 2015; Martins et al., 2019; Mikušová et al., 2005; Schultz et al., 2009; Valbuena et al., 2007). These interconnected functional complexes ensure the cell's homeostasis in a broad variety of tolerated environmental conditions. The specific molecular arrangement of CMN-type cell wall serves as pathogenicity factor in virulent representatives (Barksdale, 1970; Coyle & Lipsky, 1990; Suter, 1952). As a prominent example for such cell wall associated virulence, in *Mycobacterium tuberculosis* the hydrophobic property prevents the cells from digestion within macrophages (Mackaness, 1952; Richard A. Slayden et al., 1996). Despite species specific variations among the CMN-group, the underlying physiology is in large parts comparable

between *M. tuberculosis* and *C. glutamicum* (Dover et al., 2004). The polar organization of cell wall synthesis counts as a common hallmark (Hett & Rubin, 2008; Umeda & Amako, 1983).

1.2.1 Peptidoglycan

Peptidoglycan (PG) is a large monomolecular, honeycomb like structure that defines the sacculus of single bacterial cells (Höltje, 1998). It is formed by linear, β-(1→4)-linked chains of the alternating amino sugars N-acetylglucosamine (GlcNAc) and N-acetylmuramic acid (MurNAc). These chains are cross-linked by stem peptides which are usually bound to MurNAc. The composition and configuration of the respective amino acids are species dependent (Schleifer & Kandler, 1972). In *C. glutamicum* the structure of the peptidoglycan is described as the *Escherichia coli*-type A1γ (Schleifer & Kandler, 1972). Here, the stem peptide consists of L-alanine (L-Ala; position 1), D-glutamine (D-Glu; 2), meso-diaminopimelic acid (mDpm; 3), D-alanine (D-Ala; 4) and D-Ala (5). Direct crosslinking occurs between the positions 3→4 by a D,D-transpeptidation. Studies on the exact local PG turnover remain elusive in *C. glutamicum*. In *Corynebacterium jeikeium* and *M. tuberculosis* an alternative 3→3 L,D-transpeptidation between the mDpm residues is described (Lavollay et al., 2008, 2009). This non-canonical condensation is linked to resistance against lysozyme and certain β-lactam antibiotics, as well as more abundant in the stationary phase. In *C. glutamicum* the amidation of mDpm by LtsA has shown to facilitate the 3→3 crosslink (Levefaudes et al., 2015). The biosynthetic pathway for PG is conserved among large parts of the bacteria (Barreteau et al., 2008; Vollmer & Bertsche, 2008). This process generally involves three distinct steps: the synthesis of precursor molecules in the cytoplasm, the translocation across the phospholipid membrane (PM) and the incorporation into the existing sacculus (Barreteau et al., 2008; Pavelka et al., 2015; Raghavendra et al., 2018; Vollmer & Bertsche, 2008) (Fig.3). In *C. glutamicum* the initial step for the PG precursor synthesis starts with fructose-6-phosphate that is sequentially converted into uridine-diphospho-N-acetylglucosamine (UDP-GlcNAc) by the enzymes GlmS (respective gene: *cg2492*), GlmM (*cg0675*) and GlmU (*cg1076*). In a following two-step process UDP-GlcNAc gets converted into UDP-MurNAc by the enzymes MurA (*cg0422*) and MurB (*cg0423*). The stem peptide is formed by the consecutive addition of L-Ala (MurC; *cg2368*), D-*iso*Glu

(MurD; *cg2371*), mDpm (MurE; *cg2374*) and two D-Ala residues (MurF; *cg2373*). During this process D-Glu gets converted into D-Glu (MurI; *cg0262*). Further, the alanine racemase Alr (*cg0681*) is facilitating the conversion of D-Ala into L-Ala and *vici versa*, while DdlA (*cg1493*) ensures the formation of the terminal D-Ala-D-Ala dipeptide. The resulting UDP-MurNAc-pentapeptide is then loaded to the membrane integrated carrier-molecule decaprenyl phosphate (DP) by the integral membrane protein MraY (*cg2372*), thus forming lipid I. In a consecutive step, a molecule of GlcNAc gets β-(1→4) transferred to the MurNAc residue of lipid I by MurG (*cg2369*), consequently forming lipid II. This molecule serves as the source for PG building blocks (Fig.3A).

Regarding the translocation of lipid II across the PM, various candidate proteins have been characterized, predominantly on variants from *E. coli* (Ruiz, 2015). A broad conservation of these proteins suggests a common mechanism for most species. Recently, the MOP (multidrug/oligo-saccharidyl-lipid/polysaccharide) superfamily protein MurJ has been identified as a monofunctional lipid II flippase in *E. coli* (Sham et al., 2014). For *C. glutamicum,* the *murJ* orthologue *cg3419* is present in the genome but not further characterized. Earlier, the SEDS (shape, elongation, division, and sporulation) superfamily proteins FtsW and RodA were examined regarding lipid II translocation activity (Datta et al., 2002; Meeske et al., 2016; Sieger et al., 2013; Szwedziak & Löwe, 2013). Both proteins form a complex with a cognate penicillin binding protein and play a further role in the direct expansion of the PG sacculus (Valbuena et al., 2007). The divisome associated FtsW has shown to act as a flippase in *in vitro* experiments by using reconstituted parts of *Escherichia coli* (Mohammadi et al., 2011). The FtsW orthologues in *Mycobacterium* spp*.* and *C. glutamicum* (Cg2370) are expected to fulfill the same function as septal flippase (Ruiz, 2015). The elongasome associated SEDS protein RodA (*cg0061*) has been examined closer in *C. glutamicum* (Sieger et al., 2013). A deletion mutant showed a phenotype of diminished apical elongation growth. A further experiment with fluorescently labeled vancomycin (Van-FL) resulted in an increased signal at the lateral wall in *C. glutamicum ΔrodA* cells. Since the apical growth is still present for the respective genotype and Van-FL is supposed to bind to lipid II in the periplasm, the result was interpreted as a compensation of the locally decreased lipid II translocation by the action of FtsW and its redirection. Due to the similarity of RodA to

FtsW (31,9 %) and the obtained results, its role as apical acting flippase has been suggested (Sieger et al., 2013). Compared to SEDS proteins, MurJ shows a significant higher affinity to lipid II (Bolla et al., 2018). This, and the broad conservation among prokaryotes indicate its probable role as the major bacterial flippase (Butler et al., 2013; Ruiz, 2008; Sham et al., 2014). This opened questions about the role of the mentioned SEDS proteins and consequently revealed their major function as transglycosylases (TGs) that conduct the actual expansion of the PG sacculus.
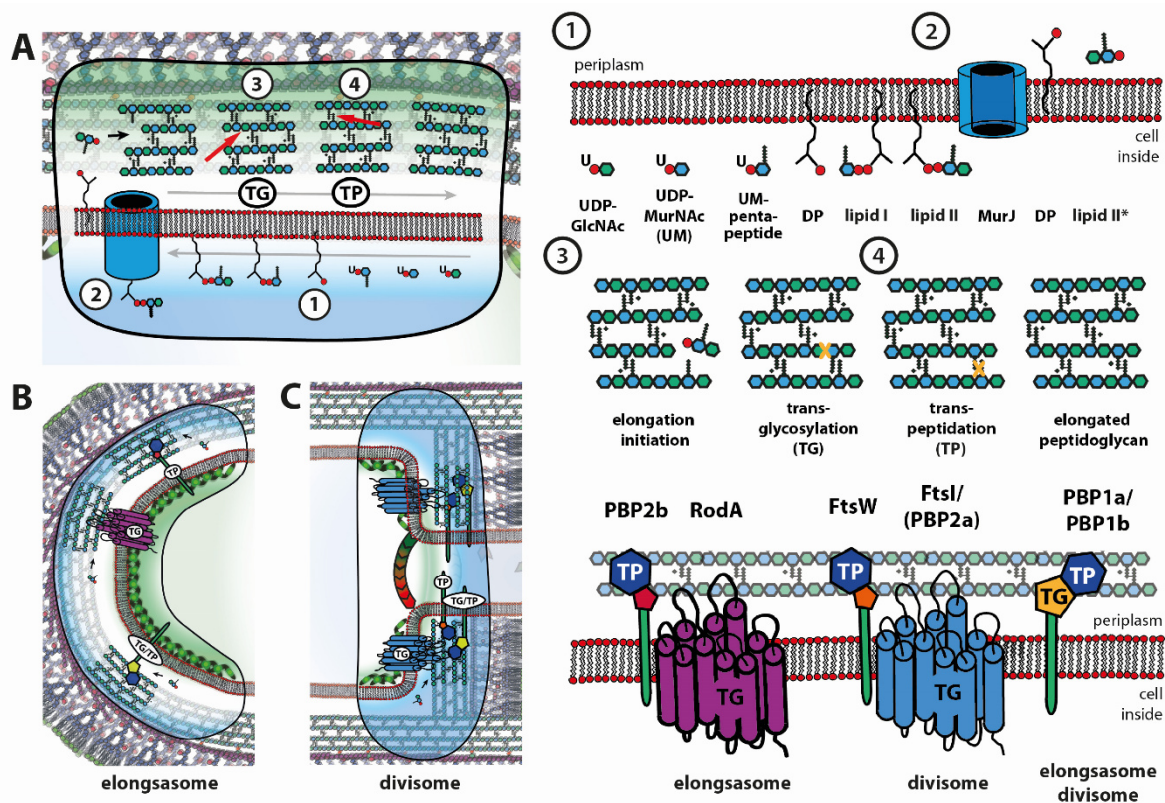

Figure 3: Mechanism of PG synthesis in *C. glutamicum*. (A) Synthesis pathway of the PG precursor lipid II and its incorporation into a present PG mesh. The precursor formation starts with a conversion of uridine-diphospho-N-acetylglucosamine (UDP-GlcNAc) to uridine-diphospho-N-acetylmuramine (UDP-MurNAc) and the addition of the pentapeptide. Loaded to the membrane associated carrier decaprenol phosphate (DP) the resulting lipid I serves as educt for lipid II formation by the addition of GlcNAc to the MurNAc residue (①). The process involves the further translocation across the plasma (②, asterisk), a transglcosylase (TG) reaction to connect the lipid II to the glycan backbone (③) and a transpeptidation (TP) reaction of the stem peptide (④). **(B)** Principal components of the apically located elongasome complex. The longitudinal growth of single cells occurs through TG and TP reactions that push new material towards the opposing pole. **(C)** Principal components of the divisome complex. Cell division is fueled by the same pool of lipid II. By the localization of the curvature sensitive DivIVA (green rods with black tips), the formation of a new elongasome is initialized.

This final integration of lipid II into the existing PG mesh includes the incorporation into the glycan backbone by TGs and the crosslinking of the stem-peptide by transpeptidases (TPs). In *C. glutamicum*, the cell cycle dependent differentiation from a divisome into two new polar elongasome sites is driven by the localization of the toposenitive, scaffold-forming protein DivIVA (Letek et al., 2008). This stands in contrast to Firmicutes and γ-Proteobacteria, where new cell wall material is synthesized along the short axis of wall, driven by the lateral acting MreB (Levin et al., 1992; van der Ploeg et al., 2015) (Fig. 3A, 3-4).

The opposing apical scaffolds, created by oligomerizations of the curvature-sensitive DivIVA, attract various proteins that are responsible for elongation growth (Kang et al., 2008; Lenarcic et al., 2009; Letek et al., 2008; Sieger & Bramkamp, 2015). Among them, the widely conserved class of bacterial penicillin binding proteins (PBPs) plays an important role for PG synthesis. The high molecular weight (HMW)-PBPs, PBP1a (*cg0336*), and PBP1b (*cg3313*), exhibit bifunctional TG/TP activity (Valbuena et al., 2007). Both have been demonstrated to localize at the cell poles, and neither is essential. For the SEDS protein RodA (*cg0061*) and the cognate, class bPBP PBP2b (*cg0060*) a colocalization with DivIVA has been shown (Sieger et al., 2013; Sieger & Bramkamp, 2015). In combination, the monofunctional activities of RodA (TG) and PBP2b (TP) act as a mechanism for the microscale apical elongation (Emami et al., 2017; Sher et al., 2021) (Fig. 3B).

Driven by the tubulin-like protein FtsZ, the divisome apparatus forms two *de novo* cell poles (Erickson, 1997). A septal SEDS/bPBP complex is found in FtsW (*cg2370*) and FtsI/PBP3 (*cg2375*) (Pogliano et al., 1997; Sher et al., 2021). The conserved role of FtsI along the cognate FtsW represents a central process of bacterial division across different phyla (L. Wang et al., 1998; Weiss et al., 1999). In *C. glutamicum*, a third HMW-bPBP, PBP2a (*cg2199*) was also associated to the divisome. Under optimal growth conditions, the deletion did not cause an altered phenotype compared to the wild-type (Valbuena et al., 2007) (Fig. 3C).

In addition to the HMW-, four low molecular (LMW)-PBPs are present in the genome of *C. glutamicum*. Acting as D,D-carboxypeptidases, PBP4 (*NCgl0650*) and DacB/PBP4b (*cg2987*/ *NCgl2606*) probably conduct mechanisms for cell wall maturation (Lavollay et

al., 2009; Valbuena et al., 2007). For PBP5 (*cg2649*) and PBP6 (*cg2478*), the structural similarity to β-lactamases accounts for a role in monitoring the status of the cell wall (Jacobs et al., 1994; Valbuena et al., 2007). Further, the L,D-transpeptidases Cg0650 and LppS (*cg2720*), catalyze a (3→3) crosslink, are described but their function was not investigated in detail (Lavollay et al., 2009).

1.2.2 Arabinogalactan

In *C. glutamicum*, the formation of the arabinogalactan (AG) layer appears connected to the PG-synthesis (McNeil et al., 1990; Yagi et al., 2003). The steps of AG precursor synthesis, translocation across the PM, and integration into the existing cell wall resemble the process around lipid II (Crick et al., 2001; Vilkas et al., 1973). A direct link is found in a common use of the membrane integrated carrier molecule DP. In *Mycobacterium* spp. the process of AG synthesis has been examined in detail (Hancock et al., 2002; Mikuová et al., 2000; Yagi et al., 2003; N. Zhang et al., 2003). Involved sugars appear in their furanoid/pyranoid ring form (*f/p*). The development and translocation of the galactan chain (Gal*f*~) appears inside the cell, uncoupled from the formation and translocation of arabinose (Ara*f*) subunits of the AG (Grover et al., 2014) (Fig. 4).

In *C. glutamicum,* the development of Gal*f*~ (GlcNAc-L-Rha-Gal*f_n*) is primed through the formation of a complex between GlcNAc and DP (DP-PP-GlcNAc) by WecA (*cg1359*) (Alderwick et al., 2005; Birch et al., 2008). The α-3-L-rhamnosyltransferase WbbL supports the addition of a single Rha*p* molecule to the GlcNAc residue (Mikušová et al., 2005; Mills et al., 2004). By using uridine-diphospho (UDP)-Gal*f* as a precursor and starting on Rha*p*, the sequential polymerization of multiple Gal*f* residues is initiated by the galactofuranosyl transferase GlfT1. The consequent Gal*f*~ elongation through alternating β-(1→5)/(1→6) linked Gal*f* is catalyzed by GlfT2 (Belánová et al., 2008; Birch et al., 2008). The length of Gal*f*~ varies among different species. For *C. glutamicum,* shorter Gal*f*~ chains were reported than for *M. tuberculosis* (Wesener et al., 2017). The translocation of Gal*f*~ across the PM is likely also conducted by Wzm/Wzt (Savková et al., 2021).

For the periplasmatic maturation of the AG, Ara*f* residues are required (Fig. 4). Derived from the pentose phosphate pathway, cytosolic ribose-5-phosphate (R5P) gets

phosphorylated to phosphoribose diphosphate (pRpp) by PrsA and subsequently gets primed for the binding to DP by UbiA (Alderwick et al., 2005). The resulting decaprenylphosphoryl-5-phosphoribose (DPPR) complex gets further dephosphorylated to decaprenylphosphoryl-β-D-ribose (DPR), likely by Cg3190. This is followed by the consequent epimerization of DPR through DprE1 (*cg0238*) and DprE2 (*cg0237*), which eventually leads to decaprenylphosphoryl-D-arabinose (DPA). Studies with fluorescent pBTZ account for a periplasmatic localization of DprE1 (Brecik et al., 2015). The protein Cg1680 is supposed to show a functional redundancy to DprE2 (Grover et al., 2014; Meniche et al., 2008). In *C. glutamicum* translocation of DPR is likely conducted by GtrA (Grover et al., 2014; Kolly et al., 2015).
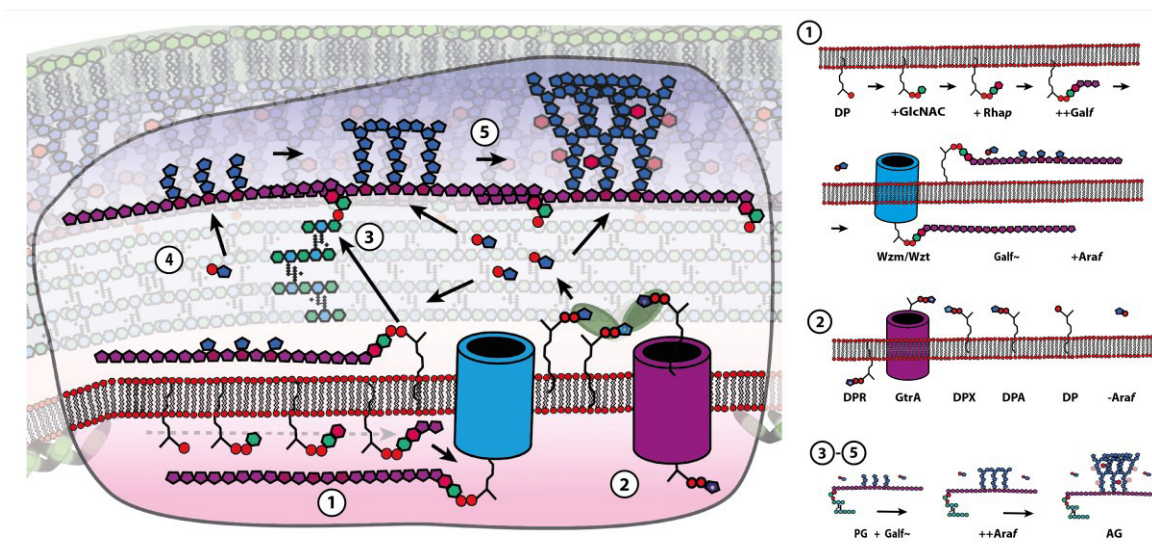

Figure 4: Mechanism of AG synthesis in *C. glutamicum*. The synthesis pathway involves the formation of decaprenyl phosphate (DP) bound Galf~ chains is starting inside the cytosol with a binding of uridine-diphospho-N-acetylglucosamine (UDP-MurNAc) to DP, followed by the addition of rhamnopyranose (Rha*p*) and galactofuranose (Gal*f*). Likely Galf~ gets translocated across the plasma membrane via Wzm/Wzt. The Galf~ get decorated with arabinofuranose (Ara*f*) residues at the positions 8, 10, and 12 (①). The free Ara*f* in the periplasm derives from a DP bound epimerization of decaprenylphosphoryl ribose (DPR) via the intermediate epimer (DPX), to decaprenylphosphoryl-D-arabinose (DPA), in prior to its translocation across the membrane by GtrA (②). The Gal~ chains get covalently linked to the peptidoglycan (PG) and successively decorated with branching arabinose residues (③-⑤). This consecutive bifurcation of parallel oriented arabinose chains renders a dense, but flexible surface towards the outside and further serves as scaffold for further mycolation.

The periplasmatic release of Gal*f*~ and of Ara*f* facilitates the ordered maturation of the AG strands. The correct branching of the Ara*f* chains is initiated and controlled by AraT

and AftABCD, while the elongation of the Ara*f* chains is conducted by proteins termed Emb (Alderwick et al., 2005, 2006; Seidel et al., 2007). *Mycobacterium* spp*.* commonly encode multiple *emb* variants, while in *C. glutamicum* only the orthologue of the mycobacterial *embC* is present (Belanger et al., 1996; Sreevatsan et al., 1997). The Gal*f* chain of Gal*f~* consequently gets decorated with three arabinan domains at the positions 8, 10 and 12 (Daffe et al., 1990). In a final step the terminal β(1→2)-Ara*f* residues become esterified by mycolic acids (MA), and hence forms a structural base for the outfacing mycomembrane (MM) (Daffe et al., 1990; Huc et al., 2013). A detailed view on the MM is found in the following section.

In *C. glutamicum*, the final transfer of the AG building block to a MurNAc residue of the PG is achieved by LcpA (*cg0847*) (Baumgart et al., 2016; Kawai et al., 2011). The accessory attachment of Rha*p* to the C2 position of α-(1→5)-linked Ara*f* is a specific feature of the AG in *C. glutamicum* (Birch et al., 2009). Together with equally distant neighbors, the upper part of the AG forms a dense, extracellular quasi-surface for the support of the MM.

C. glutamicum tolerates dysfunctional arabinan synthesis, while the galactan synthesis appears essential (Alderwick et al., 2005; Raad et al., 2010; Wesener et al., 2017). In *M. tuberculosis,* both functions are required for viability (Sassetti et al., 2003). A knockout of *ubiA* in *C. glutamicum* appears still viable, despite the Ara*f* production has been impaired at an early stage (Alderwick et al., 2005). Since cell wall associated lipoglycans were not affected from this, an alternative pathway for the Ara*f* formation was suggested (Tatituri et al., 2007). In general, the AG went into a closer focus as potential target for antibiotics with a very narrow efficacy spectrum. An established antituberculosis drug, ethambutol (EMB), is blocking the polymerization of the Ara*f* residues along the Gal*f~* by inhibiting the enzyme Emb (Forbes et al., 1962). The effect of EMB is exploited in biotechnology and for medical treatment (Kaji et al., 2021; Radmacher et al., 2005). A more recent development of an AG acting antibiotic is represented by BTZ034. This research compound is acting on the epimerase DprE1 during the formation of Ara*f* (Grover et al., 2014; Makarov et al., 2009). Using *C. glutamicum* as model organism, the effects of both antibiotics were examined in detail within this work.

1.2.3 Mycomembrane

The hydrophobic mycomembrane (MM) is a hallmark of the *Corynebacteriales* (Barksdale, 1970; Lanéelle et al., 2013). Owing to the PG/AG arrangement, the inner leaflet of the mycolic acid (MA) membrane is covalently linked to the cell wall (Fig. 5). The outer leaflet is formed by small, mobile trehalose mono (TMM)- and trehalose di-mycolates (TDM) (Fig. 5). The actual length of MA depends on the species and defines the hydrophobic property of the MM (Barry et al., 1998). In *C. glutamicum*, the surface of colonies is moist, even, and shiny. Here, the MA has a length ranging from about 22-36 carbon atoms. For *Mycobacterium* spp., a length of 60-90 carbon atoms for the MA is reported (Marrakchi et al., 2014). The colonies look dry, uneven, and waxy. The variations in the chain length of the mycolic acids between *Mycobacteria* and *Corynebacteria* allow for a differentiation by acid fast staining (Lamanna, 1946).
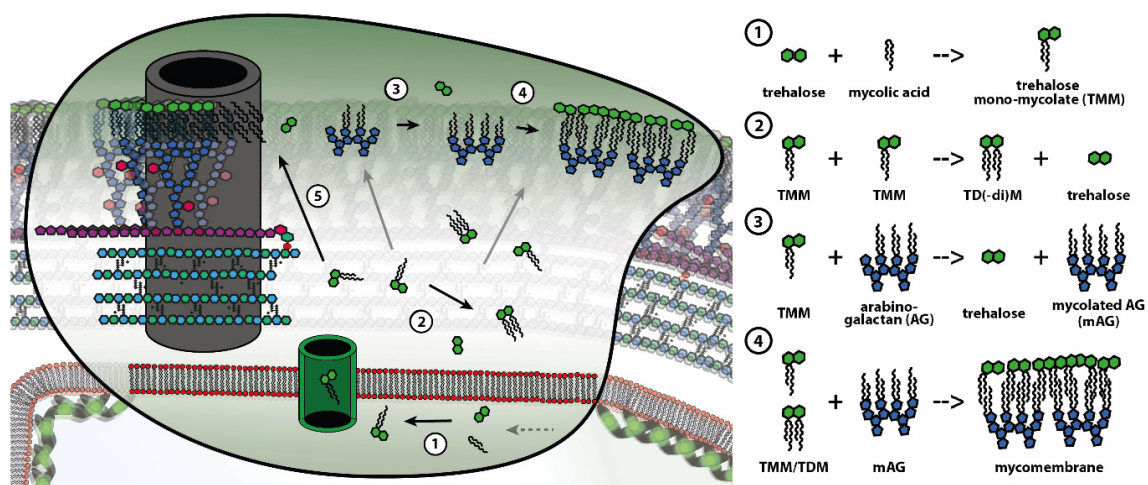
Figure 5: Mechanism of the MM assembly in *C. glutamicum*. The pathway starts with the cytosolic synthesis of free MA through the fatty acid metabolism. These get fused to free trehalose molecules and form TMM (①). Translocated to the periplasm, it serves as donor for at least three different mycolation reactions (②-④). By interacting with a second TMM molecule, TDM and free trehalose are formed (②). By the AG mycolation of the terminal arabinose residues, the static, inner leaflet of the MM is set (③). In a final step of the MM assembly, free TMM and TDM form the mobile, outer leaflet (④). In addition, cell wall spanning porins get mycolated proximal to the extracellular and to provide a stable anchor in the outer envelope (⑤).

In *C. glutamicum* the MA are formed via products derived from FasIA (*cg2743*) and FasIB (*cg0957*). These enzymes are part of the fatty acid (FA) metabolism and catalyze the production of stearic acid (C18:0), oleic acid (C18:1), and palmitic acid (C16:0) (Slayden

et al., 2000). The formation of activated FAs is mediated through FadD (*cg3179*) and AccD2 (*cg0811*), AccD3 (*cg3177*), AccBC (*cg0802*), and AccE (*cg0810*) (Gande et al., 2004). The single FA branches are fused to an α-alkyl β-ketoester by a Claisen condensation, catalyzed by the polyketide synthase Pks (*cg3178*) (R. E. Lee et al., 1997). This β-ketoester is further reduced to the mycolic motif by CmrA (Lea-Smith et al., 2007). The mycobacterial Pks orthologue, Pks13, is reported to also catalyze the transfer of a MA residue to a free trehalose molecule (Gavalda et al., 2014). This intracellular formation of TMM sets for the subsequent translocation across the PM by the transporter protein MmpL3 in *Mycobacteria*. In *C. glutamicum* the direct orthologue cmpL1 (*cg3174*) showed no reduction in the level of free or bound mycolates upon its deletion. With CmpL2 (*cg1054*), CmpL3 (*cg0722*) and CmpL4 (*cg0284*) three further putative transporters were identified. A double null mutant of *cmpL1* and *cmpL4* resulted in the complete abolishment of TMM production, likely due to feedback to Pks (Varela et al., 2012).

In the periplasmatic space, translocated TMM serve as MA donor for subsequent transfer reactions. The major recipients are the terminal Ara*f* residues of the AG and other TMM molecules, for the formation of TDM. Further, the localization of MM bound porins depend on an MA anchor. Various other proteins are suggested to be mycolated. Therefore, *C. glutamicum* encodes for the six different mycoloyl-transferases *cmytA-F* (Kacem et al., 2004). Concerning the major MA recipients, CmytA (*cg3182*) and CmytB (*cg3186*) are expected to express a higher catalytic activity compared to the redundantly acting CmytD (*cg1170*) and CmytF (*cg2394*). CmytE (*cg1052*) is described as a pseudogene. Despite the complete 483 amino acid (aa) sequence of *cmytE* being present in the genome, an emerging stop-codon terminates translation after 180 aa and leads to a non-functional fragment. (De Sousa-D'Auria et al., 2003). A supplementary MA transfer capability to certain peptides is reported for CmytC (*cg0413*). The integration of the porins PorA and PorH into the MM depend on a prior decoration with MA (Huc et al., 2013).

The hydrophobic properties of the MM, in large parts, depend on the PG/AG arrangement. Densely grouped, exposed MA-residues facilitate the formation of a PG-coupled extracellular membrane. The confluent outer MM leaflet, formed by mobile

TMM- and TDM-elements, eventually provides a versatile barrier for the cell. The integrity of the MM is connected to a protective function. The consequent shielding of the intracellular space from the aqueous environment elements appears as a successful protective strategy. In *M. tuberculosis* the physical properties of relatively long MA residues facilitate its survival upon the oxidizing conditions inside of macrophages.

1.2.4 Lipoglycans

In *Corynebacteriales,* phosphatidyl-myo-inositol (PI)-anchored glycans spans from the plasma membrane (PM) into the cell wall (Fig. 6). The detailed role of these structures is still under debate. The consecutive formation of phosphatidyl-myo-inositol mannosides (PIM), lipomannan (LM), and lipoarabinomannan (LAM) defines a notable structural trait (Rainczuk et al., 2012; Sancho-Vaello et al., 2017).
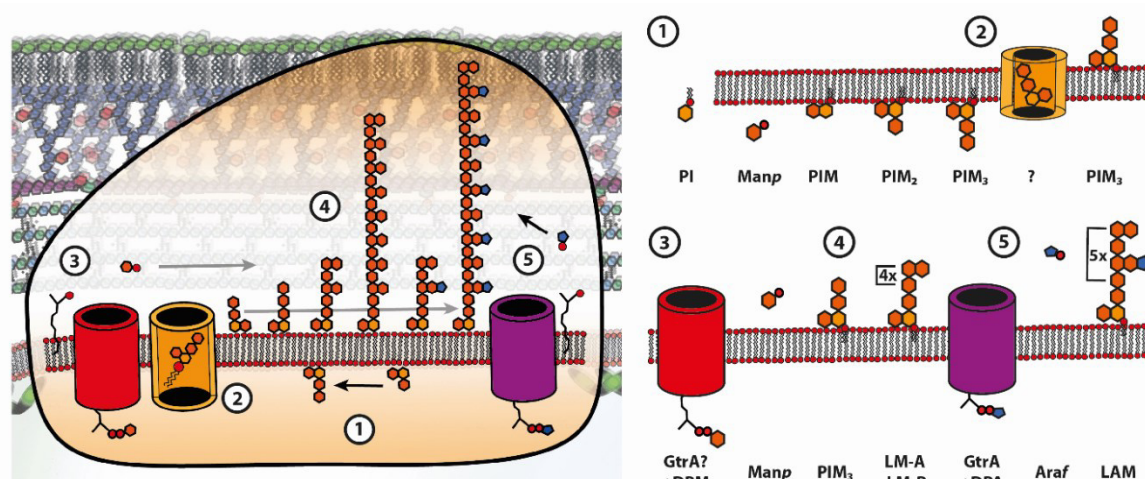
Figure 6: Mechanism of the lipoglycan synthesis in *C. glutamicum*. Lipoglycans contribute to the stability of the cell envelope since they physically connect the PM with the PG/AG/MM-complex. The synthesis starts with the formation of membrane bound phosphatidyl-myo-inositol mannosides (PIM) in the cytosol from phosphatidyl-myo-inositol (PI, ①). After the addition of a further Man*p* residue, the resulting PIM_3 gets translocated to the periplasm (②). There it serves as hub for further mannose dependent elongation and regular lateral branching (③). The resulting branched lipomannan (LM, ④) then serves as substrate for a capping of the branching mannose residues with single arabinose molecule resulting in different species of lipoarabinomannan (LAM, ⑤). The variable length of the chains is likely the subject of a regulated process.

The sequential assembly starts in the cytoplasm with the O-2 addition of a mannose residue (Man*p*) to the myo-inositol ring of PI by PimA (*cg1876*) (Gibson et al., 2003; Korduláková et al., 2002). The resulting PIM gets acetylated, likely by Cg1877

(Korduláková et al., 2003). A further addition of Man*p* to the O-6 position of the myo-inositol ring by PimB' (*cg2400*) results in AcPIM$_2$ and PIM$_3$ consecutively (Batt et al., 2010; Mishra, Klein, et al., 2008). As the processive assembly continues in the extracellular space, this molecule is suggested to be flipped across the PM, mediated by a yet uncharacterized translocase. The process involves decaprenolphosphate (DP) delivered Man*p* (DPM) (Gibson et al., 2003; Mohiman et al., 2012). The carrier molecule DP arrives from the same pool that is also utilized for PG and AG synthesis. Through the proximal and distal α(1→6) addition of Man*p* by MptA (*cg2385*) and MptB (*cg1766*), the backbone of the structure is formed (Mishra et al., 2007; Mishra, Alderwick, et al., 2008; R. Tatituri et al., 2007). With the action of MptC (*cg2393*) and MptD (*cg2390*) a regular α(1→2)-Man*p* branching is realized (Mishra et al., 2011). The intermediate LM defines already the full length Man*p* backbone. It is suggested that the progress of the Man*p* polymerization is regulated by LpqW and a membrane protein (Cg3164) of yet unknown function (Rainczuk et al., 2012). A subsequent formation of LAM is fueled by DPA (decapenyl arabinofuranose), a donor also used during the AG formation. The transfer of Ara*f* residues to LM is likely conducted by AraT (Tatituri et al., 2007).

The perpendicular orientation of the PIM-LM-LAM polymers is understood to reach into the AG, while being anchored in the PM through the PI. Molecules from this species are expected to improve the spatial stability of the cell wall. Due to the above-mentioned metabolic coupling, a potential further structural or regulatory role for PG/AG-synthesis is thinkable. Shorter PIM-LM species are suggested to populate the periplasm.

1.3 Growth and division of *C. glutamicum*

The phrase 'bacterial growth' is generally associated with the exponential increase in the cell number. The phenomenon behind the term is perceivable without any auxiliary means and appears during galloping infections, or the production of yoghurt. It has been harnessed by mankind without specific awareness for centuries (Schaechter, 2015). Regarding the fertility of soil, the preservation of food, or the conquering of the new world, microbial growth always is both, a prolific and a hostile factor (Junker, 2004; Majander et al., 2020; Visser & Parkinson, 1992). Characterized by specific environmental requirements and a respective generation time, microbes have been discovered in a manifold of niches (Rinke et al., 2013; Jiao et al., 2021). Now, recent

developments of advanced optical technologies exceed each other by breaking the resolution-limits of space and time repeatedly (Hell, 2007; Sahl et al., 2017). By this, single parts of microbial cells became prone to observation and manipulation (Schaechter, 2015).
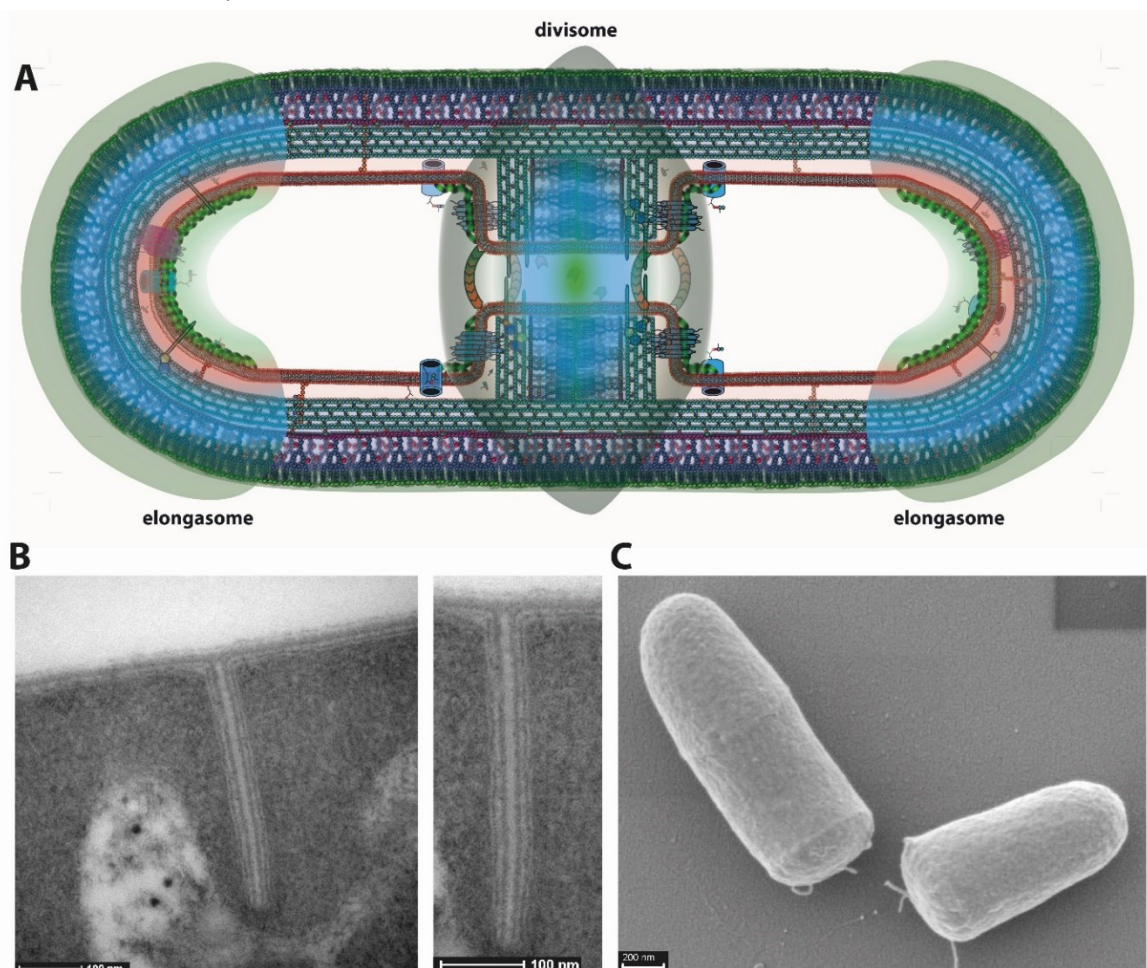
Figure 7: Zones of growth and division in *C. glutamicum*. (A) Schematic representation of the spatial organization of the apical elongasome and the central divisome complexes **(B)** A transmission electron micrograph of a division septum from *C. glutamicum*. The distinct layers get synthesized driven by the dynamic action of FtsZ. The septum is not visible from the outside, as the present layers stay preserved until the end of cytokinesis. This is reflected in the characteristic Π-shape that gets only punctuated short before division. **(C)** A scanning electron micrograph that shows the general shape of the cells and the occasional occurring asymmetric division.

By taking the cell as reference frame, the term 'bacterial growth' gets a different connotation. In particular if the exponential elongation of single cells is described for cells in the exponential growth phase. In this work, specific features of *C. glutamicum* were examined mostly from this cell centered perspective (Fig 7). Morphological characteristics were connected to genetic features and physical and chemical stress

conditions. The comparison with other model organisms offers a deeper insight in the function and organization of the corynebacterial cell cycle.

1.3.1 Biophysical aspects of bacterial growth

As prevalent model organisms, *Escherichia coli* and *Bacillus subtilis* also set the base for many theoretical considerations about bacterial growth (Amir, 2014). Current attempts aim to create a unifying concept for the cell size homeostasis. This birth centric model comprises three variants of theoretically derived strategies for the initiation of binary fission. Either the elapsed time, a critical size, or a constant threshold for the added volume, are discussed to prompt cell division. This labels the terms 'timer', 'sizer', and 'adder'. More precisely, taking the division size as a function of the size at birth, a characteristic α defines whether the species meets the timer ($\alpha = 0$), sizer ($\alpha = 1$) or adder criteria ($\alpha = 1/2$). The model is understood as a mechanism for cell size control, also with respect to a stable size distribution within the population (Amir, 2017; Campos et al., 2014; Ho & Amir, 2015; Taheri-Araghi et al., 2015). This cell size homeostasis is a prerequisite for a prospering colony and is determined by the specific mode of cell elongation and the moment of division. Given the abundance of MreB driven exponential elongation in the known bacterial kingdom, the adder type of size homeostasis regulation seems a valid approach and appears confirmed by many examples (Mao et al., 2022; Shi et al., 2018; Taheri-Araghi et al., 2015). With the respective classification of the Actinobacterium *M. smegmatis*, an exception was noted. Initially described as a hybrid of a timer and adder, the mode of single cell elongation is eventually interpreted as a parallel adder (Logsdon et al., 2017). This exception likely occurs due to the apical mode of cell elongation, the hallmark of rod-shaped Actinobacteria (Marantan & Amir, 2016). The specimen specific molecular organization seems a relevant factor for this kind of description. As a central part of this work, characteristics of single *C. glutamicum* were analyzed to get a clearer picture of the spatiotemporal dynamics.

1.3.2 Biochemical and structural aspects of bacterial growth

A comparison of the MreB-driven, lateral elongation apparatus and the DivIVA-coordinated apical elongasome shows a remarkable difference on various scales. For

B. subtilis and *E. coli*, patches of MreB migrate along the membrane, perpendicular to the long axis of the cell. By guiding the elongasome-associated proteins, new cell wall material is integrated as a single stand. This process occurs in parallel along the entire surface, except the poles. By this, bacteria like *E. coli* and *B. subtilis* grow in length (Garner et al., 2011; Shi et al., 2018). The type of lateral elongation is often connected to a precise regulation of the division symmetry. Both species harbor variants of the so-called Min-system. This dynamic arrangement of interdependent proteins helps to construct a precise central plane in the cell (Lutkenhaus, 2012). By this, a high degree of division-symmetry is ensured. Given the structural prerequisites, the growing surface enables for an increase of the number of MreB complexes. By this positive feedback, the speed of elongation undergoes an exponential acceleration (Zheng et al., 2016). The larger a cell is, the faster it grows.

In contrast to that, the actinobacterial type of elongasome organization depends on an arrangement of DivIVA (Letek et al., 2008). By showing an affinity to curved phospholipid membranes, DivIVA predominantly localizes to the cell poles (Ramamurthi & Losick, 2009). This defines the zones of active growth. Two separate, opposing complexes coordinate the production of a tube-shaped, *de novo* cell wall that is pushed towards the center of the cell. Unlike in *Firmicutes* or *γ-Proteobacteria*, no *min* homologues of the are present in the genome. Nor other known regulators for septum positioning are described. The appearance of a division septum occurs more randomly as in laterally elongating species. In contrast to the inert cell poles of *E. coli* or *B. subtilis*, the poles of rod-shaped Actinobacteria play central role for elongation. During each division, two of these structures are newly formed and persist in an active state for generations (Aldridge et al., 2012). Detailed analyses about the elongation dynamics of Actinobacteria are rare. For *M. smegmatis* a biphasic growth model was proposed. The depicted NETO ('new end take off')-model describes a gradual increase of cell wall synthesis activity of the new pole after an initial lag phase (Hannebelle et al., 2020). For *C. glutamicum*, no such studies have been done yet.

Since the cellular organization of *C. glutamicum*, in principle appears similar to *M. smegmatis*, the type of size regulation is expected to be similar. This categorization still leaves open questions about the precise dynamics of elongation and septum

placement. Parts of this study aim towards an accurate measurement of the cell cycle of *C. glutamicum*. A detailed analysis offers a new insight into the elongation dynamics of this alternative cell architecture.

For *C. glutamicum,* the optimal spatio-temporal development of cells is highly dependent on three internal scaffolding structures. The apical mode of elongation is organized by a polar aggregation of the curvature sensitive DivIVA (cg2361) (Ramos et al., 2003). Further, as in most other bacteria, the tubulin-homologue FtsZ (cg2366) is the key protein for recruitment of the proteins of the division machinery (Donovan & Bramkamp, 2014; Lutkenhaus et al., 1980). A structure that physically connects both aggregates during the cell cycle is found in the bacterial chromosome, that also serves as topological trait, since it interacts with numerous structural and regulatory proteins (Bramhill & Kornberg, 1988; Donovan et al., 2013; Yang & Inouye, 1993).

The structural role of DivIVA during the cell cycle of *C. glutamicum*

Orthologues from the DivIVA protein-superfamily appear preserved predominantly among Gram-positive *Firmicutes* and *Actinobacteria* (Cha & Stewart, 1997; Flärdh, 2003). Structurally, the proteins are characterized by a conserved, short N-terminal domain that mediates the interaction with the phospholipid membrane (Lenarcic et al., 2009; Oliva et al., 2010). Further, at least two coiled-coiled regions are essential for oligomerization and the interaction with other proteins (Letek et al., 2009). The structure of these regions differs between the mentioned species and thereby are consequently reported to cause diverse forms of functional processes (Cha & Stewart, 1997; Halbedel et al., 2012; Kaval & Halbedel, 2012; Ramos et al., 2003).

Originally, DivIVA was described during studies on cell division in *B. subtilis* (Cha & Stewart, 1997). Here, the Firmicutes orthologue of DivIVA (DivIVA$_{Fir}$) helps to ensure the proper positioning of the division site. In a dynamic process, together with MinCD, it ensures the inhibition of the Z-ring formation close to the cell poles, while it allows its formation precisely at mid-cell (Bramkamp et al., 2008; Edwards & Errington, 1997; Marston et al., 1998). Deletion mutants of *divIVA$_{Fir}$* in *Bacillus subtilis* express a filamentous phenotype (Edwards & Errington, 1997; Oliva et al., 2010).

Compared to *Firmicutes*, the orthologue of DivIVA in *Actinobacteria* (DivIVA$_{Act}$) plays a functionally different role. Initially mentioned during immunological studies, the first DivIVA$_{Act}$ homologue was assigned as antigen 84 from *Mycobacterium* spp. (Hermans et al., 1995). Later renamed to Wag31, its function is now associated with apical growth, involved in tethering DNA to the pole, and appears to be regulated by phosphorylation (Jani et al., 2010; Kang et al., 2005, 2008; Kaval & Halbedel, 2012; Melzer et al., 2018). Further DivIVA$_{Act}$ homologues were characterized in *Streptomyces* spp. and *Brevibacterium lactofermentum* (syn. *C. glutamicum*) (Flärdh, 2003; Ramos et al., 2003). The first localization study of DivIVA$_{Act}$ was achieved in *Streptomyces coelicolor* A3(2) by the construction of a fluorescently tagged allelic replacement mutant (Flärdh, 2003).

The localization of DivIVA$_{Act}$-eGFP at the tips of branching hyphae was associated with ongoing peptidoglycan synthesis (Hempel et al., 2008). This was seen in the co-localizing signal of the fluorescently labeled β-lactam antibiotic BODIPY-FL-vancomycin. Since vancomycin interferes with the PG synthesis, an accumulation of its signal serves as a proxy for actively growing sites. The induction of a new cell branch upon the prior relocalization of a DivIVA$_{Act}$-eGFP patch was reported in the same work. This already hints towards the self-organizing properties of DivIVA$_{Act}$-aggregates, with regard to cell pole formation.

In *C. glutamicum*, the DivIVA$_{Act}$ homologue is characterized as essential for viability, while overexpression or depletion of the protein leads to an irregularly enlarged cell shape (Letek et al., 2008; Ramos et al., 2003). More detailed reports revealed its role as self-organizing hub for the recruitment for at least two central processes of the cell cycle. The organization of the elongasome-specific proteins is functionally dependent on the prior and proper localization of DivIVA$_{Act}$. The cycle starts with the individual formation of the new cell poles. It requires the coordination of cytokinesis and the localization of the polar scaffold that remains in place after the division. Consequently, the polar DivIVA$_{Act}$-aggregates serve as organizational trait for a functional elongasome complex that is usually stable over many generations. In a further commission, the DivIVA$_{Act}$-aggregates serve as a tether for the chromosome to the cell pole. This occurs via ParB, by connecting chromosomal *parS* sites and DivIVA$_{Act}$.

On the molecular level, DivIVA$_{Act}$ exhibits self-organizing properties. First reports documented the tendency to localize predominantly to curved membranes (Lenarcic et al., 2009; Ramamurthi & Losick, 2009). Explained by molecular bridging, single molecules tend to form a tree dimensional semi-sphere at the inside of lipid vesicles (Oliva et al., 2010). This structural trait sets the base for the rod-shaped cell morphology of the respective Actinobacteria. Two opposing poles push recently synthesized material against each other and thereby create a rod-shaped bacterium. This occurs in contrast to the mechanism that is present in *B. subtilis*. Here, the formation and maintenance of the rod-shaped morphology are organized fundamentally differently. Circumferential moving patches of MreB mediate the cell elongation along the lateral sidewall, while DivIVA$_{Fir}$ plays a decent role in septum positioning and during cytokinesis and sporulation (Cha & Stewart, 1997; Levin et al., 1992).

The structural role of FtsZ during the cell cycle of *C. glutamicum*

The process of binary fission is one of the most characteristic events regarding the bacterial life cycle. By the selection of temperature-sensitive division mutants in *E. coli*, the subsequent mapping, confirmation, and characterization of the bacterial fission protein FtsZ became possible (Lutkenhaus et al., 1980). Appearing as a structural variant of the eukaryotic tubulin, FtsZ-family proteins possess a GTPase domain (De Boer et al., 1992). Based on initial observations, the FtsZ meta-structure was understood as a contractile ring that guides the formation of septal cell wall and finally resolves the physical connection of the daughter cells. Recent observations revealed a more fine-grained view on the dynamic process of bacterial cell division. In a treadmilling fashion, polar FtsZ protofilaments move circumferentially to the division site until the septation is finished in the center (Bisson-Filho et al., 2017).

Variants of the underlying functional machinery were abundantly discovered in different kingdoms of life. Besides being essential for nearly all bacteria, even two homologues (FtsZ1, FtsZ2) were discovered in numerous Archaea (Liao et al., 2021). Even several Eucaryotes depend on the function of FtsZ since chloroplasts and a share of mitochondria rely on FtsZ dependent binary fission (Lutkenhaus, 1998).

By localizing to the site of division, FtsZ initiates the process of cytokinesis. Independent of the species, it guides the specific cell wall synthetic machinery to the site of septation and provides a contractile track. FtsZ appears as a very old principle, since for each mentioned species the system coevolved with the respective envelope. Due to the various types of cell wall (Fig1), the actual organization of the divisome complexes in *E. coli*, *B. subtilis*, and *C. glutamicum* differ in specific details (Santana-Molina et al., 2023). Often, the parts show a functional equivalence. As a common feature, the action of FtsZ results in two mirroring layers of cell envelope at the site of division that eventually get separated. Usually, the progeny stays intact, and the cycle of elongation and division starts again.

The determination of the division site appears as a highly regulated process in *E. coli* and *B. subtilis*. By the dynamic action of Min-system proteins, a temporal gradient of inhibitors only allows the formation of FtsZ proto-filaments precisely at mid-cell (Bramkamp et al., 2008; De Boer et al., 1992; Edwards & Errington, 1997; Varley & Stewart, 1992). This ensures a high degree of self-similarity and sets the base for a stable population (Marantan & Amir, 2016). In *C. glutamicum*, homologues of the Min proteins appear missing, and the process of division-site selection is not understood in detail. An occasional asymmetric division is characteristic and has no influence on the population fitness.

The structural role of the bacterial chromosome during the cell cycle of *C. glutamicum*

The volatile topology of bacterial DNA raised the scientific interest for decades. For prokaryotic life, various forms of DNA-organization are reported. The observations span from partially linear chromosomes in *Borrelia burgdorferi* to the classic circular bacterial chromosome in *E. coli, B. subtilis* and *C. glutamicum* (Kalinowski et al., 2003; Ojaimi et al., 1994; Yoshikawa, 1968). For all of them, the proper distribution of the replicated sister chromatids to the subsequent generation defines a crucial process (Gogou et al., 2021).

By the discovery of the DNA partitioning system ParABS, the mechanism of nucleoid distribution was revealed for *B. subtilis* (Ireton et al., 1994; Lin & Grossman, 1998). A functional equivalent of the ParABS-system was also reported for *C. glutamicum*

(Donovan et al., 2010). Here as well, the defining elements include the ATPase ParA, the CTPase ParB and the *parS* sites on the bacterial chromosome (Osorio-Valeriano et al., 2019). An accumulation of these centomer-like sequences (*parS*) was mapped close to the origin of replication (*oriC*) of the *C. glutamicum* genome (Kalinowski et al., 2003). ParB molecules accumulate at the *parS* sites and serve as adaptors to tether the nucleoid to the polar aggregates of DivIVA. From there, the replicating chromatid, still decorated with ParB, gets pulled along a wave of hydrolyzing ParA molecules to the opposing side. The precise mode of the chromatid translocation is still under discussion. Either the diffusion-binding, the DNA-relay-, or the hitch-hiking via high-density DNA regions-model would explain the function of the walker-type ATPase ParA (Lim et al., 2014).

During the replication and translocation, the bacterial chromosome gets compacted by structural maintenance of the chromosome (SMC) proteins (Hirano, 1999). Loaded via bound ParB at the *oriC*, SMC-proteins facilitate the extrusion of highly ordered loops (Wilhelm et al., 2015). In this condensed form, the DNA appears more stable. The process is discussed to minimize the chance of an undesired entanglement of the structure during replication. Besides chromosomal DNA certain strains of *C. glutamicum* possess a native set of plasmids, but the commonly used laboratory strain ATCC 13032 is free of plasmids (Tauch et al., 2003).

In comparison to *B. subtilis* and *E. coli*, the genome of *C. glutamicum* lacks a sequence for nucleoid occlusion proteins (Noc) (Harry, 2001; Wu & Errington, 2004). These proteins are reported to prevent the translocating chromosome from being guillotined by the closing septum. However, homologues of the divisome associated DNA-pump FtsK are found in each of three model bacteria (Bigot et al., 2007; Donovan & Bramkamp, 2014).

1.3.3 Aspects of the regulation of growth

Regulative events play an important role in the maintenance of growth and division in all bacteria. Via sensory proteins, single cells can monitor thermodynamic parameters, the concentration of available solutes, or the integrity of internal structures. The respective regulatory effects of *C. glutamicum* include the action of sigma (σ)-factors, events of

global transcriptional regulation, and post-translational modifications. By redirecting cellular resources, these mechanisms enable the cells to adapt to changes in external conditions and thereby influence the dynamics of longitudinal growth and division (Fig. 8).
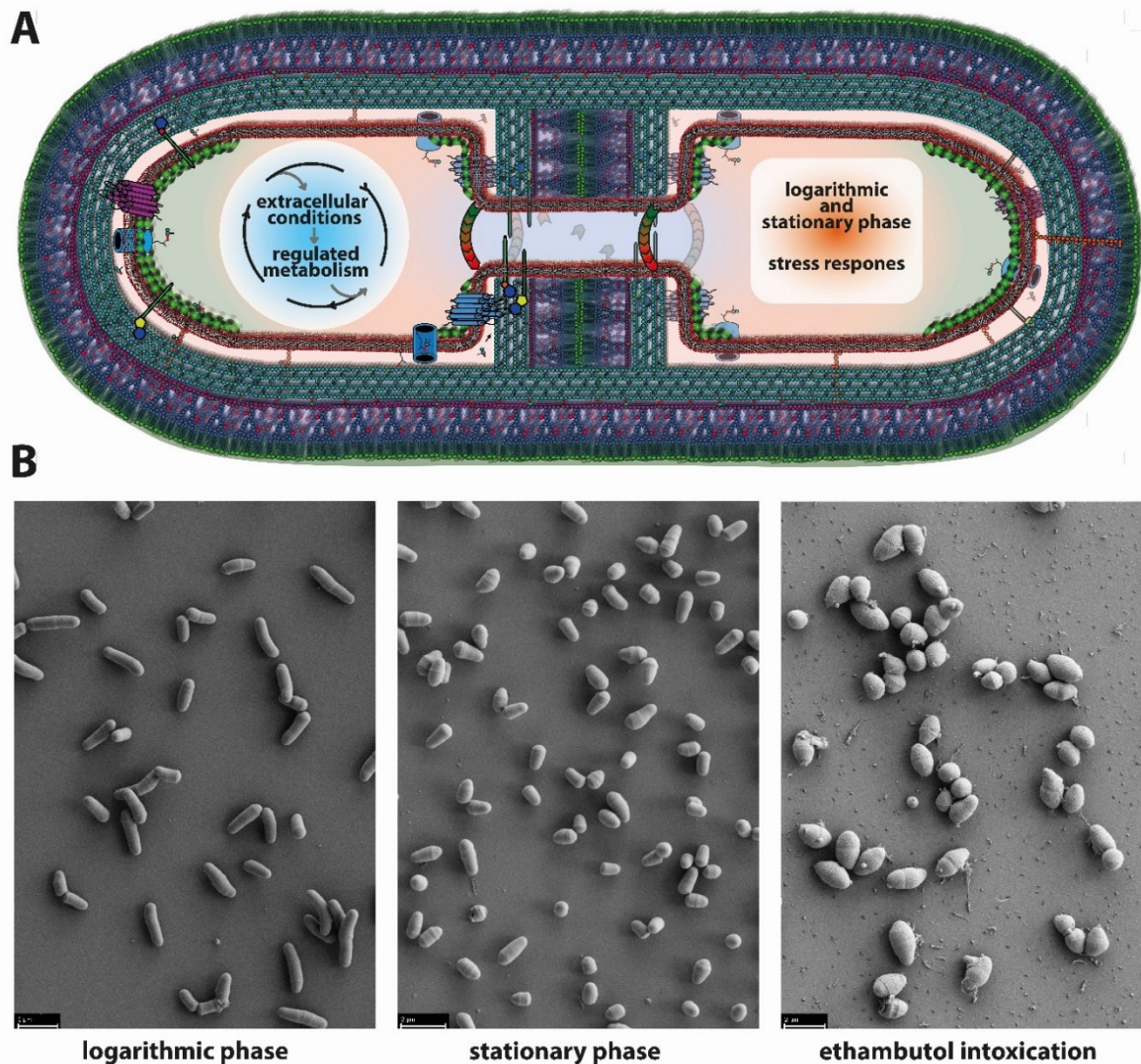
Figure 8: Illustration of the dependence between growth, division and regulation. (A) Regulative mechanisms facilitate to transition to stationary phase metabolism due to crowding. This state is also often activated during different kinds of stress responses. Thereby extrinsic factors play an important role by on elongation growth and cell division of *C. glutamicum*. **(B)** Scanning electron micrographs of *C. glutamicum* cell at different stages. Logarithmic growing cells show a typical length of about 2 µm, while cells from the stationary phase are shorter. A similar effect can be observed upon ethambutol intoxication.

The potentially strong influence of regulative events on the reproducibility of experiments is usually countered by using standardized culture conditions. However, bacteria from a petri dish behave differently compared to clones from a fresh shaking flask. Thus, for experiments, preferentially adapted cells from the exponential growth

phase are used. If the metabolic homeostasis is disturbed, e.g., by antibiotics or by reaching the stationary growth phase, regulatory events define the path to a new equilibrium, if possible (Follmann et al., 2009).

σ-factors

The regulation of bacterial physiology by σ-factors has been studied for decades (Fang, 2005; Mahadik & Srinivasan, 1971). As a variable subunit of the DNA-dependent RNA polymerase (RNAP), σ-factors guide the functional complex (RNAP holoenzyme) to σ-specific promoters and initiate the expression of the respective genes. According to their structure and function, σ-factors are grouped in four different classes and are associated with housekeeping functions and various stress responses (Feklístov et al., 2014; Nandy, 2022; Paget, 2015).

In *C. glutamicum*, the only gene for a primary class σ-factor, *sigA*, is essential (Paget, 2015). The respective promoter is found in front of more than a thousand genes, often related to housekeeping functions. The target genes of the primary-like SigB (class 2) largely overlap with the targets of SigA, but SigB occurs non-essential (Ehira et al., 2008; Oguiza et al., 1996). Studies revealed that the transition from the logarithmic to the stationary growth phase is governed by a substitution of SigA by SigB (Larisch et al., 2007). Orthologues of class 3 σ-factors that are usually related to flagellation or sporulation, are not present in *C. glutamicum*. The five remaining σ-factors all share the characteristic two-domain structure of extra cytoplasmatic function (ECF σ-factors; class 4) that is usually characterized by a cognate, transmembrane anti-σ-factor (Li et al., 2019).

For SigD, SigE, SigH, the ECF σ-factor is bound to that anti-σ-factor and therefore inactive. Triggered by specific stress conditions, the ECF σ-factor is released and able to form the RNAP holoenzyme. The two σ-factors SigC and SigM share the functional two-domain structure, but no anti-σ-factor has been described for them yet (Nakunst et al., 2007; Toyoda & Inui, 2016). For *M. tuberculosis* 13 ECF σ-factors are characterized (Gomez et al., 1997; Manganelli et al., 2023). The ECF σ-factors present in *C. glutamicum*, are found as orthologues among the ones of *M. tuberculosis*.

The function of SigH (Cg0876) is associated with the SOS-response, oxidative- and heat stress. It is regulated by the anti-σ factor RshA (Cg0877), and controls the transcriptional regulators ClgR (due to DB search, likely Cg2152), HspR (Cg3097), SulfR (Cg1765), WhcA (NCgl0275) and WhcE (NCgl0734) (Busche et al., 2012; S. Engels et al., 2004, 2005; Taniguchi & Wendisch, 2015). SigH was shown to drive the transcription of SigB and SigM (Toyoda et al., 2015). An overlapping specificity exists with parts of SigD regulated genes (Dostálová et al., 2019).

For SigE, regulated by CseE (likely Cg1272), the function is associated to surface stress response, heat shock, nitrogen starvation, and general nutritional limitation. The activity has been associated to the beginning of the stationary phase (Park et al., 2008).

The transcription of SigD is regulated by SigA and SigB while its function is controlled by RsdA (likely Cg0697). It affects the mycolate and PG synthesis/ modification and the number of available porins. An overexpression of SigD lead to more resistance against lysozyme and an increased production of trehalose-dimycolates (TDM) (Taniguchi et al., 2017).

For SigC, no anti-σ gene was found in the genome yet. A connection between the activity and the oxidative state of the cell has been demonstrated (Toyoda & Inui, 2016). SigC plays a central role in the adaptation of the respiratory chain, but its detailed physiological function remains elusive.

Also, for SigM, no anti-σ gene was found in the genome yet. The function appears connected to oxidative stress and heat stress. SigM is found to be expressed by a SigH dependent promoter (Nakunst et al., 2007).

Transcriptional regulators

Global transcriptional regulators often appear as parts of σ-regulons. Diverse in structure and context, they mediate the activation or the repression of subsets of functionally connected genes. The spectrum for this kind of transcriptional regulator systems is found connected to the balanced uptake and metabolism of the essential organic elements carbon, nitrogen, phosphate, and sulfur (Schröder & Tauch, 2010).

Parts of the central carbon metabolism are regulated via the transcriptional repressor SugR (cg2115). The regulon includes all genes for the phosphoenol-pyruvate:carbohydrate phosphotransferase system (PTS). These are characterized as specific sugar transporters, formed by the two functional subunits EI (PtsI, *cg2117*) and HPr (PtsH, *cg2121*) and a third, variable EII component that mediates the specificity for glucose (PtsG*, cg1537*)*,* fructose (PtsF*, cg2120*) or sucrose (PtsS*, cg2925*). Further FruR (*cg2118*) and RamB (cg0444) are found involved in balancing the specificity for sugars. GNtR1 (cg2783) and RbsR are reported to control the transport of gluconate and ribose, respectively (V. Engels et al., 2008). The regulative network on carbon metabolism further expands toward glycolysis, the pentose phosphate pathway, the tricarboxylic acid (TCA) cycle, L-lactate metabolism and carbon catabolite control (Schröder & Tauch, 2010).

The regulon for nitrogen homeostasis involves the repression of genes that are functionally connected by an AmtR box promoter. The binding of the related protein AmtR is consequently controlled by the level of ammonium (Jakoby et al., 2000). Under nitrogen-limiting conditions the adenylation of GlnK by GlnD facilitates its binding to AmtR which induces the expression of starvation genes (Harper et al., 2008; Michel et al., 2015). The degradation of GlnK by the divisome related protease FtsH under post-starvation conditions, suggests a cell cycle dependent downregulation of the stress response (Strösser et al., 2004).

Further, *C. glutamicum* is capable of utilizing sulfur and phosphorous from various organic and inorganic sources. Processes leading to the synthesis of methionine/cysteine or iron-sulfur clusters are controlled by McbR (*cg3253*) (Rey et al., 2003). The uptake and metabolism of the central component for DNA and phospholipids is controlled by a two-component system, formed by the sensor kinase PhoR (*cg2888*) and the response regulator PhoS (*cg2887*) (Kočan et al., 2006; Santos-Beneit, 2015; Schaaf & Bott, 2007).

Post-translational protein modifications

The mentioned σ-factors and transcription regulators take control of the physical adaptation of the cell in a hierarchical order, by activating specific subsets of genes. Post-translational modifications can also play a regulative role. At the protein level, they occur in diverse manifestations and generally aim for a functional diversification of the

proteome. In *C. glutamicum*, among others, the acetylation of metabolic enzymes or a mycoloylation of porins are notable (Huc et al., 2013; Mizuno et al., 2016).

The post-translational phosphorylation represents an ubiquitous and diverse example of post-translational modifications that is found in all domains of life. Usually only specific amino acid residues get phosphorylated. This is described for serine, threonine, and tyrosine side chains, through a phosphoester bond, for histidine, lysine and arginine through a phosphoramidate bond, and for aspartic acid and glutamic acid through a mixed anhydride linkage (A. Zhang et al., 2021).

The mentioned PTS sugar transporters, the PhoRS regulon, and Hanks-type kinases rely on their function on the transfer of phosphate residues.

The transport and simultaneous phosphorylation of various sugars is organized by PTS systems. The specific sugar is captured by the respective EII transmembrane subunit of the transporter. The acceptance can only occur if EII is in the phosphorylated state EII~P. The phosphate residue originates from phosphoenolpyruvate (PEP) and gets transferred consecutively from the cytosolic PtsI (*cg2117*) to PtsH (*cg2121*) and eventually to the EII subunit. The sugar molecule gets translocated to the cytosol only while accepting a phosphate group, where it serves as substrate for energy metabolism (Kotrba et al., 2001).

A variant of phosphate-mediated signal transduction is found in two-component systems. The mentioned example, PhoRS, allows for monitoring of the extracellular phosphate level. It consists of the sensor kinase PhoS (cg2887) and the cognate response regulator PhoR (cg2888). Under phosphate-limiting conditions, PhoA, autophosphorylated by ATP and transfers a phosphate group to PhoR. By this, a conformational change leads to the induction of phosphate scavenging genes (Kočan et al., 2006).

In *C. glutamicum,* a more complex form of regulation is attributed to a set of Hanks-type serine/threonine (Ser)/(Thr)-kinases, together with a single phosphatase Ppp (cg0062). PknA (*cg0059*), PknB (*cg0057*), PknL (*cg2388*), and the cognate Ppp are integral membrane proteins with a single transmembrane helix, while PknG (*cg3046*) appears

cytosolic. Together, they connect the central energy metabolism directly to cell elongation, cell wall maintenance, and division (Kang et al., 2005; Schultz et al., 2009).

For PknA and PknG, a direct phosphorylation of OdhI has been shown. As an inhibitor of ODHc, a key complex of the tri-chloric acid cycle (TCA), unphosphorylated OdhI impairs the conversion of 2-oxoglutarate to succinyl-CoA. The kinases regulate the energy metabolism by adjusting the binary state of OdhI phosphorylation. This process is balanced by the action of the phosphatase Ppp. Since PknA is also associated with the phosphorylation and inhibition of FtsZ (cg2366), MurC (cg2368), and RsmP (rod-shaped morphology protein, cg3264), a link between energy metabolism and morphological indications is given. The remaining PknB (cg0057) and PknL (cg2388) possess an extra-plasmatic PASTA (penicillin binding protein and serine/threonine kinase associated) domain and are hence involved in the monitoring of peptidoglycan (PG) synthesis (Schultz et al., 2009).

2. Resulting publications

2.1 Novel chromosome organization pattern in Actinomycetales

Novel chromosome organization pattern in Actinomycetales — Overlapping replication cycles combined with diploidy

Kati Böhm[a], **Fabian Meyer**[a], Agata Rhomberg[a], Jörn Kalinowski[b], Catriona Donovan[a], Marc Bramkamp[a]

[a] Ludwig-Maximilians-Universität München, Fakultät Biologie, Planegg-Martinsried, Germany
[b] Universität Bielefeld, Center for Biotechnology (CeBiTec), Bielefeld, Germany

Abstract

Bacteria regulate chromosome replication and segregation tightly with cell division to ensure faithful segregation of DNA to daughter generations. The underlying mechanisms have been addressed in several model species. It became apparent that bacteria have evolved quite different strategies to regulate DNA segregation and chromosomal organization. We have investigated here how the actinobacterium *Corynebacterium glutamicum* organizes chromosome segregation and DNA replication. Unexpectedly, we found that *C. glutamicum* cells are at least diploid under all of the conditions tested and that these organisms have overlapping C periods during replication, with both origins initiating replication simultaneously. On the basis of experimental data, we propose growth rate- dependent cell cycle models for *C. glutamicum*.

2.2 Deletion of SMC renders FtsK essential in *Corynebacterium glutamicum*

Deletion of SMC renders FtsK essential in *Corynebacterium glutamicum*

Feng Peng[a], Giacomo Giacomelli[a], **Fabian Meyer**[a], Marten Linder[b], Markus Haak[b], Christian Rückert-Reed[b], Manuela Weiß[a], Jörn Kalinowski[b], Marc Bramkamp[a]

[a] Christian-Albrechts-Universität zu Kiel, Institute for General Microbiology, Kiel, Germany
[b] Universität Bielefeld, Center for Biotechnology (CeBiTec), Bielefeld, Germany

Abstract

Structural maintenance of chromosomes (SMC) are ubiquitously distributed proteins involved in chromosome organization. Deletion of smc causes severe growth phenotypes in many organisms. Surprisingly, *smc* can be deleted in *Corynebacterium glutamicum*, a member of the Actinomycetota phylum, without any apparent growth phenotype. Earlier work has shown that SMC in *C. glutamicum* is loaded in a ParB-dependent fashion to the chromosome and functions in replichore cohesion. The unexpected absence of a growth phenotype in the *smc* mutant prompted us to screen for unknown synthetic interactions within *C. glutamicum*. Therefore, we generated a high-density Tn-5 library based on wild-type and *smc*-deleted *C. glutamicum* strains. The transposon sequencing (Tn-seq) data revealed that the DNA-translocase FtsK is essential in a *smc* deletion strain. FtsK localized to the septa and cell poles in wild type cells, however deletion of *smc* resulted in a decreased polar FtsK localization. Single-particle tracking analysis further suggests that prolonged FtsK complex activity is both required and sufficient to make up for the absence of SMC, thus achieving efficient chromosome segregation in *C. glutamicum*. Further, single molecule dynamics of FtsK is influenced, albeit indirectly, by DNA-loaded SMC. Deletion of ParB results in an increased of both SMC and FtsK mobility. While the first change agrees with previous data that show how ParB is essential for SMC loading on DNA, the latter suggests that FtsK mobility is affected in cells with defects in chromosome organization. Based on our data we propose a simple, yet efficient mechanism for efficient DNA segregation in *C. glutamicum*, even in absence of SMC proteins.

2.3 The antituberculosis drug ethambutol selectively blocks apical growth in CMN-group bacteria

The antituberculosis drug ethambutol selectively blocks apical growth in CMN group bacteria

Karin Schubert[*], Boris Sieger[*], **Fabian Meyer**[*], Giacomo Giacomelli, Kati Böhm, Angela Rieblinger, Laura Lindenthal, Nadja Sachs, Gerhard Wanner, Marc Bramkamp

[*] equal contribution

Ludwig-Maximilians-Universität München, Fakultät Biologie, Planegg-Martinsried, Germany

Abstract

Members of the genus *Mycobacterium* are the most prevalent cause of infectious diseases. Mycobacteria have a complex cell envelope containing a peptidoglycan layer and an additional arabinogalactan polymer to which a mycolic acid bilayer is linked; this complex, multilayered cell wall composition (mAGP) is conserved among all CMN group bacteria. The arabinogalactan and mycolic acid synthesis pathways constitute effective drug targets for tuberculosis treatment. Ethambutol (EMB), a classical antituberculosis drug, inhibits the synthesis of the arabinose polymer. Although EMB acts bacteriostatically, its underlying molecular mechanism remains unclear. Here, we used *Corynebacterium glutamicum* and *Mycobacterium phlei* as model organisms to study the effects of EMB at the single-cell level. Our results demonstrate that EMB specifically blocks apical cell wall synthesis, but not cell division, explaining the bacteriostatic effect of EMB. Furthermore, the data suggest that members of the family *Corynebacterineae* have two dedicated machineries for cell elongation (elongasome) and cytokinesis (divisome).

2.4 Effects of BTZ and EMB on the integrity of the corynebacterial cell envelope

Effects of benzothiazinone and ethambutol on the integrity of the corynebacterial cell envelope

Fabian M. Meyer[a, c], Urska Repnik[b], Ekaterina Karnaukhova[a], Karin Schubert[c], Marc Bramkamp[a, b, c]

[a] Christian-Albrechts-Universität zu Kiel, Institute for General Microbiology, Kiel, Germany
[b] Christian-Albrechts-Universität zu Kiel, Central Microscopy Facility, Kiel, Germany
[c] Ludwig-Maximilians-Universität München, Fakultät Biologie, Planegg-Martinsried, Germany

Abstract

The mycomembrane (MM) is a mycolic acid layer covering the surface of Mycobacteria and related species. This group includes important pathogens such as *Mycobacterium tuberculosis*, *Corynebacterium diphtheriae*, but also the biotechnologically important strain *Corynebacterium glutamicum*. Biosynthesis of the MM is an attractive target for antibiotic intervention. The first line anti-tuberculosis drug ethambutol (EMB) and the new drug candidate, benzothiazinone 043 (BTZ) interfere with the synthesis of the arabinogalactan (AG), which is a structural scaffold for covalently attached mycolic acids that form the inner leaflet of the MM. We previously showed that *C. glutamicum* cells treated with a sublethal concentration of EMB lose the integrity of the MM. In this study we examined the effects of BTZ on the cell envelope. Our work shows that BTZ efficiently blocks the apical growth machinery, however effects in combinatorial treatment with β-lactam antibiotics are only additive, not synergistic. Transmission electron microscopy (TEM) analysis revealed a distinct middle layer in the septum of control cells considered to be the inner leaflet of the MM covalently attached to the AG. This layer was not detectable in the septa of BTZ or EMB treated cells. In addition, we observed that EMB treated cells have a thicker and less electron dense peptidoglycan (PG). While EMB and BTZ both effectively block elongation growth, BTZ also strongly reduces septal cell wall synthesis, slowing down growth effectively. This renders BTZ treated cells likely more tolerant to antibiotics that act on growing bacteria.

2.5 Single-cell growth inference of *C. glutamicum* reveals asymptotically linear growth

Single-cell growth inference of *Corynebacterium glutamicum* reveals asymptotically linear growth

Joris J.B. Messelink[a*], **Fabian Meyer**[b,c*], Marc Bramkamp[b,c], Chase P. Broedersz[a,d]

[*] equal contribution

[a] Ludwig-Maximilians-Universität München, Arnold-Sommerfeld-Center for Theoretical Physics, Munich, Germany

[b] Ludwig-Maximilians-Universität München, Fakultät Biologie, Planegg-Martinsried, Germany

[c] Christian-Albrechts-Universität zu Kiel, Institute for General Microbiology, Kiel, Germany

[d] Vrije Universiteit Amsterdam, Department of Physics and Astronomy, Amsterdam, Netherlands

Abstract

Regulation of growth and cell size is crucial for the optimization of bacterial cellular function. So far, single bacterial cells have been found to grow predominantly exponentially, which implies the need for tight regulation to maintain cell size homeostasis. Here, we characterize the growth behavior of the apically growing bacterium Corynebacterium glutamicum using a novel broadly applicable inference method for single-cell growth dynamics. Using this approach, we find that *C. glutamicum* exhibits asymptotically linear single-cell growth. To explain this growth mode, we model elongation as being rate-limited by the apical growth mechanism. Our model accurately reproduces the inferred cell growth dynamics and is validated with elongation measurements on a transglycosylase deficient *ΔrodA* mutant. Finally, with simulations we show that the distribution of cell lengths is narrower for linear than exponential growth, suggesting that this asymptotically linear growth mode can act as a substitute for tight division length and division symmetry regulation.

3. Discussion

3.1 Cell cycle and chromosome organization in *C. glutamicum*

3.1.1 Diploidy and multi-fork replication

First ideas for the description of a prokaryotic cell cycle were motivated by experimental data obtained from *Escherichia coli* and *Salmonella typhimurium* (Cooper & Helmstetter, 1968; Schaechter et al., 1958). For the derived model, two essential features of the prokaryotic lifecycle, namely the cell division and DNA replication, define a reference in their sequential succession. However, only few different model species were analyzed regarding their specific cell cycles. Reports on mero-oligoploid, fast growing *E. coli* or *B. subtilis* cells account for multi-fork replication, and thus for overlapping rounds of DNA replication (Fritsch & Worcel, 1971; Pecoraro et al., 2011). In contrast, for slow growing species, like *Mycobacterium smegmatis,* initiation of replication is reported to occur only once between birth and division (Santi et al., 2013). The modern view on the bacterial cell cycle is more differentiated. Variations of the cell cycle between species are becoming obvious. Besides the intrinsic factors, like the cell morphology or chromosome organization, also the context of extrinsic factors like temperature or nutrient conditions determine the appearance of the cell cycle.

The actinobacterium *C. glutamicum* has emerged as model organism for bacterial cell biology in recent years. It shows morphological characteristics that are only in part comparable to *E. coli* or *B. subtilis*. Here, open questions about the specific cell cycle of *C. glutamicum* were experimentally addressed (Böhm et al., 2017). The previously reported influence of nutrient conditions on the DNA content already suggested an over-initiation of replication also for *C. glutamicum* (Neumeyer et al., 2013). To examine further details of this effect, we used the localization of ParB-eYFP relative to the cell length as a proxy for ongoing DNA replication and segregation (Böhm et al., 2017). As part of the ParABS DNA segregation system, ParB binds to *parS* sequences that are located in close proximity to the origin of replication (*oriC*) (Autret et al., 2001; Böhm et al., 2020; H. J. Kim et al., 2000). The systematic analysis and visualization of data from dozens of fluorescence micrographs unveiled an unexpected pattern for the dynamics of ParB-eYFP. The created demograph showed two initial polar foci for shorter cells. For

longer cells these foci split up, while one copy stays at the pole and the other gets translocated towards the center, until a distance that allows for cell septation in-between (Böhm et al., 2017). This appears in contrast to previously reported observations made on the ParB orthologue ParB1 in *Vibrio cholerae* (Fogel & Waldor, 2006). As reported there, the cell cycle stats with just a single focus of YFP-ParB1 at the old cell pole. Analogous to the mechanism that was observed in *C. glutamicum*, the focus splits, while one part stays in place, but in *V. cholerae* the other gets translocated along the whole distance to the opposite cell pole (Fogel & Waldor, 2006). Until the finding presented here, a similar mechanism was also assumed for *C. glutamicum* (Lutkenhaus, 2012; Neumeyer et al., 2013). The obtained results surprisingly suggest a diploid chromosome organization with one chromosome attached to each cell pole.

Further experiments showed that even growth in minimal medium resulted in a minimum of two chromosome copies per cell (Böhm et al., 2017). The previously suggested over-initiation of DNA replication under rich medium conditions was confirmed microscopically, by flow cytometry, and by the use of marker frequency analysis of *oriC* and terminus (*ter*) regions (Böhm et al., 2017; Neumeyer et al., 2013). Given the diploid setup, it is still not entirely clear if both chromosomes synchronize the initiation (Böhm et al., 2017). In literature, multi-fork replication is associated with a gene/dose effect. In this context, the arrangement of certain important genes in proximity to the *oriC* plays an important role (Slager et al., 2014). For *C. glutamicum,* the region clockwise from the *oriC* starts with genes coding for the replisome, like *dnaA* (*cg0001*) or *gyrB* (*cg0007*), while on the other direction genes for *parA* / *parB* (*cg3427* / *cg3426*) or the lipid II flippase *murJ* (*cg3419*) are found. This arrangement appears to favor the fast-growing state, since the first genes that occur in multiple copies are coding for proteins that control DNA replication and segregation, and for cell elongation.

The observed diploidy occurs in a sharp contrast to recent reports about the spatial organization of the taxonomically related *M. smegmatis* (Santi & McKinney, 2015). Here, the detailed characterization of the replication machinery clearly demonstrated the processing of a single, central chromatid (Santi et al., 2013; Trojanowski et al., 2015). Despite sharing a variety of structural features, *C. glutamicum* and *M. smegmatis* are

distinct genera, and thus the observed variance of DNA organization is plausible. Actinobacteria generally dwell in a broad variety of environments (Chandra & Chater, 2014; Lewin et al., 2016).

C. glutamicum was isolated from the soil (Kinoshita, Nakayama, & Akita, 1958). As a habitat, soil potentially bears various stress conditions like desiccation, radiation, or nutrient depletion. The evolutionary pressure might have consequently selected for the observed stable diploid chromosome configuration. This diploidy appears distinct to the temporal multiploidy that occurs from over-initiation, that was observed in addition (Böhm et al., 2017; Pecoraro et al., 2011; Soppa, 2014).

Current hypotheses claim that most bacterial species are in fact oligo or polyploid (Pecoraro et al., 2011). Additional copies of the genome potentially serve as template for DNA repair and are related to a better resilience towards double strand breaks (Soppa, 2014). Further advantages of multiploidy are assigned to a gene/dose effect on expression-levels and a better stability of regulatory networks (Soppa, 2014). The faster generation time of *C. glutamicum*, compared to the slower growing *M. smegmatis*, in parts, might be attributed to higher level of protein expression due to a second copy of the genome (Böhm et al., 2017).

The evolution of the ancient phylum *Actinobacteria* dates back prior to the oxygenation of the atmosphere, about 2.3 billion years ago (Battistuzzi et al., 2004). From phylogenetic analyses, a first divergence from *Firmicutes* was dated back about 3 bn years ago, while 2.7 billion years ago, *Cyanobacteria* and *Actinobacteria* developed from the common ancestor (Battistuzzi et al., 2004). The first *Actinobacteria* were likely cocci or rods and obligate anaerobic (Chandra & Chater, 2014). About 1.4 billion years ago *Corynebacteriales* differentiated from *Streptomyces,* and about 900 million years ago, the distinct genera *Corynebacterium* and *Mycobacterium* emerged (Battistuzzi et al., 2004; Gao & Gupta, 2012).

Despite the missing MM, *Streptomyces* spp. share the mode of DivIVA-regulated apical growth with the two *Corynebacteriales. Streptomyces* spp. have evolved to grow as branching hyphae. A new branch is usually initiated by the prior accumulation of phosphorylated DivIVA that recruits the respective elongasome proteins. In contrast to *Corynebacteriales, Streptomyces* spp. possess a functional orthologue of MreB. The

corresponding gene product plays an important role during sporulation, but not for elongation growth (Mazza et al., 2006). Likely, the respective sequence remained conserved from the common ancestor with *Firmicutes*, since horizontal gene transfer is reported as a rare event for *Streptomyces* spp. (Lewin et al., 2016).

All *Actinobacteria* rely on the ParABS system for the correct distribution of the DNA to their progeny (Chandra & Chater, 2014). However, for *S. coelicolor* A3(2), the detailed process is described as an adaptation to the hyphal morphology and thereby grants spore formation. In contrast to *C. glutamicum* or *M. smegmatis*, the genome of *S. coelicolor* is linear but not circular (H. J. Kim et al., 2000). The spores emerge from multi-genomic aerial hyphae. Coordinated by ParA and the polarity protein Scy, the elongation growth of the aerial hyphae stops, and sporulation gets initiated. Tens of genomic copies get equidistantly arranged in prespore compartments and finally are released synchronously as separate, mono-genomic mature spores (Ditkowski et al., 2013; H. J. Kim et al., 2000).

The common apical mechanism for cell elongation of most *Actinobacteria*, except cocci, bears interesting morphologic features. Conceptually, a branched phenotype is difficult to realize with cells that elongate from the side wall. Also, the three described variants of DNA organization, cell-pole associated diploidy in *C. glutamicum*, a singe central chromosome in *Mycobacterium* spp., and multiple copies for the hyphal *Streptomyces* spp., apparently co-evolved with the apical mode of elongation (Böhm et al., 2017; H. J. Kim et al., 2000; Santi et al., 2013; Trojanowski et al., 2015). However, future experiments will show if the observed organization is also present in other *Corynebacterium* spp. (Böhm et al., 2017).

3.1.2 The influence of DNA compaction on the function of FtsK driven DNA segregation

As discussed in Section 3.1, the progression of a bacterial cell cycle is dependent on the chromosomal organization. Usually, the topology of DNA is regulated by proteins from the SMC (structural maintenance of chromosomes) family (Strunnikov & Jessberger, 1999). Recruited via ParB, SMC proteins facilitate the extrusion of DNA loops and the chromosomes get spatially compacted by the factor 10^{-3} (Kim et al., 2023; Kois et al., 2009). This stable configuration is understood to prevent replicated arms from

interlacing and thereby facilitate an ordered segregation of the DNA to the daughter cells (Brahmachari & Marko, 2019; Sullivan et al., 2010). In *B. subtilis*, the function of the SMC complex is reported to be essential for fast growth conditions (Gruber et al., 2014; X. Wang et al., 2014). Also, in *Caulobacter crescentus*, aberrations of the cell cycle were observed upon the deletion of *smc* (Jensen & Shapiro, 1999; Schwartz & Shapiro, 2011). Surprisingly, for a few species, *smc* deletion only shows a marginal effect, among them, *Staphylococcus aureus*, *M. smegmatis* and *C. glutamicum* (Böhm et al., 2020; Güthlein et al., 2008; Yu et al., 2010). To obtain a clearer view on the underlying mechanism in *C. glutamicum*, a screening for essential genes in the absence of *smc* was conducted. By using comparative Tn5 transposon mutagenesis sequencing on the wild-type and the *Δsmc* genomic background, the function of the two DNA acting proteins ParB and FtsK rendered essential for the mutant (Peng et al., 2023).

Both proteins are involved in DNA segregation. The CTPase ParB binds to chromosomal *parS* sequences close to the *oriC*, thereby forming a phase separated region that is involved in oriC segregation and SMC loading (Osorio-Valeriano et al., 2019). During replication, ParB tethers one of the replicating chromosome arms to polar patches of DivIVA, while at the same time, it facilitates the translocation of the other arm towards the division plane along a gradient of hydrolyzing ParA. During this process, the mentioned SMC complexes, loaded to the DNA via ParB, conduct the compaction.

The other protein, FtsK, is found involved in the segregation of the replicated and compacted DNA to the daughter cells and appears as a conserved part of the divisome. Hexameric complexes are considered to function as a motor for the displacement of double stranded DNA away from the closing septum. Further, FtsK is involved in the XerCD mediated resolution of the chromosome dimers at the end of replication (Aussel et al., 2002; Bigot et al., 2007).

Our results indicate that the SMC-mediated DNA topology grants an effective function of both processes, the ParB mediated DNA translocation to midcell, and its further displacement by septal FtsK complexes. For the native genotype, frequent transposon insertions were detected for both genes, but not in the absence of *smc*. A synthetic lethal combination of *smc* and *ftsK* had also been reported before, for *B. subtilis*, *E. coli* and *S. coelicolor* (Britton & Grossman, 1999; Dedrick et al., 2009;

Sivanathan et al., 2009). For *E. coli*, the deletion of *ftsK* is reported to cause severe segregation defects and DNA damage, but could be compensated by a suppressor mutation in FtsA (Aussel et al., 2002; Berezuk et al., 2020; L. Wang & Lutkenhaus, 1998). Here, a clean deletion of *ftsK* could not be obtained, therefore the synthetic lethal interaction between FtsK and SMC was confirmed by a CRISPRi depletion of FtsK in a *Δsmc* background (Peng et al., 2023).

In cells with erroneous chromosome organization due to *smc* deletion, DNA segregation under closing septa is of particular importance. Therefore, we used single particle tracking (SPT) to analyze fluorescently labeled FtsK in the absence of *smc, parB*, and both simultaneously. We found that FtsK renders less dynamic upon the deletion of *smc*, while the deletion of *parB* showed the opposite effect (Peng et al., 2023). The calculated, virtual subcellular localization of the analytes appeared more chaotic compared to the wild-type (Peng et al., 2023). As comparable SPT data on FtsK is still rare, a report on SpoIIIE from *B. subtilis* served as hint for our interpretation (El Najjar et al., 2018). There, a fast-diffusive fraction was assigned to monomeric subunits and a second slow diffusive fraction to fully assembled complexes. We assigned a third, confined fraction to forming division septa and observed an increase of the respective fraction upon *smc* deletion (Peng et al., 2023). This was interpreted as a less effective translocation of the DNA, due to its less organized topology. The depletion of *parB* led to an increase of the fast-mobile fraction from 27.9 % to 77.7% in the mutant, accounting for even more severe loss of organizational structure compared to the *smc* mutant (Peng et al., 2023). Additionally, SPT was used to analyze labeled SMC in a *ΔparB* background. In the native scenario, SMC is loaded onto the DNA via ParB. In line with the previous finding, our result shows a shift towards a higher mobility of SMC particles upon the deletion of *parB* (Peng et al., 2023).

To cover a broader range of timescales, an additional microscopic time-lapse experiment was performed on the *Δsmc* mutant. To reveal the cell cycle dependent localization of FtsK-mCherry, we used a method that was previously developed for the analysis of time-lapse micrographs (see Appendix) (Messelink et al., 2021; Peng et al., 2023). Images were taken in a 5 min interval over multiple hours. Based on an adaptation of the analysis method, the ratio between the septal dwell-time of FtsK and the duration of the

cycle was calculated for each cell. FtsK showed an increased, prolonged, and less precise septal localization for the mutant background, while the growth rate was not affected. In line with the outcome of the SPT experiments, the results show that the cells compensate the loss of DNA organization by an increased processivity of FtsK (Peng et al., 2023). By this, the cells ensure that the closing septum gets cleared from DNA to prevent the structure from guillotining.

A different aspect of the function of FtsK is connected to diploid character of *C. glutamicum* (Böhm et al., 2017). This arrangement might be regarded as a mechanism for resilience and could in parts explain why *ftsK* is not essential in wild-type cells. It opens an interesting question about the distribution of the chromatids to the daughter cells. The FtsK associated, directed translocation of double stranded DNA would theoretically allow for a displacement of each chromosome to the respective distal side of the septum. But the spatial organization potentially allows also for the maintenance of diploidy by the preservation of the chromatid on the proximal side of the septum. Until further investigation, a detailed mechanism of diploid DNA translocation in *C. glutamicum* remains elusive.

3.2 The corynebacterial cell wall as antibiotic target

Various infectious diseases are attributed to bacteria bearing a mycolic acid (myco-) membrane (MM). Diphtheria, the Hansen's disease, and in particular tuberculosis, are caused by di-derm *Coryne-* or *Mycobacteria* (Barksdale, 1970; Zuber et al., 2008). The unique cell envelope of these bacteria is an ideal target for specific antibiotics (Abrahams & Besra, 2018). Substances that selectively act on the synthesis or maintenance of this distinct structure, ideally have only a limited effect on the patient's microbiome (Grice et al., 2009; Walker & Hoyles, 2023). An example of such an antibiotic is ethambutol (EMB) (Thomas et al., 1961). For decades, it served as an established tuberculosis medication that was mainly applied in combination therapy (Sreevatsan et al., 1997). Biochemically, it is well characterized. It inhibits the polymerization of arabinose residues by the enzyme Emb and thereby interferes with the assembly of the fine structure of the arabinogalactan (AG) layer (Forbes et al., 1962). About 10 years ago, the experimental substance benzothiazinone 043 (BTZ) was reported to act on the same metabolic route, but at a more basic stage (Makarov et al., 2009). A biochemical

characterization showed the interference of BTZ with the essential epimerization of the AG building blocks, by the inhibition of the enzyme DprE1 (Crellin et al., 2011; Trefzer et al., 2012). It was suggested that an accumulation of the intermediate epimer decaprenyl-phosphoribose (DPR) drains the pool of the shuttle molecule decaprenyl phosphate (DP), and hence impairs cell growth (Grover et al., 2014). As an outcome of a distinct search for an anti-tuberculosis medication, the drug BTZ is still tested for therapeutic side effects in clinical trial (Stop TB Partnership, 2023).

In this work, *C. glutamicum* was used to study the structural and functional effects caused by both compounds, EMB and BTZ (Meyer et al., 2023; Schubert et al., 2017). We wanted to discern the effects caused by each substance and performed a comparable set of experiments. A reproducible characterization of the induced morphologic and biochemical changes was realized by using only a sublethal concentration of each substance. The detailed characterization of the wild-type as a control, stimulated reflections about the fine-structure of the cell wall and the mechanism of division.

As the most prominent difference, the comparison revealed that the integrity of the MM becomes impaired upon EMB treatment, while it remains in a confluent state after the treatment with BTZ. The confluence of the MM grants its protective function in the native state. At a late stage of division, just prior to the characteristic v-snapping, a regulated hydrolysis of the surface proximal the septum allows for an inflow of trehalose mono- and dimycolates (TMM / TDM). These function as mobile phase and outer leaflet of the MM (Zhou et al., 2019).

Our fluorescence microscopic analysis of bio-orthogonal labeled MM revealed that the treatment with EMB leads to large discontinuities at the cell poles, while the cells exhibit a lemon-shaped morphology. This contrasts the observed phenotype induced by BTZ. Here, the morphology appeared affected, but the cell poles were less pointed, and the MM showed a confluent state around the entire cell. The effect of reduced mycolic acids upon EMB treatment was also observed from thin layer chromatography (TLC) from crude cell wall extracts and was further confirmed by testing different combinations of antibiotics. In the case of EMB, the protective MM is functionally disabled and therefore allows a synergistic effect with β-lactam antibiotics. For BTZ treated cells the MM

appeared intact, and thus only an additive effect in the respective drug combination was observed (Meyer et al., 2023; Schubert et al., 2017).

The induced morphologic alterations were further characterized microscopically. For both compounds, the staining of nascent peptidoglycan (PG) synthesis unveiled inhibition of the apically located elongasome, accompanied by an accumulation of DivIVA (Meyer et al., 2023; Schubert et al., 2017). The quantitative analysis of the respective micrographs unveiled differences in the spatial organization and timing of PG synthesis. The fraction of cells with a forming septum was much higher in comparison to the control for EMB, while for BTZ, it was lower. This also explains why BTZ treated cells are wider and less pointed. Together with the obtained growth curves, the results show that cell growth is stronger affected by BTZ, although the used sublethal dose (2.3 µM) was 20x lower compared to EMB (48.9 µM). This was previously connected to the drain of the DP pool that also serves the substrates for PG synthesis in the form of lipid II (Grover et al., 2014; Trefzer et al., 2012).

Our scanning electron microscopy (SEM) analyses of the cell surface added more detail to the previous observations. The untreated control appeared even and smooth, except for the characteristic rings that occur from division. Consistent with our fluorescence microscopy results, the EMB-treated cells exhibit superficial discontinuities at the cell poles that extend as deep longitudinal furrows along the side wall. From dividing cells, it became clear that the new cell poles have a distinct surface, which was interpreted as the total absence of mycolic acids. In contrast, the BTZ-treated cells showed a more uniform surface. Smaller longitudinal cracks were seen over the entire surface, also at the cell poles. However, from dividing cells we also observed a distinct surface of the new poles for the case of BTZ.

As this result corroborated our previous results only in parts, we also analyzed ultrathin sections of the respective specimen via transmission electron microscopy (TEM). From these analyses, we recognized an altered organization of the cell wall layers that furthermore appeared distinct for the two antibiotics (Meyer et al., 2023; Schubert et al., 2017). The native state cell wall shows a distinct electron-translucent layer between the plasma membrane and the electron-opaque PG/AG complex. This periplasmatic space appeared lost upon the treatment with both drugs. We reasoned that this is the

result of the impaired apical elongation growth. The elongasome likely starts to form just after the divisome created the new polar cell wall, hence, the effect is visible in forming septa.

Both drugs interfere with the correct formation of the elongation machinery, and hence dysfunctional cell poles occur from each division. In the case BTZ, the discussed accumulation of unprocessed DPR likely explains the crowding of the periplasmic space (Grover et al., 2014). For the case of EMB, the effect is not fully understood. The affected enzyme Emb usually conducts the polymerization of the AG (Forbes et al., 1962). Likely, native structural organization of the PG/AG is essential for functional elongasome. Based on the mode of action of both drugs the observed layers likely consist of a surrogate material distinct from the fine-structured native AG.

The PG/AG-surrogate layer of EMB-treated cells was thicker and less electron dense, compared to the control. This shows in line with a previously reported inhibition of the glutamate racemase MurI, and would imply a lower degree of PG crosslinking and hence, a decreased mechanical resistance of the cells (Pawar et al., 2019). In contrast to that, the PG layer of BTZ-treated cells appeared not significantly altered in structure, while the material of unknown structure and composition that corresponds to the AG, seemed more compact and thicker compared to the control.

The mentioned differences were most prominently visible on forming division septa. In the native state, the surface proximal to the division site remains unaffected by the formation of the new poles underneath. As visible from respective micrographs, an arrangement referred to as Π- or T-junction is formed by a splicing at the inner side of the existing PG during the first steps of septum formation, while the attached AG layer on the outside stays unaffected. The invaginating mirrored structure already shows the same arrangement as the sidewall. The central electron-translucent layer was interpreted as the opposing inner leaflets of the MM that are covalently bound to the newly formed AG layer of each side (Meyer et al., 2023). Only after the regulated hydrolysis of the Π-structure, in prior to the v-snapping, the mobile phase can enter the formed septum from the outside and keep up the MM confluency for both daughter cells (Zhou et al., 2019). This characteristic Π-structure appeared lost as a result of both drugs. The altered configuration of layers spans uniformly from the septum to the sidewall. This likely goes along with a reduced mechanical resistance of the structure

corresponding to the AG, since forming septa become visible on the surface of treated cells. Consequently, the rapid v-snapping was not observed for both treatments, the cells rather move continuously apart during division.

The distinct state of the MM is likely determined by the structure of the layer underneath. According to the described function of the molecular target of EMB, affected cells would lack the consecutive bifurcation of the arabinofuranose (Ara*f*) residues in the AG (Forbes et al., 1962). The resulting, drastically reduced surface of the inner leaflet of the MM is understood to prevent the formation of a continuous double layer. In the case of BTZ, the common model assumes a complete absence of Ara*f* residues. The composition and structure of the material that is visible instead of the AG is still unclear. Since the inhibited enzyme DprE1 only blocks the epimerization of DPR to the next intermediate product, but not the prior translocation to the periplasm, the layer likely reflects an arrangement of yet uncharacterized sugars (Grover et al., 2014). From the observed densities of the PG/AG-surrogate upon BTZ treatment, we reasoned that the exhibited surface is likely continuous, but the question about a covalently bound inner leaflet remained open. The observed phenotype rather resembled to deletion mutant of *aftB*, which was described earlier for *C. glutamicum* (Raad et al., 2010). AftB usually mediates the fusion of the terminal Ara*f* residues to the maturing AG, which then get mycolated. As described, the cells still show a continuous, confluent MM despite the missing covalently attached mycolic acids. It was suggested that the MM only consisted of mobile phase elements (TMM / TDM) that arranged as a bilayer on top of the even AG surface (Raad et al., 2010). A similar scenario is also plausible for BTZ-treated cells.

In the light of emerging multi drug resistant (MDR) and extensively drug resistant (XDR) *M. tuberculosis* strains, antibiotics targeting the CMN-type cell wall gained more importance. A detailed view on the respective effects, on various scales, provides a valuable resource for clinical settings. The treatment of the tenacious lung infection caused by *M. abcessus* profited from the growing class of CMN-cell wall acting antibiotics. The species has a natural immunity against EMB, due to a polymorphism in the respective *embB* gene (Alcaide et al., 1997). A synergy test with the experimental DprE1 inhibitor OPC-167832 showed also an additive effect with a β-lactam antibiotic,

here cefoxitin (Sarathy et al., 2022). This indicates that the observed effect is likewise similar among the mycolata, as it shows consistent with our results (Meyer et al., 2023).

We have shown that the apical elongasome of *C. glutamicum* becomes functionally inactivated as the result of sublethal EMB and BTZ treatment. In the case of EMB, cells continue to grow slowly and form a defective MM, while for the case of BTZ growth was strongly inhibited, but the confluency of the MM was less affected.

3.3 Elongation growth of *C. glutamicum*

The rod-shaped cell morphology appears reasonably simple. Many of the common model species in bacteriology such as *E. coli* or *B. subtilis,* are typical rod-shaped cells. Individual cells from both species elongate along their lateral cell wall (Cabeen & Jacobs-Wagner, 2005). In contrast, a cluster of the Actinobacteria phylum, called the CMN *(Corynebacterium, Mycobacterium,* and *Nocardia*)-group, also shows the characteristic of rod-shaped cell morphology, but bears a mechanistic variant for its maintenance. Elongation growth only occurs from the cell poles, similar to the apical growth of filamentous *Streptomyces* spp. (Daniel & Errington, 2003; Flärdh, 2003; Hett & Rubin, 2008).

Over decades, the lateral mode of cell elongation has been characterized in detail. Based on fundamental considerations about the bacterial cell cycle, exponential elongation of *E. coli* and *Salmonella typhimurium* cells was postulated and later experimentally confirmed (Cooper & Helmstetter, 1968; Schaechter et al., 1958). This observed exponential cell elongation has even been proposed as a universal pattern for elongating bacterial cells during the phase of balanced growth (Cooper, 2006). In contrast to cells that elongate by cell wall synthesis on the lateral side, the development of cells with a (bi-) polar located elongasome are only poorly characterized. Here, we harnessed detailed measurements and analyses of the cell cycle of *C. glutamicum,* to test whether the proposed assumption for an exponential cell elongation holds also true for apically growing cells (Messelink et al., 2021). Therefore, a comprehensive set of individual cells obtained from growing microcolonies were geometrically characterized and further analyzed with a novel growth trajectory inference method. The resulting rate-limiting apical growth (RAG) model shows that *C. glutamicum* cells exhibits an initial increase of

the individual growth rate, followed by a leveling off towards a constant rate. We termed the observed pattern asymptotically linear growth and linked the dynamics to the maturation of the elongasome complex at the new cell pole.

For the validation of the RAG model, we also tested the growth of the transglycosylase deficient mutant *C. glutamicum ΔrodA.* The obtained results confirmed the asymptotically linear pattern of cell elongation, while the total rate of elongation was diminished compared to the wild-type.

Additionally, the data was used for a comparative simulation of exponentially- and asymptotically linear elongation growth and resulted in the description of an intrinsic mechanism for cell size homeostasis provided by saturating growth rates. From this, we reasoned that the absence of a distinct division-site selection mechanism in *C. glutamicum* is consequently explained by the apical mode of elongation (Messelink et al., 2021).

Since for exponentially elongating cells, the actual length correspondents to the rate of elongation, a strict division symmetry guarantees an equal growth rate for the daughter cells. This prevents from the formation of large, fast growing individual cells.

The predominant lateral type of cell wall synthesis, as found in *E. coli* and *B. subtilis*, is spatially regulated by MreB (Garner et al., 2011; Shi et al., 2018). This group includes ten diverse phyla, among them Protobacteria, Firmicutes, Fusobacteria, Spirochaetes, Cyanobacteria, and others (Takahashi et al., 2020). The cellular organization of the respective cell wall synthetic complexes appears as dynamic movement of parallel acting patches along the side wall (Garner et al., 2011). Mediated by the associated transglycosylases (TG) and transpeptidases (TP), single strands of nascent PG get integrated into the sidewall. This lateral mode of elongation is characterized by an exponential increase in cell length, since the growing surface allows for more MreB complexes to contribute (Zheng et al., 2016). During this process, the cell poles stay inert. Hence, division resets the turnover per cell. This mechanism ensures a stable distribution of cell sizes. In *E. coli* the regulation of division symmetry and cell size homeostasis are biochemically well characterized (Hu et al., 1999). This mechanism of homeostasis provides a characteristic cell size distribution in an exponentially growing culture. Both predictive and experimental methods, speak for a strong interdependence

between exponential elongating cells and a high degree of division symmetry (Taheri-Araghi et al., 2015; Zheng et al., 2016).

For CMN-group bacteria, the rod-shaped morphology has evolved differently. Two polar localized elongasome complexes produce nascent PG and thereby form a closed tube that expands from the tips. The subcellular organization of the poles depends on the scaffold protein DivIVA (Letek et al., 2008). Associated to that, SEDS proteins mediate the integration of building blocks. This apical mode of elongation includes the assembly of two stably anchored, mirroring elongasome complexes at the division site that consequently form the new poles (Donovan & Bramkamp, 2014; Sieger et al., 2013). In the case of *C. glutamicum*, the growth rate of single cells runs into a saturation. Due to the maturation of the new cell pole, cells are approaching a constant growth rate that is independent from the actual cell length. This mechanism also ensures that both daughter cells start with an equal growth rate, since each cell inherits a fully matured and a newly formed elongasome complex. Hence, the division symmetry is less important in cells that use the apical mode of elongation.

Aiming on a simplified and general description of the bacterial cell elongation, the so-called 'adder'-model of elongation was proposed (J. Lin & Amir, 2017). It describes a constant amount of added cell mass as a trigger for division. The model also includes the two theoretical borders, defined as the 'sizer' that describes the dependence of division on a critical cell size, and the 'timer' that defines a constant elapsed time as a trigger for division. For *E. coli*, *B. subtilis* and *Pseudomonas aeruginosa,* the analyses of time-lapse micrographs obtained with the mentioned mother-machines, confirmed the addition of a constant amount of cell mass as trigger for cell division, independent from the final size or the elapsed time (Sauls et al., 2016; Taheri-Araghi et al., 2015).

The 'adder' model for cell-size homeostasis links the metabolic activity to the actual size of the cell. The model implies an absolute (threshold) concentration of a certain metabolite as trigger for cell division, this further implies an optimal cell size. Any occurring deviations from this size, either shorter, or longer cells are adjusted in length within a few generations. With this intrinsic mechanism, cell-size homeostasis is gradually maintained (Si et al., 2019).

For *Mycobacterium smegmatis*, the classification along the criteria of the 'adder' model resulted in a theoretical hybrid of a 'timer' and an 'adder' (Willis & Huang, 2017). Here, the dependence of the 'adder' model on the morphogenic mechanism became visible. A less accurate division symmetry of the examined specimen, at a first glance, appeared as hard to interpret by the provided model. Later, this discrepancy was solved by taking the independence of both polar elongasome complexes into account and interpreted the data as a parallel adder (Logsdon et al., 2017).

Distinct from the 'adder'-approach, an atomic force characterization of the biphasic growth of *M. smegmatis* and *M. tuberculosis* provided a useful comparison since the elongation rates of single cells were measured. The concluded 'new end take off' (NETO) model describes the jumping onset of the elongation growth of the new pole after an initial inactive phase (Hannebelle et al., 2020). It appears as a consistent observation specific for *Mycobacterium* spp*.* and a rapidly doubling of growth rates by the activation of the new pole was not observed for *C. glutamicum*. Here, the growth rates gradually increase towards a static plateau (Messelink et al., 2021). This difference to the reported delay of polar maturation for *Mycobacterium* spp*.*, together with the prolonged generation time, might be associated to a gene/dose effect that is caused by the diploidy (Böhm et al., 2017). The study about the atomic force characterization of the biphasic growth of *M. smegmatis* and *M. tuberculosis* only deals with a small sample number, but a species-specific effect appears likely (Hannebelle et al., 2020). This discrepancy also shows the limits for the use of *Corynebacterium* as a model for cell growth in *Mycobacterium*.

The quality of the cell cycle model is highly dependent on the precision of the raw data. By the time the project stared, the only method for an automated analysis of time-lapse micrographs was realized for the so-called mother machine (Fig. 9) (P. Wang et al., 2010). This microfluidic device consists of parallel microtubes that roughly fit the width of *E. coli* cells. It turned out that this setup is insufficient for *C. glutamicum* cells. The characteristic v-snapping and the occasionally occurring asymmetric division led to a bias by randomly orientated cells that in few cases even clogged the chambers due to crosswise trapping. Because of this limitation, an alternative solution was developed that is based on a different microfluidic setup, which allows any orientation of the cells.

(Messelink et al., 2021). The respective processing of the time-lapse micrographs was realized by evolving the algorithm of a previously developed automated image analysis method (Schubert et al., 2017).
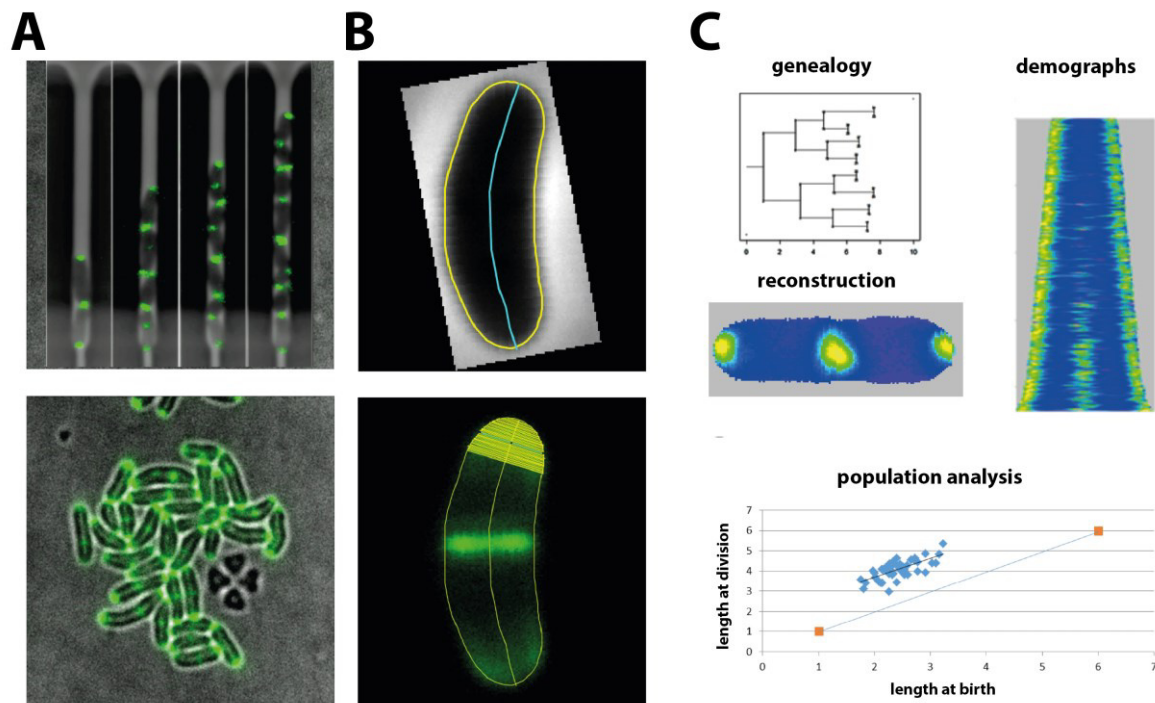

Figure 9: Computer vision of time-lapse micrographs. (A) Different microfluidic devices bear distinct advantages and disadvantages. The 'mother-machine' was developed for *E. coli* and works nicely with a provided software on this setup (A, upper panel). Due to morphological characteristics, for *C. glutamicum* the setup appeared inferior. This limitation was circumvented by the development of a novel image analysis method that uses a microfluidic setup without spatial constraints as raw data (A, lower panel). **(B)** The developed algorithm is based on the analysis of single cells, extracted from the raw image. It is able to process virtually any cell morphology and was therefore termed 'Morpholyzer'. A more detailed description of the algorithm can be found in the Appendix. **(C)** The obtained data include the genealogic context of the cells, information on fluorescence intensity and localization, and geometric features like the cell length or width. The obtained numeric data then is used for further analysis and visualization.

By adding the dimension of time and the orientation of the new pole to the dataset, the spatial development of individual cells can be consequently displayed as a list of numbers. Individual elements of the list further bear information about the genealogical context of the growing microcolony. We used the reporter strain *C. glutamicum divIVA::divIVA-mNeonGreen* as a proxy for the onset, duration, and position of cell division was included to the dataset of each cell (Messelink et al., 2021). From earlier experiments, we learned that DivIVA localizes to the forming division plane just before the synthesis of nascent PG becomes visible (Schubert et al., 2017). In the used time-lapse setup, this enabled measurements of the individual timing of division and the

positioning relative to the new pole. This numeric set resulted in a precise measurement of complex optical raw-data and served as base for the development of the reported single-cell growth inference method. Through an initial binning of the data according to the measured lengths at birth, the developed model accounts for the occasional asymmetry that naturally occurs for *C. glutamicum*. Thus, the limitations of models developed under the premise of strict division symmetry, as it is the case for *E. coli* and *B. subtilis,* were compensated (J. F. Collins & Richmond, 1962; Messelink et al., 2021; Taheri-Araghi et al., 2015).

Our results suggest that the proposed universal pattern of exponential bacterial elongation is limited to only certain species (Cooper, 2006; Messelink et al., 2021). It was further suggested that observed linear components of single cell growth are explained by experimental bias (Cooper, 2006). In contrast to that, our results suggest that the dynamics of bacterial cell elongation is strongly dependent on the molecular arrangement of growth zones and a general approach for bacteria is not trivial (Messelink et al., 2021).

References

Abe, S., Takayama, K. I., & Kinoshita, S. (1967). Taxonomical studies on glutamic acid-producing bacteria. *The Journal of General and Applied Microbiology*, *13*(3), 279–301. https://doi.org/10.2323/jgam.13.279

Abrahams, K. A., & Besra, G. S. (2018). Mycobacterial cell wall biosynthesis: A multifaceted antibiotic target. In *Parasitology* (Vol. 145, Issue 2, pp. 116–133). Cambridge University Press. https://doi.org/10.1017/S0031182016002377

Alcaide, F., Pfyffer, G. E., & Telenti, A. (1997). Role of *embB* in natural and acquired resistance to ethambutol in mycobacteria. *Antimicrobial Agents and Chemotherapy*, *41*(10), 2270–2273. https://doi.org/10.1128/aac.41.10.2270

Alderwick, L. J., James Harrison, Lloyd, G. S., & Birch, H. L. (2015). The mycobacterial cell wall—peptidoglycan and arabinogalactan. *Cold Spring Harbor Perspectives in Medicine*, *5*(8), a021113. https://doi.org/10.1101/cshperspect.a021113

Alderwick, L. J., Radmacher, E., Seidel, M., Gande, R., Hitchen, P. G., Morris, H. R., Dell, A., Sahm, H., Eggeling, L., & Besra, G. S. (2005). Deletion of *Cg-emb* in *Corynebacterianeae* leads to a novel truncated cell wall arabinogalactan, whereas inactivation of *Cg-ubiA* results in an arabinan-deficient mutant with a cell wall galactan core. *Journal of Biological Chemistry*, *280*, 32362–32371. https://doi.org/10.1074/jbc.M506339200

Alderwick, L. J., Seidel, M., Sahm, H., Besra, G. S., & Eggeling, L. (2006). Identification of a novel arabinofuranosyltransferase (AftA) involved in cell wall arabinan biosynthesis in *Mycobacterium tuberculosis*. *Journal of Biological Chemistry*, *281*, 15653–15661. https://doi.org/10.1074/jbc.M600045200

Aldridge, B. B., Fernandez-Suarez, M., Heller, D., Ambravaneswaran, V., Irimia, D., Toner, M., & Fortune, S. M. (2012). Asymmetry and aging of mycobacterial cells lead to variable growth and antibiotic susceptibility. *Science*, *335*(December), 100–104. https://doi.org/10.1126/science.1216166

Alliedmarketresearch. (2023). https://www.xn--alliedmarketresearch-o0a.xn--com-bfa/glutamic-acid-market-A15523; Access: 23.07.2023

Amir, A. (2014). Cell size regulation in bacteria. *Physical Review Letters*, *112*(20), 1–5. https://doi.org/10.1103/PhysRevLett.112.208102

Amir, A. (2017). Is cell size a spandrel? *ELife*, *6*, 1–8. https://doi.org/10.7554/eLife.22186

Aussel, L., Barre, F. X., Aroyo, M., Stasiak, A., Stasiak, A. Z., & Sherratt, D. (2002). FtsK is a DNA motor protein that activates chromosome dimer resolution by switching the catalytic state of the XerC and XerD recombinases. *Cell*, *108*(2), 195–205. https://doi.org/10.1016/S0092-8674(02)00624-4

Autret, S., Nair, R., & Errington, J. (2001). Genetic analysis of the chromosome segregation protein Spo0j of *Bacillus subtilis*: Evidence for separate domains involved in DNA binding and interactions with Soj protein. *Molecular Microbiology*, *41*(3), 743–755. https://doi.org/10.1046/j.1365-2958.2001.02551.x

Bakkes, P. J., Ramp, P., Bida, A., Dohmen-Olma, D., Bott, M., & Freudl, R. (2020). Improved *pEKEx2*-derived expression vectors for tightly controlled production of recombinant proteins in *Corynebacterium glutamicum*. *Plasmid*, *112*, 102540. https://doi.org/10.1016/j.plasmid.2020.102540

Barksdale, L. (1970). *Corynebacterium diphtheriae* and its relatives. *Bacteriological Reviews*, *34*(4), 378–422.

Barreteau, H., Kovač, A., Boniface, A., Sova, M., Gobec, S., & Blanot, D. (2008). Cytoplasmic steps of peptidoglycan biosynthesis. *FEMS Microbiology Reviews*, *32*(2), 168–207. https://doi.org/10.1111/j.1574-6976.2008.00104.x

Barry, C. E., Lee, R. E., Mdluli, K., Sampson, A. E., Schroeder, B. G., Slayden, R. A., & Yuan, Y. (1998). Mycolic acids: Structure, biosynthesis and physiological functions. *Progress in Lipid Research*, *37*(2–3), 143–179. https://doi.org/10.1016/S0163-7827(98)00008-3

Batt, S. M., Jabeen, T., Mishra, A. K., Veerapen, N., Krumbach, K., Eggeling, L., Besra, G. S., & Fütterer, K. (2010). Acceptor substrate discrimination in phosphatidyl-myo-inositol mannoside synthesis: Structural and mutational analysis of mannosyltransferase *Corynebacterium glutami*cum PimB'. *Journal of Biological Chemistry*, *285*(48), 37741–37752. https://doi.org/10.1074/jbc.M110.165407

Battistuzzi, F. U., Feijao, A., & Hedges, S. B. (2004). A genomic timescale of prokaryote evolution: Insights into the origin of methanogenesis, phototrophy, and the colonization of land. *BMC Evolutionary Biology*, *4*, 1–14. https://doi.org/10.1186/1471-2148-4-44

Baumgart, M., Schubert, K., Bramkamp, M., & Frunzke, J. (2016). Impact of LytRCpsA-Psr proteins on cell wall biosynthesis in *Corynebacterium glutamicum*. *Journal of Bacteriology*, *198*(22), 3045–3059. https://doi.org/10.1128/JB.00406-16

Bechelli, L. M., & Guinto, R. S. (1970). Some recent laboratory findings on *Mycobacterium leprae*. Implications for the therapy, epidemiology and control of leprosy. *Bulletin of the World Health Organization*, *43*(4), 559–569.

Belanger, A. E., Besra, G. S., Ford, M. E., Mikušová, K., Belisle, J. T., Brennan, P. J., & Inamine, J. M. (1996). The *embAB* genes of *Mycobacterium avium* encode an arabinosyl transferase involved in cell wall arabinan biosynthesis that is the target for the antimycobacterial drug ethambutol. *Proceedings of the National Academy of Sciences of the United States of America*, *93*(21), 11919–11924. https://doi.org/10.1073/pnas.93.21.11919

Belánová, M., Dianišková, P., Brennan, P. J., Completo, G. C., Rose, N. L., Lowary, T. L., & Mikušova, K. (2008). Galactosyl transferases in mycobacterial cell wall synthesis. *Journal of Bacteriology*, *190*(3), 1141–1145. https://doi.org/10.1128/JB.01326-07

Berezuk, A. M., Roach, E. J., Seidel, L., Lo, R. Y., & Khursigara, C. M. (2020). FtsA G50E mutant suppresses the essential requirement for ftsk during bacterial cell division in *Escherichia coli*. *Canadian Journal of Microbiology*, *66*(4), 313–327. https://doi.org/10.1139/cjm-2019-0493

Bigot, S., Sivanathan, V., Possoz, C., Barre, F. X., & Cornet, F. (2007). FtsK, a literate chromosome segregation machine. *Molecular Microbiology*, *64*(6), 1434–1441. https://doi.org/10.1111/j.1365-2958.2007.05755.x

Birch, H. L., Alderwick, L. J., Bhatt, A., Rittmann, D., Krumbach, K., Singh, A., Bai, Y., Lowary, T. L., Eggeling, L., & Besra, G. S. (2008). Biosynthesis of mycobacterial arabinogalactan: Identification of a novel α(1→3) arabinofuranosyltransferase. *Molecular Microbiology*, *69*(5), 1191–1206. https://doi.org/10.1111/j.1365-2958.2008.06354.x

References

Birch, H. L., Alderwick, L. J., Rittmann, D., Krumbach, K., Etterich, H., Grzegorzewicz, A., McNeil, M. R., Eggeling, L., & Besra, G. S. (2009). Identification of a terminal rhamnopyranosyltransferase (RptA) involved in *Corynebacterium glutamicum* cell wall biosynthesis. *Journal of Bacteriology*, *191*(15), 4879–4887. https://doi.org/10.1128/JB.00296-09

Bisson-Filho, A. W., Hsu, Y. P., Squyres, G. R., Kuru, E., Wu, F., Jukes, C., Sun, Y., Dekker, C., Holden, S., VanNieuwenhze, M. S., Brun, Y. V., & Garner, E. C. (2017). Treadmilling by FtsZ filaments drives peptidoglycan synthesis and bacterial cell division. *Science*, *355*(6326), 739–743. https://doi.org/10.1126/science.aak9973

Böhm, K., Giacomelli, G., Schmidt, A., Imhof, A., Koszul, R., Marbouty, M., & Bramkamp, M. (2020). Chromosome organization by a conserved condensin-ParB system in the actinobacterium *Corynebacterium glutamicum*. *Nature Communications*, *11*(1), 1–17. https://doi.org/10.1038/s41467-020-15238-4

Böhm, K., Meyer, F., Rhomberg, A., Kalinowski, J., Donovan, C., & Bramkampa, M. (2017). Novel chromosome organization pattern in Actinomycetales-overlapping replication cycles combined with diploidy. *MBio*, *8*(3), 1–18. https://doi.org/10.1128/mBio.00511-17

Bolla, J. R., Sauer, J. B., Wu, D., Mehmood, S., Allison, T. M., & Robinson, C. V. (2018). Direct observation of the influence of cardiolipin and antibiotics on lipid II binding to MurJ. *Nature Chemistry*, *10*(3), 363–371. https://doi.org/10.1038/nchem.2919

Brahmachari, S., & Marko, J. F. (2019). Chromosome disentanglement driven via optimal compaction of loop-extruded brush structures. *Proceedings of the National Academy of Sciences of the United States of America*, *116*(50), 24956–24965. https://doi.org/10.1073/pnas.1906355116

Bramhill, D., & Kornberg, A. (1988). A model for initiation at origins of DNA replication. *Cell*, *54*(7), 915–918. https://doi.org/10.1016/0092-8674(88)90102-X

Bramkamp, M., Emmins, R., Weston, L., Donovan, C., Daniel, R. A., & Errington, J. (2008). A novel component of the division-site selection system of *Bacillus subtilis* and a new mode of action for the division inhibitor MinCD. *Molecular Microbiology*, *70*(6), 1556–1569. https://doi.org/10.1111/j.1365-2958.2008.06501.x

Brecik, M., Centárová, I., Mukherjee, R., Kolly, G. S., Huszár, S., Bobovská, A., Kilacsková, E., Mokošová, V., Svetlíková, Z., Šarkan, M., Neres, J., Korduláková, J., Cole, S. T., & Mikušová, K. (2015). DprE1 is a vulnerable tuberculosis drug target due to its cell wall localization. *ACS Chemical Biology*, *10*(7), 1631–1636. https://doi.org/10.1021/acschembio.5b00237

Britton, R. A., & Grossman, A. D. (1999). Synthetic lethal phenotypes caused by mutations affecting chromosome partitioning in *Bacillus subtilis*. *Journal of Bacteriology*, *181*(18), 5860–5864. https://doi.org/10.1128/jb.181.18.5860-5864.1999

Busche, T., Šilar, R., Pičmanová, M., Pátek, M., & Kalinowski, J. (2012). Transcriptional regulation of the operon encoding stress-responsive ECF sigma factor SigH and its anti-sigma factor RshA, and control of its regulatory network in *Corynebacterium glutamicum*. *BMC Genomics*, *13*(1), 1–19. https://doi.org/10.1186/1471-2164-13-445

Butler, E. K., Davis, R. M., Bari, V., Nicholson, P. A., & Ruiz, N. (2013). Structure-function analysis of MurJ reveals a solvent-exposed cavity containing residues essential for peptidoglycan biogenesis in *Escherichia coli*. *Journal of Bacteriology*, *195*(20), 4639–4649. https://doi.org/10.1128/JB.00731-13

Cabeen, M. T., & Jacobs-Wagner, C. (2005). Bacterial cell shape. *Nature Reviews Microbiology*, *3*(8), 601–610. https://doi.org/10.1038/nrmicro1205

Campos, M., Surovtsev, I. V., Kato, S., Paintdakhi, A., Beltran, B., Ebmeier, S. E., & Jacobs-Wagner, C. (2014). A constant size extension drives bacterial cell size homeostasis. *Cell*, *159*(6), 1433–1446. https://doi.org/10.1016/j.cell.2014.11.022

Cha, J. H., & Stewart, G. C. (1997). The *divIVA* minicell locus of *Bacillus subtilis*. *Journal of Bacteriology*, *179*(5), 1671–1683. https://doi.org/10.1128/jb.179.5.1671-1683.1997

Chandra, G., & Chater, K. F. (2014). Developmental biology of *Streptomyces* from the perspective of 100 actinobacterial genome sequences. *FEMS Microbiology Reviews*, *38*(3), 345–379. https://doi.org/10.1111/1574-6976.12047

Cho, J. S., Choi, K. R., Prabowo, C. P. S., Shin, J. H., Yang, D., Jang, J., & Lee, S. Y. (2017). CRISPR/Cas9-coupled recombineering for metabolic engineering of *Corynebacterium glutamicum*. *Metabolic Engineering*, *42*, 157–167. https://doi.org/10.1016/j.ymben.2017.06.010

Claus, G. W., & Roth, L. E. (1964). Fine structure of the Gram-negative bacterium *Acetobacter suboxydans*. *The Journal of Cell Biology*, *20*(44), 217–233. https://doi.org/10.1083/jcb.20.2.217

Cleto, S., Jensen, J. V. K., Wendisch, V. F., & Lu, T. K. (2016). *Corynebacterium glutamicum* metabolic engineering with CRISPR interference (CRISPRi). *ACS Synthetic Biology*, *5*(5), 375–385. https://doi.org/10.1021/acssynbio.5b00216

Collins, J. F., & Richmond, M. H. (1962). Rate of growth of *Bacillus cereus* between divisions. *Journal of General Microbiology*, *28*(1), 15–33. https://doi.org/10.1099/00221287-28-1-15

Collins, M. D., Goodfellow, M., & Minnikin, D. E. (1982). A survey of the structures of mycolic acids in *Corynebacterium* and related taxa. *Journal of General Microbiology*, *128*(1), 129–149. https://doi.org/10.1099/00221287-128-1-129

Cooper, S. (2006). Distinguishing between linear and exponential cell growth during the division cycle: Single-cell studies, cell-culture studies, and the object of cell-cycle research. *Theoretical Biology and Medical Modelling*, *3*(1), 10. https://doi.org/10.1186/1742-4682-3-10

Cooper, S., & Helmstetter, C. (1968). Chromosome replication and the division cycle of *Escherichia coli* B/r. *Journal of Molecular Biology*, *31*, 519–540.

Coyle, M. B., & Lipsky, B. A. (1990). Coryneform bacteria in infectious diseases: Clinical and laboratory aspects. *Clinical Microbiology Reviews*, *3*(3), 227–246. https://doi.org/10.1128/CMR.3.3.227

Crellin, P. K., Brammananth, R., & Coppel, R. L. (2011). Decaprenylphosphoryl-β-D-Ribose 2'-epimerase, the target of benzothiazinones and dinitrobenzamides, is an essential enzyme in *Mycobacterium smegmatis*. *PLoS ONE*, *6*(2). https://doi.org/10.1371/journal.pone.0016869

Crick, D. C., Mahapatra, S., & Brennan, P. J. (2001). Biosynthesis of the arabinogalactan-peptidoglycan complex of *Mycobacterium tuberculosis*. *Glycobiology*, *11*(9), 107R-118R. https://doi.org/10.1093/glycob/11.9.107R

Cummins, C. S., & Harris, H. (1958). Studies on the Cell-Wall Composition and Taxonomy of *Actinomycetales* and Related Groups. *Microbiology*, *18*(1), 173–189.

Daffé, M. (2005). The cell envelope of *Corynebacteria*. In L. Eggeling & M. Bott (Eds.), *Handbook of Corynebacterium glutamicum* (pp. 121–148). CRC Press.

Daffe, M., Brennan, P. J., & McNeil, M. (1990). Predominant structural features of the cell wall arabinogalactan of *Mycobacterium tuberculosis* as revealed through characterization of oligoglycosyl alditol fragments by gas chromatography/mass spectrometry and by 1H and 13C NMR analyses. *Journal of Biological Chemistry*, *265*(12), 6734–6743. https://doi.org/10.1016/s0021-9258(19)39211-7

Danhaive, P., Hoet, P., & Cocito, C. (1982). Base compositions and homologies of deoxyribonucleic acids of *Corynebacteria* isolated from human leprosy lesions and related microorganisms. *International Journal of Systematic Bacteriology*, *32*(1), 70–76. https://doi.org/10.1099/00207713-32-1-70

Daniel, R. A., & Errington, J. (2003). Control of cell morphogenesis in bacteria: Two distinct ways to make a rod-shaped cell. *Cell*, *113*, 767–776. https://doi.org/10.1016/S0092-8674(03)00421-5

Datta, P., Dasgupta, A., Bhakta, S., & Basu, J. (2002). Interaction between FtsZ and FtsW of *Mycobacterium tuberculosis*. *Journal of Biological Chemistry*, *277*(28), 24983–24987. https://doi.org/10.1074/jbc.M203847200

De Boer, P., Crossley, R. E., & Rothfield, L. I. (1992). Roles of MinC and MinD in the site-specific septation block mediated by the MinCDE system of *Escherichia coli*. *Journal of Bacteriology*, *174*(1), 63–70. https://doi.org/10.1128/jb.174.1.63-70.1992

De Sousa-D'Auria, C., Kacem, R., Puech, V., Tropis, M., Leblon, G., Houssin, C., & Daffé, M. (2003). New insights into the biogenesis of the cell envelope of *Corynebacteria*: Identification and functional characterization of five new mycoloyltransferase genes in *Corynebacterium glutamicum*. *FEMS Microbiology Letters*, *224*, 35–44. https://doi.org/10.1016/S0378-1097(03)00396-3

Dedrick, R. M., Wildschutte, H., & McCormick, J. R. (2009). Genetic interactions of smc, ftsK, and parB genes in Streptomyces coelicolor and their developmental genome segregation phenotypes. *Journal of Bacteriology*, *91*(1), 320–332. https://doi.org/10.1128/JB.00858-08

Den Blaauwen, T., De Pedro, M. A., Nguyen-Distèche, M., & Ayala, J. A. (2008). Morphogenesis of rod-shaped sacculi. *FEMS Microbiology Reviews*, *32*(2), 321–344. https://doi.org/10.1111/j.1574-6976.2007.00090.x

Ditkowski, B., Holmes, N., Rydzak, J., Donczew, M., Bezulska, M., Ginda, K., Kędzierski, P., Zakrzewska-Czerwińska, J., Kelemen, G. H., & Jakimowicz, D. (2013). Dynamic interplay of ParA with the polarity protein, Scy, coordinates the growth with chromosome segregation in *Streptomyces coelicolor*. *Open Biology*, *3*(MAR). https://doi.org/10.1098/rsob.130006

Donovan, C., & Bramkamp, M. (2014). Cell division in *Corynebacterineae*. *Frontiers in Microbiology*, *5*(APR), 132. https://doi.org/10.3389/fmicb.2014.00132

Donovan, C., Schauss, A., Krämer, R., & Bramkamp, M. (2013). Chromosome Segregation Impacts on Cell Growth and Division Site Selection in *Corynebacterium glutamicum*. *PLoS ONE*, *8*(2). https://doi.org/10.1371/journal.pone.0055078

Donovan, C., Schwaiger, A., Krämer, R., & Bramkamp, M. (2010). Subcellular localization and characterization of the ParAB system from *Corynebacterium glutamicum*. *Journal of Bacteriology*, *192*(13), 3441–3451. https://doi.org/10.1128/JB.00214-10

Dostálová, H., Busche, T., Holátko, J., Ruцká, L., Štěpánek, V., Barvík, I., Nešvera, J., Kalinowski, J., & Pátek, M. (2019). Overlap of promoter recognition specificity of stress response sigma factors SigD and SigH in *Corynebacterium glutamicum* ATCC 13032. *Frontiers in Microbiology*, *10*(JAN), 1–17. https://doi.org/10.3389/fmicb.2018.03287

Dover, L. G., Cerdeño-Tárraga, A. M., Pallen, M. J., Parkhill, J., & Besra, G. S. (2004). Comparative cell wall core biosynthesis in the mycolated pathogens, *Mycobacterium tuberculosis* and *Corynebacterium diphtheriae*. *FEMS Microbiology Reviews*, *28*(2), 225–250. https://doi.org/10.1016/j.femsre.2003.10.001

Edwards, D. H., & Errington, J. (1997). The Bacillus subtilis DivIVA protein targets to the division septum and controls the site specificity of cell division. *Molecular Microbiology*, *24*(5), 905–915. https://doi.org/10.1046/j.1365-2958.1997.3811764.x

Ehira, S., Shirai, T., Teramoto, H., Inui, M., & Yukawa, H. (2008). Group 2 sigma factor *sigB* of *Corynebacterium glutamicum* positively regulates glucose metabolism under conditions of oxygen deprivation. *Applied and Environmental Microbiology*, *74*(16), 5146–5152. https://doi.org/10.1128/AEM.00944-08

El Najjar, N., El Andari, J., Kaimer, C., Fritz, G., Rösch, T. C., & Graumann, P. L. (2018). Singlemolecule tracking of DNA translocases in *Bacillus subtilis* reveals strikingly different dynamics of SftA, SpoIIIE, and FtsA. *Applied and Environmental Microbiology*, *84*(8), 1–16. https://doi.org/10.1128/AEM.02610-17

Emami, K., Guyet, A., Kawai, Y., Devi, J., Wu, L. J., Allenby, N., Daniel, R. A., & Errington, J. (2017). RodA as the missing glycosyltransferase in *Bacillus subtilis* and antibiotic discovery for the peptidoglycan polymerase pathway. *Nature Microbiology*, *2*(3), 16253. https://doi.org/10.1038/nmicrobiol.2016.253

Engels, S., Ludwig, C., Schweitzer, J. E., Mack, C., Bott, M., & Schaffer, S. (2005). The transcriptional activator ClgR controls transcription of genes involved in proteolysis and DNA repair in *Corynebacterium glutamicum*. *Molecular Microbiology*, *57*(2), 576–591. https://doi.org/10.1111/j.1365-2958.2005.04710.x

Engels, S., Schweitzer, J. E., Ludwig, C., Bott, M., & Schaffer, S. (2004). clpC and clpP1P2 gene expression in *Corynebacterium glutamicum* is controlled by a regulatory network involving the transcriptional regulators ClgR and HspR as well as the ECF sigma factor σH. *Molecular Microbiology*, *52*(1), 285–302. https://doi.org/10.1111/j.1365-2958.2003.03979.x

Engels, V., Lindner, S. N., & Wendisch, V. F. (2008). The global repressor SugR controls expression of genes of glycolysis and of the L-lactate dehydrogenase LdhA in *Corynebacterium glutamicum*. *Journal of Bacteriology*, *190*(24), 8033–8044. https://doi.org/10.1128/JB.00705-08

Erickson, H. P. (1997). FtsZ, a tubulin homologue in prokaryote cell division. In *Trends in Cell Biology* (Vol. 7, Issue 9, pp. 362–367). Elsevier Current Trends. https://doi.org/10.1016/S0962-8924(97)01108-2

Fang, F. C. (2005). Sigma cascades in prokaryotic regulatory networks. *Proceedings of the National Academy of Sciences of the United States of America*, *102*(14), 4933–4934. https://doi.org/10.1073/pnas.0501417102

Feklístov, A., Sharon, B. D., Darst, S. A., & Gross, C. A. (2014). Bacterial sigma factors: A historical, structural, and genomic perspective. *Annual Review of Microbiology*, *68*, 357–376. https://doi.org/10.1146/annurev-micro-092412-155737

References

Flärdh, K. (2003). Essential role of DivlVA in polar growth and morphogenesis in *Streptomyces coelicolor* A3(2). *Molecular Microbiology*, *49*(6), 1523–1536. https://doi.org/10.1046/j.1365-2958.2003.03660.x

Fogel, M. A., & Waldor, M. K. (2006). A dynamic, mitotic-like mechanism for bacterial chromosome segregation. *Genes and Development*, *20*(23), 3269–3282. https://doi.org/10.1101/gad.1496506

Follmann, M., Ochrombel, I., Krämer, R., Trötschel, C., Poetsch, A., Rückert, C., Hüser, A., Persicke, M., Seiferling, D., Kalinowski, J., & Marin, K. (2009). Functional genomics of pH homeostasis in *Corynebacterium glutamicum* revealed novel links between pH response, oxidative stress, iron homeostasis and methionine synthesis. *BMC Genomics*, *10*, 621. https://doi.org/10.1186/1471-2164-10-621

Forbes, M., Kuck, N. A., & Peets, E. A. (1962). Mode of action of ethambutol. *Journal of Bacteriology*, *84*(5), 1099–1103. https://doi.org/10.1128/jb.84.5.1099-1103.1962

Fritsch, A., & Worcel, A. (1971). Symmetric multifork chromosome replication in fast-growing *Escherichia coli*. *Journal of Molecular Biology*, *59*(1), 207–211. https://doi.org/10.1016/0022-2836(71)90422-0

Gande, R., Gibson, K. J. C., Brown, A. K., Krumbach, K., Dover, L. G., Sahm, H., Shioyama, S., Oikawa, T., Besra, G. S., & Eggeling, L. (2004). Acyl-CoA carboxylases (*accD2* and *accD3*), together with a unique polyketide synthase (*Cg-pks*), are key to mycolic acid biosynthesis in *Corynebacterianeae* such as *Corynebacterium glutamicum* and *Mycobacterium tuberculosis*. *Journal of Biological Chemistry*, *279*(43), 44847–44857. https://doi.org/10.1074/jbc.M408648200

Gao, B., & Gupta, R. S. (2012). Phylogenetic framework and molecular signatures for the main clades of the phylum *Actinobacteria*. *Microbiology and Molecular Biology Reviews*, *76*(1), 66–112. https://doi.org/10.1128/mmbr.05011-11

Garner, E. C., Bernard, R., Wang, W., Zhuang, X., Rudner, D. Z., & Mitchison, T. (2011). Coupled, circumferential motions of the cell wall synthesis machinery and MreB filaments in *B. subtilis*. *Science*, *333*(6039), 222–225. https://doi.org/10.1126/science.1203285

Gavalda, S., Bardou, F., Laval, F., Bon, C., Malaga, W., Chalut, C., Guilhot, C., Mourey, L., Daffé, M., & Quémard, A. (2014). The polyketide synthase Pks13 catalyzes a novel mechanism of lipid transfer in *Mycobacteria*. *Chemistry and Biology*, *21*(12), 1660–1669. https://doi.org/10.1016/j.chembiol.2014.10.011

Gibson, K. J. C., Eggeling, L., Maughan, W. N., Krumbach, K., Gurcha, S. S., Nigou, J., Puzo, G., Sahm, H., & Besra, G. S. (2003). Disruption of Cg-Ppm1, a polyprenyl monophosphomannose synthase, and the generation of lipoglycan-less mutants in *Corynebacterium glutamicum*. *Journal of Biological Chemistry*, *278*(42), 40842–40850. https://doi.org/10.1074/jbc.M307988200

Gogou, C., Japaridze, A., & Dekker, C. (2021). Mechanisms for chromosome segregation in bacteria. *Frontiers in Microbiology*, *12*(June), 1–15. https://doi.org/10.3389/fmicb.2021.685687

Gomez, J. E., Chen, J. M., & Bishai, W. R. (1997). Sigma factors of *Mycobacterium tuberculosis*. *Tubercle and Lung Disease*, *78*(3–4), 175–183. https://doi.org/10.1016/S0962-8479(97)90024-1

Grice, E. A., Kong, H. H., Conlan, S., Deming, C. B., Davis, J., Young, A. C., Bouffard, G. G., Blakesley, R. W., Murray, P. R., Green, E. D., Turner, M. L., & Segre, J. A. (2009). Topographical and temporal diversity of the human skin microbiome. *Science*, *324*(5931), 1190–1192. https://doi.org/10.1126/science.1171700

Grigoriou, S., Kugler, P., Kulcinskaja, E., Walter, F., King, J., Hill, P., Wendisch, V. F., O'Reilly, E., & O'Reilly, E. (2020). Development of a *Corynebacterium glutamicum* bio-factory for self-sufficient transaminase reactions. *Green Chemistry*, *22*(13), 4128–4132. https://doi.org/10.1039/D0GC01432J

Grover, S., Alderwick, L. J., Mishra, A. K., Krumbach, K., Marienhagen, J., Eggeling, L., Bhatt, A., & Besra, G. S. (2014). Benzothiazinones mediate killing of *Corynebacterineae* by blocking decaprenyl phosphate recycling involved in cell wall biosynthesis. *Journal of Biological Chemistry*, *289*(9), 6177–6187. https://doi.org/10.1074/jbc.M113.522623

Gruber, S., Veening, J. W., Bach, J., Blettinger, M., Bramkamp, M., & Errington, J. (2014). Interlinked sister chromosomes arise in the absence of condensin during fast replication in *B. subtilis*. *Current Biology*, *24*(3), 293–298. https://doi.org/10.1016/j.cub.2013.12.049

Güthlein, C., Wanner, R. M., Sander, P., Böttger, E. C., & Springer, B. (2008). A mycobacterial *smc* null mutant is proficient in DNA repair and long-term survival. *Journal of Bacteriology*, *190*(1), 452–456. https://doi.org/10.1128/JB.01315-07

Haase, R., Fazeli, E., Legland, D., Doube, M., Culley, S., Belevich, I., Jokitalo, E., Schorb, M., Klemm, A., & Tischer, C. (2022). A Hitchhiker's guide through the bio-image analysis software universe. *FEBS Letters*, *596*(19), 2472–2485. https://doi.org/10.1002/1873-3468.14451

Hagino, H., & Nakayama, K. (1973). L-tyrosine production by analog-resistant mutants derived from a phenylalanine auxotroph of *Corynebacterium glutamicum*. *Agricultural and Biological Chemistry*, *37*(9), 2013–2023. https://doi.org/10.1080/00021369.1973.10860958

Hagino, H., & Nakayama, K. (1974). L-phenylalanine production by analog-resistant mutants of *Corynebacterium glutamicum*. *Agricultural and Biological Chemistry*, *38*(1), 157–161. https://doi.org/10.1080/00021369.1974.10861130

Hagino, H., & Nakayama, K. (1975). L-Tryptophan production by analog-resistant mutants derived from a phenylalanine and tyrosine double auxotroph of *Corynebacterium glutamicum*. *Agricultural and Biological Chemistry*, *39*(2), 343–349. https://doi.org/10.1080/00021369.1975.10861621

Halbedel, S., Hahn, B., Daniel, R. A., & Flieger, A. (2012). DivIVA affects secretion of virulence-related autolysins in *Listeria monocytogenes*. *Molecular Microbiology*, *83*(4), 821–839. https://doi.org/10.1111/j.1365-2958.2012.07969.x

Hancock, I. C., Carman, S., Besra, G. S., Brennan, P. J., & Waite, E. (2002). Ligation of arabinogalactan to peptidoglycan in the cell wall of *Mycobacterium smegmatis* requires concomitant synthesis of the two wall polymers. *Microbiology*, *148*, 3059–3067.

Hannebelle, M. T. M., Ven, J. X. Y., Toniolo, C., Eskandarian, H. A., Vuaridel-Thurre, G., McKinney, J. D., & Fantner, G. E. (2020). A biphasic growth model for cell pole elongation in *Mycobacteria*. *Nature Communications*, *11*(1). https://doi.org/10.1038/s41467-019-14088-z

Harper, C., Hayward, D., Wiid, I., & Van Helden, P. (2008). Regulation of nitrogen metabolism in *Mycobacterium tuberculosis*: A comparison with mechanisms in *Corynebacterium glutamicum* and *Streptomyces coelicolor*. *IUBMB Life*, *60*(10), 643–650. https://doi.org/10.1002/iub.100

Harry, E. J. (2001). MicroReview Bacterial cell division: regulating Z-ring formation. *Molecular Microbiology*, *40*(4), 795–803.

Hartbrich, A., Schmitz, G., Weuster-Botz, D., De Graaf, A. A., & Wandrey, C. (1996). Development and application of a membrane cyclone reactor for in vivo NMR spectroscopy with high microbial cell densities. *Biotechnology and Bioengineering*, *51*(6), 624–635. https://doi.org/10.1002/(SICI)1097-0290(19960920)51:6<624::AID-BIT2>3.0.CO;2-J

Hartmann, R., van Teeseling, M. C. F., Thanbichler, M., & Drescher, K. (2020). BacStalk: A comprehensive and interactive image analysis software tool for bacterial cell biology. *Molecular Microbiology*, *114*(1), 140–150. https://doi.org/10.1111/mmi.14501

Heider, S. A. E., & Wendisch, V. F. (2015). Engineering microbial cell factories: Metabolic engineering of *Corynebacterium glutamicum* with a focus on non-natural products. *Biotechnology Journal*, *10*(8), 1170–1184. https://doi.org/10.1002/BIOT.201400590

Hell, S. W. (2007). Far-field optical nanoscopy. *Science*, *316*(5828), 1153–1158. https://doi.org/10.1126/SCIENCE.1137395/SUPPL_FILE/HELL.SOM.PDF

Hempel, A., Wang, S. B., Letek, M., Gil, J., & Flärdh, K. (2008). Assemblies of DivIVA mark sites for hyphal branching and can establish new zones of cell wall growth in *Streptomyces coelicolor*. *Journal of Bacteriology*, *190*(22), 7579–7583. https://doi.org/10.1128/JB.00839-08

Hermans, P. W. M., Abebe, F., Kuteyi, V. I. O., Kolk, A. H. J., Thole, J. E. R., & Harboe, M. (1995). Molecular and immunological characterization of the highly conserved antigen 84 from *Mycobacterium tuberculosis* and *Mycobacterium leprae*. *Infection and Immunity*, *63*(3), 954–960. https://doi.org/10.1128/iai.63.3.954-960.1995

Hett, E. C., & Rubin, E. J. (2008). Bacterial growth and cell division: a mycobacterial perspective. *Microbiology and Molecular Biology Reviews*, *72*(1), 126–156. https://doi.org/10.1128/mmbr.00028-07

Hirano, T. (1999). SMC-mediated chromosome mechanics: A conserved scheme from bacteria to vertebrates? In *Genes and Development* (Vol. 13, Issue 1, pp. 11–19). https://doi.org/10.1101/gad.13.1.11

Ho, P. Y., & Amir, A. (2015). Simultaneous regulation of cell size and chromosome replication in bacteria. *Frontiers in Microbiology*, *6*(JUL), 1–10. https://doi.org/10.3389/fmicb.2015.00662

Höltje, J. (1998). Growth of the stress-bearing and shape-maintaining murein sacculus of *Escherichia coli*. *Microbiology and Molecular Biology Reviews : MMBR*, *62*(1), 181–203.

Houssin, C., D'Auria, C. de S., Constantinesco, F., Dietrich, C., Labarre, C., & Bayan, N. (2020). *Corynebacterium glutamicum: biology and biotechnology* (M. Inui & K. Toyoda (Eds.); Vol. 23). Springer Nature.

Hu, Z., Mukherjee, A., Pichoff, S., & Lutkenhaus, J. (1999). The MinC component of the division site selection system in *Escherichia coli* interacts with FtsZ to prevent polymerization. *Proceedings of the National Academy of Sciences of the United States of America*, *96*(26), 14819–14824. https://doi.org/10.1073/pnas.96.26.14819

Huc, E., de Sousa-D'Auria, C., de la Sierra-Gallay, I. L., Salmeron, C., Tilbeurgh, H. van, Bayan, N., Houssin, C., Daffé, M., & Tropisa, M. (2013). Identification of a mycoloyl transferase selectively involved in O-acylation of polypeptides in *Corynebacteriales*. *Journal of Bacteriology*, *195*(18), 4121–4128. https://doi.org/10.1128/JB.00285-13

Ikeda, M., & Katsumata, R. (1992). Metabolic engineering to produce tyrosine or phenylalanine in a tryptophan-producing Corynebacterium glutamicum strain. *Applied and Environmental Microbiology*, *58*(3), 781–785. https://doi.org/10.1128/aem.58.3.781-785.1992

Ikeda, M., & Nakagawa, S. (2003). The Corynebacterium glutamicum genome: Features and impacts on biotechnological processes. *Applied Microbiology and Biotechnology*, *62*(2–3), 99–109. https://doi.org/10.1007/S00253-003-1328-1/METRICS

Ireton, K., Gunther IV, N. W., & Grossman, A. D. (1994). spo0J is required for normal chromosome segregation as well as the initiation of sporulation in *Bacillus subtilis*. *Journal of Bacteriology*, *176*(17), 5320–5329. https://doi.org/10.1128/jb.176.17.5320-5329.1994

Jacobs, C., Huang, L. J., Bartowsky, E., Normark, S., & Park, J. T. (1994). Bacterial cell wall recycling provides cytosolic muropeptides as effectors for β-lactamase induction. *EMBO Journal*, *13*(19), 4684–4694. https://doi.org/10.1002/j.1460-2075.1994.tb06792.x

Jakoby, M., Nolden, L., Meier-Wagner, J., Krämer, R., & Burkovski, A. (2000). AmtR, a global repressor in the nitrogen regulation system of *Corynebacterium glutamicum*. *Molecular Microbiology*, *37*(4), 964–977. https://doi.org/10.1046/j.1365-2958.2000.02073.x

Jani, C., Eoh, H., Lee, J. J., Hamasha, K., Sahana, M. B., Han, J. S., Nyayapathy, S., Lee, J. Y., Suh, J. W., Lee, S. H., Rehse, S. J., Crick, D. C., & Kang, C. M. (2010). Regulation of polar peptidoglycan biosynthesis by Wag31 phosphorylation in mycobacteria. *BMC Microbiology*, *10*(1), 327. https://doi.org/10.1186/1471-2180-10-327

Jankute, M., Cox, J. A. G., Harrison, J., & Besra, G. S. (2015). Assembly of the mycobacterial cell wall. In *Annual Review of Microbiology* (Vol. 69, Issue 1, pp. 405–423). Annual Reviews. https://doi.org/10.1146/annurev-micro-091014-104121

Jensen, R. B., & Shapiro, L. (1999). The *Caulobacter crescentus smc* gene is required for cell cycle progression and chromosome segregation. *Proceedings of the National Academy of Sciences of the United States of America*, *96*(19), 10661–10666. https://doi.org/10.1073/pnas.96.19.10661

Jiao, J. Y., Liu, L., Hua, Z. S., Fang, B. Z., Zhou, E. M., Salam, N., Hedlund, B. P., & Li, W. J. (2021). Microbial dark matter coming to light: Challenges and opportunities. *National Science Review*, *8*(3), 1–5. https://doi.org/10.1093/nsr/nwaa280

Jones, T. R., Kang, I. H., Wheeler, D. B., Lindquist, R. A., Papallo, A., Sabatini, D. M., Golland, P., & Carpenter, A. E. (2008). CellProfiler Analyst: Data exploration and analysis software for complex image-based screens. *BMC Bioinformatics*, *9*, 1–16. https://doi.org/10.1186/1471-2105-9-482

Junker, B. (2004). Fermentation. *Kirk-Othmer Encyclopedia of Chemical Technology*. https://doi.org/10.1002/0471238961.0605181319051407.A01.PUB2

Kacem, R., De Sousa-D'Auria, C., Tropis, M., Chami, M., Gounon, P., Leblon, G., Houssin, C., & Daffé, M. (2004). Importance of mycoloyltransferases on the physiology of *Corynebacterium glutamicum*. *Microbiology*, *150*(1), 73–84. https://doi.org/10.1099/mic.0.26583-0

Kaji, Y., Nakamura, O., Yamaguchi, K., Nomura, Y., Oka, K., & Yamamoto, T. (2021). Combined administration of rifampicin, ethambutol, and clarithromycin for the treatment of tenosynovitis of the hand caused by *Mycobacterium avium* complex: Case series and literature review. *Medicine*, *100*(17), e25283. https://doi.org/10.1097/MD.0000000000025283

Kalinowski, J., Bathe, B., Bartels, D., Bischoff, N., Bott, M., Burkovski, A., Dusch, N., Eggeling, L., Eikmanns, B. J., Gaigalat, L., Goesmann, A., Hartmann, M., Huthmacher, K., Krämer, R., Linke, B., McHardy, A. C., Meyer, F., Möckel, B., Pfefferle, W., … Tauch, A. (2003). The complete *Corynebacterium glutamicum* ATCC 13032 genome sequence and its impact on the production of L-aspartate-derived amino acids and vitamins. *Journal of Biotechnology*, *104*(1–3), 5–25. https://doi.org/10.1016/S0168-1656(03)00154-8

Kallscheuer, N., & Marienhagen, J. (2018). *Corynebacterium glutamicum* as platform for the production of hydroxybenzoic acids. *Microbial Cell Factories*, *17*(1), 1–13. https://doi.org/10.1186/s12934-018-0923-x

Kang, C. M., Abbott, D. W., Sang, T. P., Dascher, C. C., Cantley, L. C., & Husson, R. N. (2005). The *Mycobacterium tuberculosis* serine/threonine kinases PknA and PknB: Substrate identification and regulation of cell shape. *Genes and Development*, *19*(14), 1692–1704. https://doi.org/10.1101/gad.1311105

Kang, C. M., Nyayapathy, S., Lee, J. Y., Suh, J. W., & Husson, R. N. (2008). Wag31, a homologue of the cell division protein DivIVA, regulates growth, morphology and polar cell wall synthesis in *Mycobacteria*. *Microbiology*, *154*(3), 725–735. https://doi.org/10.1099/mic.0.2007/014076-0

Kaval, K. G., & Halbedel, S. (2012). Architecturally the same, but playing a different game: the diverse species-specific roles of DivIVA proteins. *Virulence*, *3*(4), 406–407. https://doi.org/10.4161/viru.20747

Kawaguchi, H., Sasaki, M., Vertès, A. A., Inui, M., & Yukawa, H. (2009). Identification and functional analysis of the gene cluster for L-arabinose utilization in *Corynebacterium glutamicum*. *Applied and Environmental Microbiology*, *75*(11), 3419–3429. https://doi.org/10.1128/AEM.02912-08

Kawai, Y., Marles-Wright, J., Cleverley, R. M., Emmins, R., Ishikawa, S., Kuwano, M., Heinz, N., Bui, N. K., Hoyland, C. N., Ogasawara, N., Lewis, R. J., Vollmer, W., Daniel, R. A., & Errington, J. (2011). A widespread family of bacterial cell wall assembly proteins. *EMBO Journal*, *30*(24), 4931–4941. https://doi.org/10.1038/emboj.2011.358

Kim, E., Barth, R., & Dekker, C. (2023). Looping the Genome with SMC Complexes. *Annual Review of Biochemistry*, *92*, 15–41. https://doi.org/10.1146/annurev-biochem-032620-110506

Kim, H. J., Calcutt, M. J., Schmidt, F. J., & Chater, K. F. (2000). Partitioning of the linear chromosome during sporulation of *Streptomyces coelicolor* A3(2) involves an oriC-linked parAB locus. *Journal of Bacteriology*, *182*(5), 1313–1320. https://doi.org/10.1128/JB.182.5.1313-1320.2000

Kinoshita, S., Nakayama, K., & Akita, S. (1958). Taxonomical study of glutamic acid accumulating bacteria, *Micrococcus glutamicus* nov. sp. *Bulletin of the Agricultural Chemical Society of Japan*, *22*(3), 176–185. https://doi.org/10.1271/bbb1924.22.176

Kinoshita, S., Nakayama, K., & Kitada, S. (1958). L-lysine production using microbial auxotroph. *The Journal of General and Applied Microbiology*, *4*(2), 128–129.

Kinoshita, S., Udaka, S., & Shimono, M. (1957). Studies on the amino acid fermentation Part I. Production of L-glutamic acid by various microorganisms. *The Journal of General and Applied Microbiology*, *3*(3), 193–205. https://doi.org/10.2323/jgam.3.193

Kočan, M., Schaffer, S., Ishige, T., Sorger-Herrmann, U., Wendisch, V. F., & Bott, M. (2006). Two-component systems of *Corynebacterium glutamicum*: Deletion analysis and involvement of the *phoS-phoR* system in the phosphate starvation response. *Journal of Bacteriology*, *188*(2), 724–732. https://doi.org/10.1128/JB.188.2.724-732.2006

Kois, A., Świątek, M., Jakimowicz, D., & Zakrzewska-Czerwińska, J. (2009). SMC protein-dependent chromosome condensation during aerial hyphal development in *Streptomyces*. *Journal of Bacteriology*, *91*(1), 310–319. https://doi.org/10.1128/JB.00513-08

Kolly, G. S., Mukherjee, R., Kilacsková, E., Abriata, L. A., Raccaud, M., Blaško, J., Sala, C., Dal Peraro, M., Mikušová, K., & Cole, S. T. (2015). GtrA protein Rv3789 is required for arabinosylation of arabinogalactan in *Mycobacterium tuberculosis*. *Journal of Bacteriology*, *197*(23), 3686–3697. https://doi.org/10.1128/JB.00628-15

Korduláková, J., Gilleron, M., Mikuová, K., Puzo, G., Brennan, P. J., Gicquel, B., & Jackson, M. (2002). Definition of the first mannosylation step in phosphatidylinositol mannoside synthesis: PimA is essential for growth of *Mycobacteria*. *Journal of Biological Chemistry*, *277*(35), 31335–31344. https://doi.org/10.1074/jbc.M204060200

Korduláková, J., Gilleron, M., Puzo, G., Brennan, P. J., Gicquel, B., Mikušová, K., & Jackson, M. (2003). Identification of the required acyltransferase step in the biosynthesis of the phosphatidylinositol mannosides of *Mycobacterium* species. *Journal of Biological Chemistry*, *278*(38), 36285–36295. https://doi.org/10.1074/jbc.M303639200

Kotrba, P., Inui, M., & Yukawa, H. (2001). Bacterial phosphotransferase system (PTS) in carbohydrate uptake and control of carbon metabolism. *Journal of Bioscience and Bioengineering*, *92*(6), 502–517. https://doi.org/10.1016/S1389-1723(01)80308-X

Lamanna, C. (1946). The nature of the acid-fast stain. *Journal of Bacteriology*, *52*(1), 99–103.

Lanéelle, M.-A., Tropis, M., & Daffé, M. (2013). Current knowledge on mycolic acids in *Corynebacterium glutamicum* and their relevance for biotechnological processes. *Applied Microbiology and Biotechnology*, *97*(23), 9923–9930. https://doi.org/10.1007/s00253-013-5265-3

Larisch, C., Nakunst, D., Hüser, A. T., Tauch, A., & Kalinowski, J. (2007). The alternative sigma factor SigB of *Corynebacterium glutamicum* modulates global gene expression during transition from exponential growth to stationary phase. *BMC Genomics*, *8*, 1–14. https://doi.org/10.1186/1471-2164-8-4

Lavollay, M., Arthur, M., Fourgeaud, M., Dubost, L., Marie, A., Riegel, P., Gutmann, L., & Mainardi, J. L. (2009). The β-lactam-sensitive d,d-carboxypeptidase activity of Pbp4 controls the l,d and d,d transpeptidation pathways in *Corynebacterium jeikeium*. *Molecular Microbiology*, *74*(3), 650–661. https://doi.org/10.1111/j.1365-2958.2009.06887.x

Lavollay, M., Arthur, M., Fourgeaud, M., Dubost, L., Marie, A., Veziris, N., Blanot, D., Gutmann, L., & Mainardi, J. L. (2008). The peptidoglycan of stationary-phase *Mycobacterium tuberculosi*s predominantly contains cross-links generated by L,D-transpeptidation. *Journal of Bacteriology*, *190*(12), 4360–4366. https://doi.org/10.1128/JB.00239-08

Lea-Smith, D. J., Pyke, J. S., Tull, D., McConville, M. J., Coppel, R. L., & Crellin, P. K. (2007). The reductase that catalyzes mycolic motif synthesis is required for efficient attachment of mycolic acids to arabinogalactan. *Journal of Biological Chemistry*, *282*(15), 11000–11008. https://doi.org/10.1074/jbc.M608686200

Lee, B., Lee, S., Kim, H., Jeong, K., Park, J., Park, K., & Lee, J. (2015). Whole cell bioconversion of ricinoleic acid to 1,2-ketooleic acid by recombinant *Corynebacterium glutamicum*-based biocatalyst. *Journal of Microbiology and Biotechnology*, *25*(4), 452–458. https://doi.org/10.4014/jmb.1501.01001

Lee, J. (2014). Development and characterization of expression vectors for *Corynebacterium glutamicum*. *Journal of Microbiology and Biotechnology*, *24*(1), 70–79. https://doi.org/10.4014/jmb.1310.10032

Lee, J. Y., Na, Y. A., Kim, E., Lee, H. S., & Kim, P. (2016). The actinobacterium *Corynebacterium glutamicum*, an industrial workhorse. *Journal of Microbiology and Biotechnology*, *26*(5), 807–822. https://doi.org/10.4014/jmb.1601.01053

Lee, M. J., & Kim, P. (2018). Recombinant protein expression system in Corynebacterium glutamicum and its application. *Frontiers in Microbiology*, *9*(OCT). https://doi.org/10.3389/fmicb.2018.02523

Lee, R. E., Armour, J. W., Takayama, K., Brennan, P. J., & Besra, G. S. (1997). Mycolic acid biosynthesis: Definition and targeting of the Claisen condensation step. *Biochimica et Biophysica Acta - Lipids and Lipid Metabolism*, *1346*, 275–284. https://doi.org/10.1016/S0005-2760(97)00051-9

Lenarcic, R., Halbedel, S., Visser, L., Shaw, M., Wu, L. J., Errington, J., Marenduzzo, D., & Hamoen, L. W. (2009). Localisation of DivIVA by targeting to negatively curved membranes. *EMBO Journal*, *28*(15), 2272–2282. https://doi.org/10.1038/emboj.2009.129

Letek, M., Fiuza, M., Ordóñez, E., Villadangos, A. F., Flärdh, K., Mateos, L. M., & Gil, J. A. (2009). DivIVA uses an N-terminal conserved region and two coiled-coil domains to localize and sustain the polar growth in *Corynebacterium glutamicum*. *FEMS Microbiology Letters*, *297*(1), 110–116. https://doi.org/10.1111/j.1574-6968.2009.01679.x

Letek, M., Ordóñez, E., Vaquera, J., Margolin, W., Flärdh, K., Mateos, L. M., & Gil, J. A. (2008). DivIVA is required for polar growth in the MreB-lacking rod-shaped actinomycete *Corynebacterium glutamicum*. *Journal of Bacteriology*, *190*(9), 3283–3292. https://doi.org/10.1128/JB.01934-07

Levefaudes, M., Patin, D., De Sousa-D'Auria, C., Chami, M., Blanot, D., Hervé, M., Arthur, M., Houssin, C., & Mengin-Lecreulx, D. (2015). Diaminopimelic acid amidation in *Corynebacteriales* new insights into the role of ltsa in peptidoglycan modification. *Journal of Biological Chemistry*, *290*(21), 13079–13094. https://doi.org/10.1074/jbc.M115.642843

Levin, P. A., Margolis, P. S., Setlow, P., Losick, R., & Sun, D. (1992). Identification of *Bacillus subtilis* genes for septum placement and shape determination. *Journal of Bacteriology*, *174*(21), 6717–6728. https://doi.org/10.1128/jb.174.21.6717-6728.1992

Lewin, G. R., Carlos, C., Chevrette, M. G., Horn, H. A., McDonald, B. R., Stankey, R. J., Fox, B. G., & Currie, C. R. (2016). Evolution and Ecology of Actinobacteria and Their Bioenergy Applications. *Annual Review of Microbiology*, *70*(58), 235–254. https://doi.org/10.1146/annurev-micro-102215-095748

Li, L., Fang, C., Zhuang, N., Wang, T., & Zhang, Y. (2019). Structural basis for transcription initiation by bacterial ECF σ factors. *Nature Communications*, *10*(1). https://doi.org/10.1038/s41467-019-09096-y

Liao, Y., Ithurbide, S., Evenhuis, C., Löwe, J., & Duggin, I. G. (2021). Cell division in the archaeon *Haloferax volcanii* relies on two FtsZ proteins with distinct functions in division ring assembly and constriction. *Nature Microbiology*, *6*(5), 594–605. https://doi.org/10.1038/s41564-021-00894-z

Liebl, W., Ehrmann, M., Ludwig, W., & Schleifer, K. H. (1991). Transfer of *Brevibacterium divaricatum* DSM 20297, "'*Brevibacterium flavum*'" DSM 20411, " '*Brevibacterium lactofermentum*'" DSM 20412 and DSM 1412, and *Corynebacterium lilium* DSM 20137 to *Corynebacterium glutamicum* and their distinction by rRNA gene restriction patterns. *International Journal of Systematic Bacteriology*, *41*(2), 255–260. https://doi.org/10.1099/00207713-41-2-255

Lim, H. C., Surovtsev, I. V., Beltran, B. G., Huang, F., Bewersdorf, J., & Jacobs-Wagner, C. (2014). Evidence for a DNA-relay mechanism in ParABS-mediated chromosome segregation. *ELife*, *2014*(3), 1–32. https://doi.org/10.7554/eLife.02758

Lin, D. C. H., & Grossman, A. D. (1998). Identification and characterization of a bacterial chromosome partitioning site. *Cell*, *92*(5), 675–685. https://doi.org/10.1016/S0092-8674(00)81135-6

Lin, J., & Amir, A. (2017). The effects of stochasticity at the single-cell level and cell size control on the population growth. *Cell Systems*, *5*(4), 358-367.e4. https://doi.org/10.1016/j.cels.2017.08.015

Lipsky, B. A., Goldberger, A. C., Tompkins, L. S., & Plorde, J. J. (1982). Infections caused by nondiphtheria *Corynebacteria*. *Reviews of Infectious Diseases*, *4*(6), 1220–1235. https://doi.org/10.1093/clinids/4.6.1220

Liu, Q., Ouyang, S. ping, Kim, J., & Chen, G. Q. (2007). The impact of PHB accumulation on l-glutamate production by recombinant *Corynebacterium glutamicum*. *Journal of Biotechnology*, *132*(3), 273–279. https://doi.org/10.1016/j.jbiotec.2007.03.014

Logsdon, M. M., Ho, P. Y., Papavinasasundaram, K., Richardson, K., Cokol, M., Sassetti, C. M., Amir, A., & Aldridge, B. B. (2017). A parallel adder coordinates mycobacterial cell-cycle progression and cell-size homeostasis in the context of asymmetric growth and organization. *Current Biology*, *27*(21), 3367-3374.e7. https://doi.org/10.1016/j.cub.2017.09.046

Loos, A., Glanemann, C., Willis, L. B., O'Brien, X. M., Lessard, P. A., Gerstmeir, R., Guillouet, S., & Sinskey, A. J. (2001). Development and validation of *Corynebacterium* DNA microarrays. *Applied and Environmental Microbiology*, *67*(5), 2310–2318. https://doi.org/10.1128/AEM.67.5.2310-2318.2001

Lutkenhaus, J. (1998). Organelle division: From *coli* to chloroplasts. *Current Biology*, *8*(17), 619–621. https://doi.org/10.1016/s0960-9822(98)70391-4

Lutkenhaus, J. (2012). The ParA/MinD family puts things in their place. *Trends in Microbiology*, *20*(9), 411–418. https://doi.org/10.1016/j.tim.2012.05.002

Lutkenhaus, J., Wolf-Watz, H., & Donachie, W. D. (1980). Organization of genes in the *ftsA-envA* region of the *Escherichia coli* genetic map and identification of a new *fts* locus (*ftsZ*). *Journal of Bacteriology*, *142*(2), 615–620. https://doi.org/10.1128/jb.142.2.615-620.1980

References

Mackaness, G. B. (1952). The action of drugs on intra-cellular tubercle Bacilli. *Journal of Pathology and Bacteriolgy*, *64*(3), 429–446.

Mahadik, S. P., & Srinivasan, P. R. (1971). Stimulation of DNA-dependent RNA synthesis by a protein associated with ribosomes. *Proceedings of the National Academy of Sciences of the United States of America*, *68*(8), 1898–1901. https://doi.org/10.1073/pnas.68.8.1898

Majander, K., Pfrengle, S., Kocher, A., Neukamm, J., du Plessis, L., Pla-Díaz, M., Arora, N., Akgül, G., Salo, K., Schats, R., Inskip, S., Oinonen, M., Valk, H., Malve, M., Kriiska, A., Onkamo, P., González-Candelas, F., Kühnert, D., Krause, J., & Schuenemann, V. J. (2020). Ancient bacterial genomes reveal a high diversity of *Treponema pallidum* strains in early modern Europe. *Current Biology*, *30*(19), 3788-3803.e10. https://doi.org/10.1016/j.cub.2020.07.058

Makarov, V., Manina, G., Mikusova, K., Möllmann, U., Ryabova, O., Saint-Joanis, B., Dhar, N., Pasca, M. R., Buroni, S., Lucarelli, A. P., Milano, A., De Rossi, E., Belanova, M., Bobovska, A., Dianiskova, P., Kordulakova, J., Sala, C., Fullam, E., Schneider, P., … Cole, S. T. (2009). Benzothiazinones kill *Mycobacterium tuberculosis* by blocking arabinan synthesis. *Science*, *324*(5928), 801–804. https://doi.org/10.1126/science.1171583

Manganelli, R., Cioetto-Mazzabò, L., Segafreddo, G., Boldrin, F., Sorze, D., Conflitti, M., Serafini, A., & Provvedi, R. (2023). SigE: A master regulator of *Mycobacterium tuberculosis*. *Frontiers in Microbiology*, *14*(March), 1–8. https://doi.org/10.3389/fmicb.2023.1075143

Mao, W., Renner, L. D., Cornilleau, C., Sierra-Gallay, I. L. de la, Benlamara, S., Ah-Seng, Y., Tilbeurgh, H. Van, Nessler, S., Bertin, A., Chastanet, A., & Carballido-López, R. (2022). Polymerization cycle of actin homolog MreB from a Gram-positive bacterium. *BioRxiv*, 2022.10.19.512861. https://www.biorxiv.org/content/10.1101/2022.10.19.512861v1%0Ahttps://www.biorxiv.org/content/10.1101/2022.10.19.512861v1.abstract

Marantan, A., & Amir, A. (2016). Stochastic modeling of cell growth with symmetric or asymmetric division. *Physical Review E*, *94*(1), 1–18. https://doi.org/10.1103/PhysRevE.94.012405

Marrakchi, H., Lanéelle, M. A., & Daffé, M. (2014). Mycolic acids: Structures, biosynthesis, and beyond. In *Chemistry and Biology* (Vol. 21, Issue 1, pp. 67–85). Cell Press. https://doi.org/10.1016/j.chembiol.2013.11.011

Marston, A. L., Thomaides, H. B., Edwards, D. H., Sharpe, M. E., & Errington, J. (1998). Polar localization of the MinD protein of *Bacillus subtilis* and its role in selection of the mid-cell division site. *Genes and Development*, *12*(21), 3419–3430. https://doi.org/10.1101/gad.12.21.3419

Martins, G. B., Giacomelli, G., Goldbeck, O., Seibold, G. M., & Bramkamp, M. (2019). Substrate-dependent cluster density dynamics of *Corynebacterium glutamicum* phosphotransferase system permeases. *Molecular Microbiology*, *111*(5), 1335–1354. https://doi.org/10.1111/mmi.14224

Mazza, P., Noens, E. E., Schirner, K., Grantcharova, N., Mommaas, A. M., Koerten, H. K., Muth, G., Flärdh, K., Van Wezel, G. P., & Wohlleben, W. (2006). MreB of *Streptomyces coelicolor* is not essential for vegetative growth but is required for the integrity of aerial hyphae and spores. *Molecular Microbiology*, *60*(4), 838–852. https://doi.org/10.1111/j.1365-2958.2006.05134.x

McNeil, M., Daffe, M., & Brennan, P. J. (1990). Evidence for the nature of the link between the arabinogalactan and peptidoglycan of mycobacterial cell walls. *Journal of Biological Chemistry*, *265*(30), 18200–18206. https://doi.org/10.1016/s0021-9258(17)44738-7

Meeske, A. J., Riley, E. P., Robins, W. P., Uehara, T., Mekalanos, J. J., Kahne, D., Walker, S., Kruse, A. C., Bernhardt, T. G., & Rudner, D. Z. (2016). SEDS proteins are a widespread family of bacterial cell wall polymerases. *Nature, 537*(7622), 634–638. https://doi.org/10.1038/nature19331

Melzer, E. S., Sein, C. E., Chambers, J. J., & Sloan Siegrist, M. (2018). DivIVA concentrates mycobacterial cell envelope assembly for initiation and stabilization of polar growth. *Cytoskeleton*, *75*(12), 498–507. https://doi.org/10.1002/cm.21490

Meniche, X., de Sousa-d'Auria, C., Van-der-Rest, B., Bhamidi, S., Huc, E., Huang, H., De Paepe, D., Tropis, M., McNeil, M., Daffé, M., & Houssin, C. (2008). Partial redundancy in the synthesis of the D-arabinose incorporated in the cell wall arabinan of *Corynebacterineae*. *Microbiology*, *154*(8), 2315–2326. https://doi.org/10.1099/mic.0.2008/016378-0

Messelink, J. J., Meyer, F., Bramkamp, M., & Broedersz, C. P. (2021). Single-cell growth inference of *Corynebacterium glutamicum* reveals asymptotically linear growth. *ELife*, *10*, e70106. https://doi.org/10.7554/eLife.70106

Meyer, F. M., Repnik, U., Karnaukhova, E., Schubert, K., & Bramkamp, M. (2023). Effects of benzothiazinone and ethambutol on the integrity of the corynebacterial cell envelope. *The Cell Surface*, 100116.

Michel, A., Koch-Koerfges, A., Krumbach, K., Brocker, M., & Bott, M. (2015). Anaerobic growth of *Corynebacterium glutamicum* via mixed-acid fermentation. *Applied and Environmental Microbiology*, *81*(21), 7496–7508. https://doi.org/10.1128/AEM.02413-15

Mikuová, K., Yagi, T., Stern, R., McNeil, M. R., Besra, G. S., Crick, D. C., & Brennan, P. J. (2000). Biosynthesis of the galactan component of the mycobacterial cell wall. *Journal of Biological Chemistry*, *275*(43), 33890–33897. https://doi.org/10.1074/jbc.M006875200

Mikušová, K., Huang, H., Yagi, T., Holsters, M., Vereecke, D., D'Haeze, W., Scherman, M. S., Brennan, P. J., McNeil, M. R., & Crick, D. C. (2005). Decaprenylphosphoryl arabinofuranose, the donor of the D-arabinofuranosyl residues of mycobacterial arabinan, is formed via a two-step epimerization of decaprenylphosphoryl ribose. *Journal of Bacteriology*, *187*(23), 8020–8025. https://doi.org/10.1128/JB.187.23.8020-8025.2005

Mills, J. A., Motichka, K., Jucker, M., Wu, H. P., Uhlik, B. C., Stern, R. J., Scherman, M. S., Vissa, V. D., Pan, F., Kundu, M., Yu, F. M., & McNeil, M. (2004). Inactivation of the mycobacterial rhamnosyltransferase, which is needed for the formation of the arabinogalactan-peptidoglycan linker, leads to irreversible loss of viability. *Journal of Biological Chemistry*, *279*(42), 43540–43546. https://doi.org/10.1074/jbc.M407782200

Mishra, A. K., Alderwick, L. J., Rittmann, D., Tatituri, R. V. V., Nigou, J., Gilleron, M., Eggeling, L., & Besra, G. S. (2007). Identification of an $\alpha(1\rightarrow6)$ mannopyranosyltransferase (MptA), involved in *Corynebacterium glutamicum* lipomanann biosynthesis, and identification of its orthologue in Mycobacterium tuberculosis. *Molecular Microbiology*, *65*(6), 1503–1517. https://doi.org/10.1111/j.1365-2958.2007.05884.x

Mishra, A. K., Alderwick, L. J., Rittmann, D., Wang, C., Bhatt, A., Jacobs, W. R., Takayama, K., Eggeling, L., & Besra, G. S. (2008). Identification of a novel α(1→6) mannopyranosyltransferase MptB from *Corynebacterium glutamicum* by deletion of a conserved gene, *NCgl1505*, affords a lipomannan- and lipoarabinomannan-deficient mutant. *Molecular Microbiology*, *68*(6), 1595–1613. https://doi.org/10.1111/j.1365-2958.2008.06265.x

Mishra, A. K., Klein, C., Gurcha, S. S., Alderwick, L. J., Babu, P., Hitchen, P. G., Morris, H. R., Dell, A., Besra, G. S., & Eggeling, L. (2008). Structural characterization and functional properties of a novel lipomannan variant isolated from a *Corynebacterium glutamicum pimB'* mutant. *Antonie van Leeuwenhoek, International Journal of General and Molecular Microbiology*, *94*(2), 277–287. https://doi.org/10.1007/s10482-008-9243-1

Mishra, A. K., Krumbach, K., Rittmann, D., Appelmelk, B., Pathak, V., Pathak, A. K., Nigou, J., Geurtsen, J., Eggeling, L., & Besra, G. S. (2011). Lipoarabinomannan biosynthesis in *Corynebacterineae*: The interplay of two α(1→2)-mannopyranosyltransferases MptC and MptD in mannan branching. *Molecular Microbiology*, *80*(5), 1241–1259. https://doi.org/10.1111/j.1365-2958.2011.07640.x

Mizukami, T., Hamu, A., Ikeda, M., Oka, T., & Katsumata, R. (1994). Cloning of the ATP phosphoribosyl transferase gene of *Corynebacterium glutamicum* and application of the gene to L-histidine production. *Bioscience, Biotechnology, and Biochemistry*, *58*(4), 635–638. https://doi.org/10.1271/bbb.58.635

Mizuno, Y., Nagano-Shoji, M., Kubo, S., Kawamura, Y., Yoshida, A., Kawasaki, H., Nishiyama, M., Yoshida, M., & Kosono, S. (2016). Altered acetylation and succinylation profiles in *Corynebacterium glutamicum* in response to conditions inducing glutamate overproduction. *MicrobiologyOpen*, *5*(1), 152–173. https://doi.org/10.1002/mbo3.320

Mohammadi, T., Van Dam, V., Sijbrandi, R., Vernet, T., Zapun, A., Bouhss, A., Diepeveen-De Bruin, M., Nguyen-Distéche, M., De Kruijff, B., & Breukink, E. (2011). Identification of FtsW as a transporter of lipid-linked cell wall precursors across the membrane. *EMBO Journal*, *30*(8), 1425–1432. https://doi.org/10.1038/emboj.2011.61

Mohiman, N., Argentini, M., Batt, S. M., Cornu, D., Masi, M., Eggeling, L., Besra, G., & Bayan, N. (2012). The *ppm* operon is essential for acylation and glycosylation of lipoproteins in *Corynebacterium glutamicum*. *PLoS ONE*, *7*(9). https://doi.org/10.1371/journal.pone.0046225

Nakamura, Y., Nishio, Y., Ikeo, K., & Gojobori, T. (2003). The genome stability in *Corynebacterium* species due to lack of the recombinational repair system. *Gene*, *317*(1–2), 149–155. https://doi.org/10.1016/S0378-1119(03)00653-X

Nakunst, D., Larisch, C., Hüser, A. T., Tauch, A., Pühler, A., & Kalinowski, J. (2007). The extracytoplasmic function-type sigma factor SigM of *Corynebacterium glutamicum* ATCC 13032 is involved in transcription of disulfide stress-related genes. *Journal of Bacteriology*, *189*(13), 4696–4707. https://doi.org/10.1128/JB.00382-07

Nandy, P. (2022). The role of sigma factor competition in bacterial adaptation under prolonged starvation. *Microbiology (United Kingdom)*, *168*(5), 1–11. https://doi.org/10.1099/mic.0.001195

Nešvera, J., & Pátek, M. (2011). Tools for genetic manipulations in *Corynebacterium glutamicum* and their applications. In *Applied Microbiology and Biotechnology* (Vol. 90, Issue 5, pp. 1641–1654). Springer. https://doi.org/10.1007/s00253-011-3272-9

Neumeyer, A., Hübschmann, T., Müller, S., & Frunzke, J. (2013). Monitoring of population dynamics of *Corynebacterium glutamicum* by multiparameter flow cytometry. *Microbial Biotechnology*, *6*(2), 157–167. https://doi.org/10.1111/1751-7915.12018

Oberreuter, H., Charzinski, J., & Scherer, S. (2002). Intraspecific diversity of Brevibacterium linens, *Corynebacterium glutamicum* and *Rhodococcus erythropolis* based on partial 16S rDNA sequence analysis and Fourier-transform infrared (FT-IR) spectroscopy. *Microbiology*, *148*(5), 1523–1532. https://doi.org/10.1099/00221287-148-5-1523

Oguiza, J. A., Marcos, A. T., Malumbres, M., & Martín, J. F. (1996). Multiple sigma factor genes in *Brevibacterium lactofermentum*: Characterization of sigA and sigB. *Journal of Bacteriology*, *178*(2), 550–553. https://doi.org/10.1128/jb.178.2.550-553.1996

Ojaimi, C., Davidson, B. E., Girons, I. S., & Old, I. G. (1994). Conservation of gene arrangement and an unusual organization of rRNA genes in the linear chromosomes of the Lyme disease spirochaetes *Borrelia burgdorferi*, *B. garinii* and *B. afzelii*. *Microbiology*, *140*(11), 2931–2940. https://doi.org/10.1099/13500872-140-11-2931

Oliva, M. A., Halbedel, S., Freund, S. M., Dutow, P., Leonard, T. A., Veprintsev, D. B., Hamoen, L. W., & Löwe, J. (2010). Features critical for membrane binding revealed by DivIVA crystal structure. *EMBO Journal*, *29*(12), 1988–2001. https://doi.org/10.1038/emboj.2010.99

Osorio-Valeriano, M., Altegoer, F., Steinchen, W., Urban, S., Liu, Y., Bange, G., & Thanbichler, M. (2019). ParB-type DNA segregation proteins are CTP-dependent molecular switches. *Cell*, *179*(7), 1512-1524.e15. https://doi.org/10.1016/j.cell.2019.11.015

Paget, M. S. (2015). Bacterial sigma factors and anti-sigma factors: Structure, function and distribution. *Biomolecules*, *5*(3), 1245–1265. https://doi.org/10.3390/biom5031245

Park, S. D., Youn, J. W., Kim, Y. J., Lee, S. M., Kim, Y., & Lee, H. S. (2008). *Corynebacterium glutamicum* σE is involved in responses to cell surface stresses and its activity is controlled by the anti-σ factor CseE. *Microbiology*, *154*(3), 915–923. https://doi.org/10.1099/mic.0.2007/012690-0

Pavelka, M. S., Mahapatra, S., & Crick, D. C. (2015). Genetics of peptidoglycan biosynthesis. *Molecular Genetics of Mycobacteria*, *3*, 511–533. https://doi.org/10.1128/9781555818845.ch26

Pawar, A., Jha, P., Konwar, C., Chaudhry, U., Chopra, M., & Saluja, D. (2019). Ethambutol targets the glutamate racemase of *Mycobacterium tuberculosis*—an enzyme involved in peptidoglycan biosynthesis. *Applied Microbiology and Biotechnology*, *103*(2), 843–851. https://doi.org/10.1007/s00253-018-9518-z

Pecoraro, V., Zerulla, K., Lange, C., & Soppa, J. (2011). Quantification of ploidy in proteobacteria revealed the existence of monoploid, (mero-)oligoploid and polyploid species. *PLoS ONE*, *6*(1). https://doi.org/10.1371/journal.pone.0016392

Peng, F., Giacomelli, G., Meyer, F. M., Linder, M., Haak, M., Rueckert-Reed, C., … & Bramkamp, M. (2023). Deletion of SMC renders FtsK essential in Corynebacterium glutamicum. bioRxiv, 2023-10.

Peschek, N., Herzog, R., Singh, P. K., Sprenger, M., Meyer, F., Fröhlich, K. S., Schröger, L., Bramkamp, M., Drescher, K., & Papenfort, K. (2020). RNA-mediated control of cell shape modulates antibiotic resistance in *Vibrio cholerae*. *Nature Communications*, *11*(1). https://doi.org/10.1038/s41467-020-19890-8

References

Poehl, S., Giacomelli, G., Meyer, F., Bramkamp, M., & Thanbichler, M. (in preparation). PapS in *R. rubrum*.

Pogliano, J., Pogliano, K., Weiss, D. S., Losick, R., & Beckwith, J. (1997). Inactivation of FtsI inhibits constriction of the FtsZ cytokinetic ring and delays the assembly of FtsZ rings at potential division sites. *Proceedings of the National Academy of Sciences of the United States of America*, *94*(2), 559–564. https://doi.org/10.1073/pnas.94.2.559

Puech, V., Chami, M., Lemassu, a, Lanéelle, M. a, Schiffler, B., Gounon, P., Bayan, N., Benz, R., & Daffé, M. (2001). Structure of the cell envelope of *Corynebacteria*: importance of the non-covalently bound lipids in the formation of the cell wall permeability barrier and fracture plane. *Microbiology (Reading, England)*, *147*(Pt 5), 1365–1382. http://www.ncbi.nlm.nih.gov/pubmed/11320139

R Development Core Team. (2003). *R: A Language and Environment for Statistical Computing*. R Foundation for Statistical Computing, Vienna, Austria.

Raad, R. B., Méniche, X., De Sousa-D'Auria, C., Chami, M., Salmeron, C., Tropis, M., Labarre, C., Daffé, M., Houssin, C., & Bayan, N. (2010). A deficiency in arabinogalactan biosynthesis affects *Corynebacterium glutamicum* mycolate outer membrane stability. *Journal of Bacteriology*, *192*(11), 2691–2700. https://doi.org/10.1128/JB.00009-10

Radmacher, E., Stansen, K. C., Besra, G. S., Alderwick, L. J., Maughan, W. N., Hollweg, G., Sahm, H., Wendisch, V. F., & Eggeling, L. (2005). Ethambutol, a cell wall inhibitor of Mycobacterium tuberculosis, elicits L-glutamate efflux of *Corynebacterium glutamicum*. *Microbiology*, *151*, 1359–1368. https://doi.org/10.1099/mic.0.27804-0

Raghavendra, T., Patil, S., & Mukherjee, R. (2018). Peptidoglycan in Mycobacteria: chemistry, biology and intervention. In *Glycoconjugate Journal* (Vol. 35, Issue 5, pp. 421–432). Springer. https://doi.org/10.1007/s10719-018-9842-7

Rainczuk, A. K., Yamaryo-Botte, Y., Brammananth, R., Stinear, T. P., Seemann, T., Coppel, R. L., McConville, M. J., & Crellin, P. K. (2012). The lipoprotein LpqW is essential for the mannosylation of periplasmic glycolipids in corynebacteria. *Journal of Biological Chemistry*, *287*(51), 42726–42738. https://doi.org/10.1074/jbc.M112.373415

Ramamurthi, K. S., & Losick, R. (2009). Negative membrane curvature as a cue for subcellular localization of a bacterial protein. *Proceedings of the National Academy of Sciences of the United States of America*, *106*(32), 13541–13545. https://doi.org/10.1073/pnas.0906851106

Ramos, A., Honrubia, M. P., Valbuena, N., Vaquera, J., Mateos, L. M., & Gil, J. A. (2003). Involvement of DivIVA in the morphology of the rod-shaped actinomycete *Brevibacterium lactofermentum*. *Microbiology*, *149*(12), 3531–3542. https://doi.org/10.1099/mic.0.26653-0

Rankine-Wilson, L. I., Shapira, T., Emani, C. S., & Av-Gay, Y. (2021). From infection niche to therapeutic target: The intracellular lifestyle of *Mycobacterium tuberculosis*. *Microbiology (United Kingdom)*, *167*(4). https://doi.org/10.1099/MIC.0.001041

Ravasi, P., Peiru, S., Gramajo, H., & Menzella, H. G. (2012). Design and testing of a synthetic biology framework for genetic engineering of *Corynebacterium glutamicum*. *Microbial Cell Factories*, *11*, 1–11. https://doi.org/10.1186/1475-2859-11-147

Rey, D. A., Pühler, A., & Kalinowski, J. (2003). The putative transcriptional repressor McbR, member of the TetR-family, is involved in the regulation of the metabolic network directing the synthesis of sulfur containing amino acids in *Corynebacterium glutamicum*. *Journal of Biotechnology*, *103*(1), 51–65. https://doi.org/10.1016/S0168-1656(03)00073-7

Rinke, C., Schwientek, P., Sczyrba, A., Ivanova, N. N., Anderson, I. J., Cheng, J. F., Darling, A., Malfatti, S., Swan, B. K., Gies, E. A., Dodsworth, J. A., Hedlund, B. P., Tsiamis, G., Sievert, S. M., Liu, W. T., Eisen, J. A., Hallam, S. J., Kyrpides, N. C., Stepanauskas, R., … Woyke, T. (2013). Insights into the phylogeny and coding potential of microbial dark matter. *Nature*, *499*(7459), 431–437. https://doi.org/10.1038/nature12352

Ruiz, N. (2008). Bioinformatics identification of MurJ (MviN) as the peptidoglycan lipid II flippase in Escherichia coli. *Proceedings of the National Academy of Sciences of the United States of America*, *105*(40), 15553–15557. https://doi.org/10.1073/pnas.0808352105

Ruiz, N. (2015). Lipid flippases for bacterial peptidoglycan biosynthesis. *Lipid Insights*, *2015*, 21–31. https://doi.org/10.4137/Lpi.s31783

Sahl, S. J., Hell, S. W., & Jakobs, S. (2017). Fluorescence nanoscopy in cell biology. *Nature Reviews Molecular Cell Biology 2017 18:11*, *18*(11), 685–701. https://doi.org/10.1038/nrm.2017.71

Sancho-Vaello, E., Albesa-Jové, D., Rodrigo-Unzueta, A., & Guerin, M. E. (2017). Structural basis of phosphatidyl-myo-inositol mannosides biosynthesis in *Mycobacteria*. *Biochimica et Biophysica Acta (BBA) - Molecular and Cell Biology of Lipids*, *1862*(11), 1355–1367. https://doi.org/10.1016/J.BBALIP.2016.11.002

Santana-Molina, C., Saz-Navarro, Dm. del, & Devos, D. P. (2023). Early origin and evolution of the FtsZ/tubulin protein family. *Frontiers in Microbiology*, *13*(January), 1–14. https://doi.org/10.3389/fmicb.2022.1100249

Santi, I., Dhar, N., Bousbaine, D., Wakamoto, Y., & McKinney, J. D. (2013). Single-cell dynamics of the chromosome replication and cell division cycles in *Mycobacteria*. *Nature Communications*, *4*(May), 3–8. https://doi.org/10.1038/ncomms3470

Santi, I., & McKinney, J. D. (2015). Chromosome organization and replisome dynamics in *Mycobacterium smegmatis*. *MBio*, *6*(1). https://doi.org/10.1128/mBio.01999-14

Santos-Beneit, F. (2015). The Pho regulon: A huge regulatory network in bacteria. *Frontiers in Microbiology*, *6*(APR), 1–13. https://doi.org/10.3389/fmicb.2015.00402

Sarathy, J. P., Zimmerman, M. D., Gengenbacher, M., Dartois, V., & Dick, T. (2022). *Mycobacterium tuberculosis* DprE1 Inhibitor OPC-167832 Is active against *Mycobacterium abscessus* in vitro. *Antimicrobial Agents and Chemotherapy*, *66*(12). https://doi.org/10.1128/aac.01237-22

Sassetti, C. M., Boyd, D. H., & Rubin, E. J. (2003). Genes required for mycobacterial growth defined by high density mutagenesis. *Molecular Microbiology*, *48*(1), 77–84. https://doi.org/10.1046/j.1365-2958.2003.03425.x

Sauls, J. T., Li, D., & Jun, S. (2016). Adder and a coarse-grained approach to cell size homeostasis in bacteria. *Current Opinion in Cell Biology*, *38*, 38–44. https://doi.org/10.1016/j.ceb.2016.02.004

Savková, K., Huszár, S., Baráth, P., Pakanová, Z., Kozmon, S., Vancová, M., ... & Mikušová, K. (2021). An ABC transporter Wzm–Wzt catalyzes translocation of lipid-linked galactan across the plasma membrane in mycobacteria. *Proceedings of the National Academy of Sciences*, *118*(17), e2023663118

Schaaf, S., & Bott, M. (2007). Target genes and DNA-binding sites of the response regulator PhoR from *Corynebacterium glutamicum*. *Journal of Bacteriology*, *189*(14), 5002–5011. https://doi.org/10.1128/JB.00121-07

Schaechter, M. (2015). A brief history of bacterial growth physiology. *Frontiers in Microbiology*, *6*(MAR), 1–5. https://doi.org/10.3389/fmicb.2015.00289

Schaechter, M., Maaløe, O., & Kjeldgaard, N. O. (1958). Dependency on Medium and Temperature of Cell Size and Chemical Composition during Balanced Growth of *Salmonella typhimurium*. *Journal of General Microbiology*, *19*(3), 592–606. https://doi.org/10.1099/00221287-19-3-592

Schäfer, A., Tauch, A., Jäger, W., Kalinowski, J., Thierbach, G., & Pühler, A. (1994). Small mobilizable multi-purpose cloning vectors derived from the *Escherichia coli* plasmids *pK18* and *pK19*: selection of defined deletions in the chromosome of *Corynebacterium glutamicum*. *Gene*, *145*(1), 69–73. https://doi.org/10.1016/0378-1119(94)90324-7

Schindelin, J., Arganda-Carreras, I., Frise, E., Kaynig, V., Longair, M., Pietzsch, T., Preibisch, S., Rueden, C., Saalfeld, S., Schmid, B., Tinevez, J.-Y., White, D. J., Hartenstein, V., Eliceiri, K., Tomancak, P., & Cardona, A. (2012). Fiji: an open-source platform for biological-image analysis. *Nature Methods*, *9*(7), 676–682. https://doi.org/10.1038/nmeth.2019

Schleifer, K. H., & Kandler, O. (1972). Peptidoglycan types of bacterial cell walls and their taxonomic implications. *Bacteriological Reviews*, *36*(4), 407–477.

Schröder, J., & Tauch, A. (2010). Transcriptional regulation of gene expression in Corynebacterium glutamicum: The role of global, master and local regulators in the modular and hierarchical gene regulatory network. *FEMS Microbiology Reviews*, *34*(5), 685–737. https://doi.org/10.1111/j.1574-6976.2010.00228.x

Schubert, K., Sieger, B., Meyer, F., Giacomelli, G., Böhm, K., Rieblinger, A., Lindenthal, L., Sachs, N., Wanner, G., & Bramkamp, M. (2017). The antituberculosis drug ethambutol selectively blocks apical growth in CMN group bacteria. *MBio*, *8*(1), 1–21. https://doi.org/10.1128/mBio.02213-16

Schultz, C., Niebisch, A., Schwaiger, A., Viets, U., Metzger, S., Bramkamp, M., & Bott, M. (2009). Genetic and biochemical analysis of the serine/threonine protein kinases PknA, PknB, PknG and PknL of *Corynebacterium glutamicum*: Evidence for non-essentiality and for phosphorylation of OdhI and FtsZ by multiple kinases. *Molecular Microbiology*, *74*(3), 724–741. https://doi.org/10.1111/j.1365-2958.2009.06897.x

Schwartz, M. A., & Shapiro, L. (2011). An SMC ATPase mutant disrupts chromosome segregation in *Caulobacter*. *Molecular Microbiology*, *82*(6), 1359–1374. https://doi.org/10.1111/j.1365-2958.2011.07836.x

Seidel, M., Alderwick, L. J., Sahm, H., Besra, G. S., & Eggeling, L. (2007). Topology and mutational analysis of the single Emb arabinofuranosyltransferase of *Corynebacterium glutamicum* as a model of Emb proteins of Mycobacterium tuberculosis. *Glycobiology*, *17*(2), 210–219. https://doi.org/10.1093/glycob/cwl066

Sham, L. T., Butler, E. K., Lebar, M. D., Kahne, D., Bernhardt, T. G., & Ruiz, N. (2014). MurJ is the flippase of lipid-linked precursors for peptidoglycan biogenesis. *Science*, *345*(6193), 220–222. https://doi.org/10.1126/science.1254522

Sher, J. W., Lim, H. C., & Bernhardt, T. G. (2021). Polar growth in *Corynebacterium glutamicum* has a flexible cell wall synthase requirement. *MBio*, *12*(3). https://doi.org/10.1128/mBio.00682-21

Shi, H., Bratton, B. P., Gitai, Z., & Huang, K. C. (2018). How to build a bacterial cell: MreB as the foreman of *E. coli* construction. In *Cell* (Vol. 172, Issue 6, pp. 1294–1305). Elsevier Inc. https://doi.org/10.1016/j.cell.2018.02.050

Si, F., Le Treut, G., Sauls, J. T., Vadia, S., Levin, P. A., & Jun, S. (2019). Mechanistic origin of cell-size control and homeostasis in bacteria. *Current Biology*, *29*(11), 1760-1770.e7. https://doi.org/10.1016/j.cub.2019.04.062

Siebert, D., & Wendisch, V. F. (2015). Metabolic pathway engineering for production of 1,2-propanediol and 1-propanol by *Corynebacterium glutamicum*. *Biotechnology for Biofuels*, *8*(1), 1–13. https://doi.org/10.1186/s13068-015-0269-0

Sieger, B., & Bramkamp, M. (2015). Interaction sites of DivIVA and RodA from *Corynebacterium glutamicum*. *Frontiers in Microbiology*, *5*(January), 1–11. https://doi.org/10.3389/fmicb.2014.00738

Sieger, B., Schubert, K., Donovan, C., & Bramkamp, M. (2013). The lipid II flippase RodA determines morphology and growth in *Corynebacterium glutamicum*. *Molecular Microbiology*, *90*(5), 966–982. https://doi.org/10.1111/mmi.12411

Sivanathan, V., Emerson, J. E., Pages, C., Cornet, F., Sherratt, D. J., & Arciszewska, L. K. (2009). KOPS-guided DNA translocation by FtsK safeguards *Escherichia coli* chromosome segregation. *Molecular Microbiology*, *71*(4), 1031–1042. https://doi.org/10.1111/j.1365-2958.2008.06586.x

Slager, J., Kjos, M., Attaiech, L., & Veening, J. W. (2014). Antibiotic-induced replication stress triggers bacterial competence by increasing gene dosage near the origin. *Cell*, *157*(2), 395–406. https://doi.org/10.1016/j.cell.2014.01.068

Slayden, R. A., Lee, R. E., & Barry, C. E. (2000). Isoniazid affects multiple components of the type II fatty acid synthase system of *Mycobacterium tuberculosis*. *Molecular Microbiology*, *38*(3), 514–525. https://doi.org/10.1046/j.1365-2958.2000.02145.x

Slayden, Richard A., Lee, R. E., Armour, J. W., Cooper, A. M., Orme, I. M., Brennan, P. J., & Besra, G. S. (1996). Antimycobacterial action of thiolactomycin: An inhibitor of fatty acid and mycolic acid synthesis. *Antimicrobial Agents and Chemotherapy*, *40*(12), 2813–2819. https://doi.org/10.1128/aac.40.12.2813

Soppa, J. (2014). Polyploidy in archaea and bacteria: About desiccation resistance, giant cell size, long-term survival, enforcement by a eukaryotic host and additional aspects. In *Journal of Molecular Microbiology and Biotechnology* (Vol. 24, Issues 5–6, pp. 409–419). S. Karger AG. https://doi.org/10.1159/000368855

Sreevatsan, S., Stockbauer, K. E., Pan, X., Kreiswirth, B. N., Moghazeh, S. L., Jacobs, W. R., Telenti, A., & Musser, J. M. (1997). Ethambutol resistance in *Mycobacterium tuberculosis*: Critical role of embB mutations. *Antimicrobial Agents and Chemotherapy*, *41*(8), 1677–1681. https://doi.org/10.1128/aac.41.8.1677

Stackebrandt, E., Rainey, F. A., & Ward-Rainey, N. L. (1997). Proposal for a new hierarchic classification system, Actinobacteria classis nov. *International Journal of Systematic Bacteriology*, *47*(2), 479–491. https://doi.org/10.1099/00207713-47-2-479

Stop TB Partnership. (2023). *Pipeline | Working Group for New TB Drugs*. http://www.newtbdrugs.org/pipeline/clinical, Access: 08.10.2023

Strösser, J., Lüdke, A., Schaffer, S., Krämer, R., & Burkovski, A. (2004). Regulation of GlnK activity: Modification, membrane sequestration and proteolysis as regulatory principles in the network of nitrogen control in *Corynebacterium glutamicum*. *Molecular Microbiology*, *54*(1), 132–147. https://doi.org/10.1111/j.1365-2958.2004.04247.x

Strunnikov, A. V., & Jessberger, R. (1999). Structural maintenance of chromosomes (SMC) proteins: Conserved molecular properties for multiple biological functions. *European Journal of Biochemistry*, *263*(1), 6–13. https://doi.org/10.1046/j.1432-1327.1999.00509.x

Sullivan, N. L., Marquis, K. A., Rudner, D. Z., & Boston, A. (2010). Recruitment of SMC to the origin by ParB-*parS* organizes the origin and promotes efficient chromosome segregation. *Cell, 137*(4), 697–707. https://doi.org/10.1016/j.cell.2009.04.044.Recruitment

Suter, E. (1952). The multiplication of tubercle bacilli within normal phagocytes in tissue culture. *The Journal of Experimental Medicine*, *96*(2), 137–150. https://doi.org/10.1084/jem.96.2.137

Suzuki, N., Okai, N., Nonaka, H., Tsuge, Y., Inui, M., & Yukawa, H. (2006). High-throughput transposon mutagenesis of *Corynebacterium glutamicum* and construction of a single-gene disruptant mutant library. *Applied and Environmental Microbiology*, *72*(5), 3750–3755. https://doi.org/10.1128/AEM.72.5.3750-3755.2006

Szwedziak, P., & Löwe, J. (2013). Do the divisome and elongasome share a common evolutionary past ? *Current Opinion in Microbiology*, *16*(6), 745–751. https://doi.org/10.1016/j.mib.2013.09.003

Taheri-Araghi, S., Bradde, S., Sauls, J. T., Hill, N. S., Levin, P. A., Paulsson, J., Vergassola, M., & Jun, S. (2015). Cell-size control and homeostasis in bacteria. *Current Biology*, *25*(3), 385–391. https://doi.org/10.1016/j.cub.2014.12.009

Takahashi, D., Fujiwara, I., & Miyata, M. (2020). Phylogenetic origin and sequence features of MreB from the wall-less swimming bacteria *Spiroplasma. Biochemical and Biophysical Research Communications*, *533*(4), 638–644. https://doi.org/10.1016/j.bbrc.2020.09.060

Taniguchi, H., Busche, T., Patschkowski, T., Niehaus, K., Pátek, M., Kalinowski, J., & Wendisch, V. F. (2017). Physiological roles of sigma factor SigD in *Corynebacterium glutamicum*. *BMC Microbiology*, *17*(1), 1–10. https://doi.org/10.1186/s12866-017-1067-6

Taniguchi, H., & Wendisch, V. F. (2015). Exploring the role of sigma factor gene expression on production by *Corynebacterium glutamicum*: Sigma factor H and FMN as example. *Frontiers in Microbiology*, *6*(JUL), 1–12. https://doi.org/10.3389/fmicb.2015.00740

Tatituri, R., Illarionov, P., Dover, L., Nigou, J., Gilleron, M., Hitchen, P., Krumbach, K., Morris, H., Spencer, N., Dell, A., Eggeling, L., & Besra, G. (2007). Inactivation of *Corynebacterium glutamicum NCgl0452* and the role of MgtA in the biosynthesis of a novel mannosylated glycolipid involved in lipomannan biosynthesis. *Journal of Biological Chemistry*, *282*(7), 4561–4572. https://doi.org/10.1074/jbc.M608695200

Tatituri, R. V. V., Alderwick, L. J., Mishra, A. K., Nigou, J., Gilleron, M., Krumbach, K., Hitchen, P., Giordano, A., Morris, H. R., Dell, A., Eggeling, L., & Besra, G. S. (2007). Structural characterization of a partially arabinosylated lipoarabinomannan variant isolated from a *Corynebacterium glutamicum ubiA* mutant. *Microbiology*, *153*(8), 2621–2629. https://doi.org/10.1099/mic.0.2007/008078-0

Tauch, A., Pühler, A., Kalinowski, J., & Thierbach, G. (2003). Plasmids in *Corynebacterium glutamicum* and their molecular classification by comparative genomics. *Journal of Biotechnology*, *104*(1–3), 27–40. https://doi.org/10.1016/S0168-1656(03)00157-3

Thomas, J. P., Baughn, C. O., Wilkinson, R. G., & Shepherd, R. G. (1961). A new synthetic compound with antituberculous activity in mice: ethambutol (dextro-2,2'-(ethylenediimino)-di-l-butanol). *The American Review of Respiratory Disease*, *83*, 891–893. https://doi.org/10.1164/arrd.1961.83.6.891

Toyoda, K., & Inui, M. (2016). The extracytoplasmic function σ factor σC regulates expression of a branched quinol oxidation pathway in *Corynebacterium glutamicum*. *Molecular Microbiology*, *100*(3), 486–509. https://doi.org/10.1111/mmi.13330

Toyoda, K., Teramoto, H., Yukawa, H., & Inui, M. (2015). Expanding the regulatory network governed by the extracytoplasmic function sigma factor σH in *Corynebacterium glutamicum*. *Journal of Bacteriology*, *197*(3), 483–496. https://doi.org/10.1128/JB.02248-14

Trefzer, C., Škovierová, H., Buroni, S., Bobovská, A., Nenci, S., Molteni, E., Pojer, F., Pasca, M. R., Makarov, V., Cole, S. T., Riccardi, G., Mikušová, K., & Johnsson, K. (2012). Benzothiazinones are suicide inhibitors of mycobacterial decaprenylphosphoryl-β-d-ribofuranose 2'-oxidase DprE1. *Journal of the American Chemical Society*, *134*(2), 912–915. https://doi.org/10.1021/ja211042r

Trojanowski, D., Ginda, K., Pióro, M., Hołówka, J., Skut, P., Jakimowicz, D., & Zakrzewska-Czerwińska, J. (2015). Choreography of the *Mycobacterium* replication machinery during the cell cycle. *MBio*, *6*(1). https://doi.org/10.1128/mBio.02125-14

Umeda, A., & Amako, K. (1983). Growth of the surface of *Corynebacterium diphtheriae*. *Microbiology and Immunology*, *27*(8), 663–671. https://doi.org/10.1111/j.1348-0421.1983.tb00629.x

Vadillo-Rodriguez, V., Schooling, S. R., & Dutcher, J. R. (2009). In situ characterization of differences in the viscoelastic response of individual Gram-negative and Gram-positive bacterial cells. *Journal of Bacteriology*, *191*(17), 5518–5525. https://doi.org/10.1128/JB.00528-09

Valbuena, N., Letek, M., Ordóñez, E., Ayala, J., Daniel, R. A., Gil, J. A., & Mateos, L. M. (2007). Characterization of HMW-PBPs from the rod-shaped actinomycete *Corynebacterium glutamicum*: Peptidoglycan synthesis in cells lacking actin-like cytoskeletal structures. *Molecular Microbiology*, *66*(3), 643–657. https://doi.org/10.1111/j.1365-2958.2007.05943.x

van der Ploeg, R., Goudelis, S. T., & den Blaauwen, T. (2015). Validation of FRET assay for the screening of growth inhibitors of *Escherichia coli* reveals elongasome assembly dynamics. *International Journal of Molecular Sciences*, *16*(8), 17637–17654. https://doi.org/10.3390/ijms160817637

van Raaphorst, R., Kjos, M., & Veening, J.-W. (2017). Chromosome segregation drives division site selection in *Streptococcus pneumoniae*. *Proceedings of the National Academy of Sciences*, *114*(29), E5959–E5968. https://doi.org/10.1073/pnas.1620608114

Varela, C., Rittmann, D., Singh, A., Krumbach, K., Bhatt, K., Eggeling, L., Besra, G. S., & Bhatt, A. (2012). MmpL genes are associated with mycolic acid metabolism in *Mycobacteria* and *Corynebacteria*. *Chemistry and Biology*, *19*(4), 498–506. https://doi.org/10.1016/j.chembiol.2012.03.006

Varley, A. W., & Stewart, G. C. (1992). The *divIVB* region of the *Bacillus subtilis* chromosome encodes homologs of *Escherichia coli* septum placement (MinCD) and cell shape (MreBCD) determinants. *Journal of Bacteriology*, *174*(21), 6729–6742. https://doi.org/10.1128/jb.174.21.6729-6742.1992

Vilkas, E., Amar, C., Markovits, J., Vliegenthart, J. F. G., & Kamerling, J. P. (1973). Occurrence of a galactofuranose disaccharide in immunoadjuvant fractions of *Mycobacterium tubercolosis* (cell walls and wax D). *BBA - General Subjects*, *297*(2), 423–435. https://doi.org/10.1016/0304-4165(73)90089-5

Visser, S., & Parkinson, D. (1992). Soil biological criteria as indicators of soil quality: Soil microorganisms. *American Journal of Alternative Agriculture*, *7*(1–2), 33–37. https://doi.org/10.1017/S0889189300004434

Vollmer, W., & Bertsche, U. (2008). Murein (peptidoglycan) structure, architecture and biosynthesis in *Escherichia coli*. *Biochimica et Biophysica Acta - Biomembranes*, *1778*(9), 1714–1734. https://doi.org/10.1016/j.bbamem.2007.06.007

Walker, A. W., & Hoyles, L. (2023). Human microbiome myths and misconceptions. *Nature Microbiology*, *8*(8), 1392–1396. https://doi.org/10.1038/s41564-023-01426-7

Wang, L., Khattar, M. K., Donachie, W. D., & Lutkenhaus, J. (1998). FtsI and FtsW are localized to the septum in *Escherichia coli*. *Journal of Bacteriology*, *180*(11), 2810–2816. https://doi.org/10.1128/jb.180.11.2810-2816.1998

Wang, L., & Lutkenhaus, J. (1998). FtsK is an essential cell division protein that is localized to the septum and induced as part of the SOS response. *Molecular Microbiology*, *29*(3), 731–740. https://doi.org/10.1046/j.1365-2958.1998.00958.x

Wang, P., Robert, L., Pelletier, J., Dang, W. L., Taddei, F., Wright, A., & Jun, S. (2010). Robust growth of *Escherichia coli*. *Current Biology*, *20*(12), 1099–1103. https://doi.org/10.1016/j.cub.2010.04.045

Wang, X., Tang, O. W., Riley, E. P., & Rudner, D. Z. (2014). The SMC condensin complex is required for origin segregation in *Bacillus subtilis*. *Current Biology*, *24*(3), 287–292. https://doi.org/10.1016/j.cub.2013.11.050

Weiss, D. S., Chen, J. C., Ghigo, J. M., Boyd, D., & Beckwith, J. (1999). Localization of FtsI (PBP3) to the septal ring requires its membrane anchor, the Z ring, FtsA, FtsQ, and FtsL. *Journal of Bacteriology*, *181*(2), 508–520. https://doi.org/10.1128/jb.181.2.508-520.1999

Wendisch, V. F. (2020). Metabolic engineering advances and prospects for amino acid production. In *Metabolic Engineering* (Vol. 58, pp. 17–34). Academic Press. https://doi.org/10.1016/j.ymben.2019.03.008

Wendisch, V. F., Bott, M., & Eikmanns, B. J. (2006). Metabolic engineering of Escherichia coli and *Corynebacterium glutamicum* for biotechnological production of organic acids and amino acids. In *Current Opinion in Microbiology* (Vol. 9, Issue 3, pp. 268–274). Elsevier Current Trends. https://doi.org/10.1016/j.mib.2006.03.001

Wendisch, V. F., Bott, M., Kalinowski, J., Oldiges, M., & Wiechert, W. (2006). Emerging *Corynebacterium glutamicum* systems biology. *Journal of Biotechnology*, *124*(1), 74–92. https://doi.org/10.1016/j.jbiotec.2005.12.002

Wesener, D. A., Levengood, M. R., & Kiessling, L. L. (2017). Comparing Galactan Biosynthesis in *Mycobacterium tuberculosis* and *Corynebacterium diphtheriae*. *Journal of Biological Chemistry*, *292*(7), 2944–2955. https://doi.org/10.1074/jbc.M116.759340

WHO (Ed.). (2021). *Global tuberculosis report 2021*. https://www.who.int/publications/i/item/9789240037021

Wickham, M. H. (2011). "ggplot2." *Wiley Interdisciplinary Reviews: Computational Statistics*, *3*(2), 180–185.

Wilhelm, L., Bürmann, F., Minnen, A., Shin, H. C., Toseland, C. P., Oh, B. H., & Gruber, S. (2015). SMC condensin entraps chromosomal DNA by an ATP hydrolysis dependent loading mechanism in Bacillus subtilis. *ELife*, *4*(MAY), 1–18. https://doi.org/10.7554/eLife.06659

Willis, L., & Huang, K. C. (2017). Sizing up the bacterial cell cycle. *Nature Reviews Microbiology*, *15*(10), 606–620. https://doi.org/10.1038/nrmicro.2017.79

Wu, L. J., & Errington, J. (2004). Coordination of cell division and chromosome segregation by a nucleoid occlusion protein in *Bacillus subtilis*. *Cell*, *117*(7), 915–925. https://doi.org/10.1016/j.cell.2004.06.002

Yagi, T., Mahapatra, S., Mikušová, K., Crick, D. C., & Brennan, P. J. (2003). Polymerization of mycobacterial arabinogalactan and ligation to peptidoglycan. *Journal of Biological Chemistry*, *278*(29), 26497–26504. https://doi.org/10.1074/jbc.M302216200

Yang, Y., & Inouye, M. (1993). Requirement of both kinase and phosphatase activities of an *Escherichia coli* receptor (Taz1) for ligand-dependent signal transduction. *Journal of Molecular Biology*, *231*(2), 335–342. https://doi.org/10.1006/jmbi.1993.1286

Yoshikawa, H. (1968). Chromosomes in *Bacillus subtilis* spores and their segregation during germination. *Journal of Bacteriology*, *95*(6), 2282–2292. https://doi.org/10.1128/jb.95.6.2282-2292.1968

Young, R. M., & Mood, G. M. (1945). Effect of penicillin on infection of guinea pigs with *Corynebacterium diphtheriae*. *Journal of Bacteriology*, *50*, 205–212. https://doi.org/10.1128/jb.50.2.205-212.1945

Yu, W., Herbert, S., Graumann, P. L., & Götz, F. (2010). Contribution of SMC (Structural Maintenance of Chromosomes) and spoIIIE to chromosome segregation in *Staphylococci*. *Journal of Bacteriology*, *192*(15), 4067–4073. https://doi.org/10.1128/JB.00010-10

Zhang, A., Pompeo, F., & Galinier, A. (2021). Overview of protein phosphorylation in bacteria with a main focus on unusual protein kinases in *Bacillus subtilis*. *Research in Microbiology*, *172*(7–8), 103871. https://doi.org/10.1016/j.resmic.2021.103871

References

Zhang, N., Torrelles, J. B., McNeil, M. R., Escuyer, V. E., Khoo, K. H., Brennan, P. J., & Chatterjee, D. (2003). The Emb proteins of mycobacteria direct arabinosylation of lipoarabinomannan and arabinogalactan via an N-terminal recognition region and a C-terminal synthetic region. *Molecular Microbiology*, *50*, 69–76. https://doi.org/10.1046/j.1365-2958.2003.03681.x

Zheng, H., Ho, P.-Y., Jiang, M., Tang, B., Liu, W., Li, D., Yu, X., Kleckner, N. E., Amir, A., & Liu, C. (2016). Interrogating the *Escherichia coli* cell cycle by cell dimension perturbations. *Proceedings of the National Academy of Sciences*, *113*(52), 15000–15005. https://doi.org/10.1073/pnas.1617932114

Zhou, X., Rodriguez-Rivera, F. P., Lim, H. C., Bell, J. C., Bernhardt, T. G., Bertozzi, C. R., & Theriot, J. A. (2019). Sequential assembly of the septal cell envelope prior to V snapping in *Corynebacterium glutamicum*. *Nature Chemical Biology*, *15*(3), 221–231. https://doi.org/10.1038/s41589-018-0206-1

Zuber, B., Chami, M., Houssin, C., Dubochet, J., Griffiths, G., & Daffé, M. (2008). Direct visualization of the outer membrane of *Mycobacteria* and *Corynebacteria* in their native state. *Journal of Bacteriology*, *190*(16), 5672–5680. https://doi.org/10.1128/JB.01919-07

Appendix

Development of a custom image analysis method for epifluorescence micrographs

1.4.1 Image structure

Modern epifluorescence micrographs typically contain multiple dimensions, organized as a stack of images. These are usually recorded by the same black/white camera and show a single focal plane. Potentially organized as a multiple (hyper) stack, the image can contain additional channels that bear further information about the sample, depending on the used imaging protocol.

The first image of the stack usually shows a non-fluorescent micrograph. By this, only the basic geometric features of the specimen become visible. The image is usually taken with a transmitted full spectrum VIS (visible light) illumination and an objective dependent contrasting method. Typically, either phase contrast or differential interference contrast (DIC) are available at the microscope. The two dimensions of the image can be expanded in space and time. The use of motorized stages opens up the second dimension by potentially adding multiple spots of the specimen that can be later examined individually. By acquiring a series of images with a defined focal range, the third spatial dimension can be added to a micrograph. The repetitive acquisition of the same focal plane would add the dimension of time in a separate channel. All three are optional.

In the simplest form, further channels only contain the fluorescence information. An additional image shows the captured signal that was emitted under a certain illumination condition. The spectrum and time of illumination are dependent on the characteristics of the used fluorophore or dye and the respective optical setup. Common targets for chemical dyes are structures like membranes or DNA. Modern approaches use bio-orthogonal labeling via click-chemistry on other structures. Dyes are also used as reporter systems for DNA sequence specific fluorescence *in situ* hybridization (FISH)-probes. With the use of fluorescent proteins, potentially every protein can be labeled in almost any desired color, already at the genetic level. In modern microscopic systems, up to nine sharply distinct bands of the light-spectrum can be used in parallel, but

usually one to three is common practice. For usual applications, the sample size of the examined trait is commonly limited. The extraction of quantitative features from images is often laborious and rather requires different methods. This is currently changing (Haase et al., 2022; Hartmann et al., 2020; Jones et al., 2008; van Raaphorst et al., 2017). The awareness about the amount of data that is produced by a single micrograph primes a path to the idea of automated image processing and analysis. Respective software environments that enabled the handling of multi-dimensional micrographs entered the field about a decade ago. Due to a very active community, the open-source project FIJI meanwhile provides a considerable collection of established tools (Schindelin et al., 2012). Since then, a whole ecosystem of specialized solutions appeared for various topics and hence formed the discipline of scientific image analysis.

Since available tools often appear as a black box when it comes to details, the purpose of this project was to create a transparent, powerful, and adaptable process, that could be adapted for different questions within this work. The initial problem was that available tools were unable to cope with the irregular morphology of *C. glutamicum*. Therefore, the developed algorithm was termed 'Morpholyzer'. For the processing and measurements, the program FIJI and the internal ImageJ macro language were used (Schindelin et al., 2012). The analysis and visualization of the acquired data was developed in R (R Development Core Team, 2003).

The general idea behind the procedure is a decoupling of the raw-data and the actual subject of interest, a single bacterial cell. This bears various advantages and is realized by systematic data storage. The key element of the data organization is a unique identifier for every cell, independent from the source image. By this, a series of images is treated as a whole, but single elements are kept traceable from the beginning. This identifier-code helps to organize the storage of every significant intermediate step. The procedure is divided into three general tasks. In the beginning, single cells are gathered semi-automatically from a series of raw images and get stored separately. The following, automated step, determines all relevant geometric parameters for each single cell. Based on that, the cell poles, a shape-adaptive centerline, and the profile of the cell halves are constructed individually. All fluorescence signals are measured pixel wise. The

obtained data, then serves as input for further sorting, analyses, and visualizations. In the following, basic functions and key features of the algorithm are summarized.

1.4.2 Creation of a binary mask and single cell gathering

For the process of gathering single cells, a phase contrast/ DIC image is obligatory. It is used to create a binary (black/white) mask of the image (Fig. 10). The script uses a FIJI-provided threshold algorithm, and the mask is automatically calculated and added to the first position of the stack. The respective threshold algorithm can be chosen according to the image composition. To a certain extent, the artifacts in the resulting image get cleared automatically. In a following manual step, the remaining undesired elements can be removed with a large black brush, and touching cells can be separated either manually or by the application of the watershed function. The resulting cleared mask should now only contain separated white cells on black background. After a confirmation, the outlines of the single cells are automatically recognized by edge-detection and stored as separate regions of interest (ROIs). From each of these ROIs, a bounding rectangle is calculated, and the respective selection is duplicated. This cut-out of a single cell includes all present fluorescence channels and formatting. Since all these cells are stored individually but at the same place, the procedure includes a repetition on technical replicates until a sufficient sample number of cells is reached.

The original images, plus a channel containing the mask are saved. Also, the respective coordinates of the cell ROIs on the large image. By monitoring the count of files in the image folder the systematic naming for the cells is generated. A typical name is Tf023Ti044T and follows the syntax: 'f' is the number of the technical replicate (or frame in time-lapse analysis) and 'i' is the individual cell ID for that image, while 'T' is used as a delimiter for later processing.
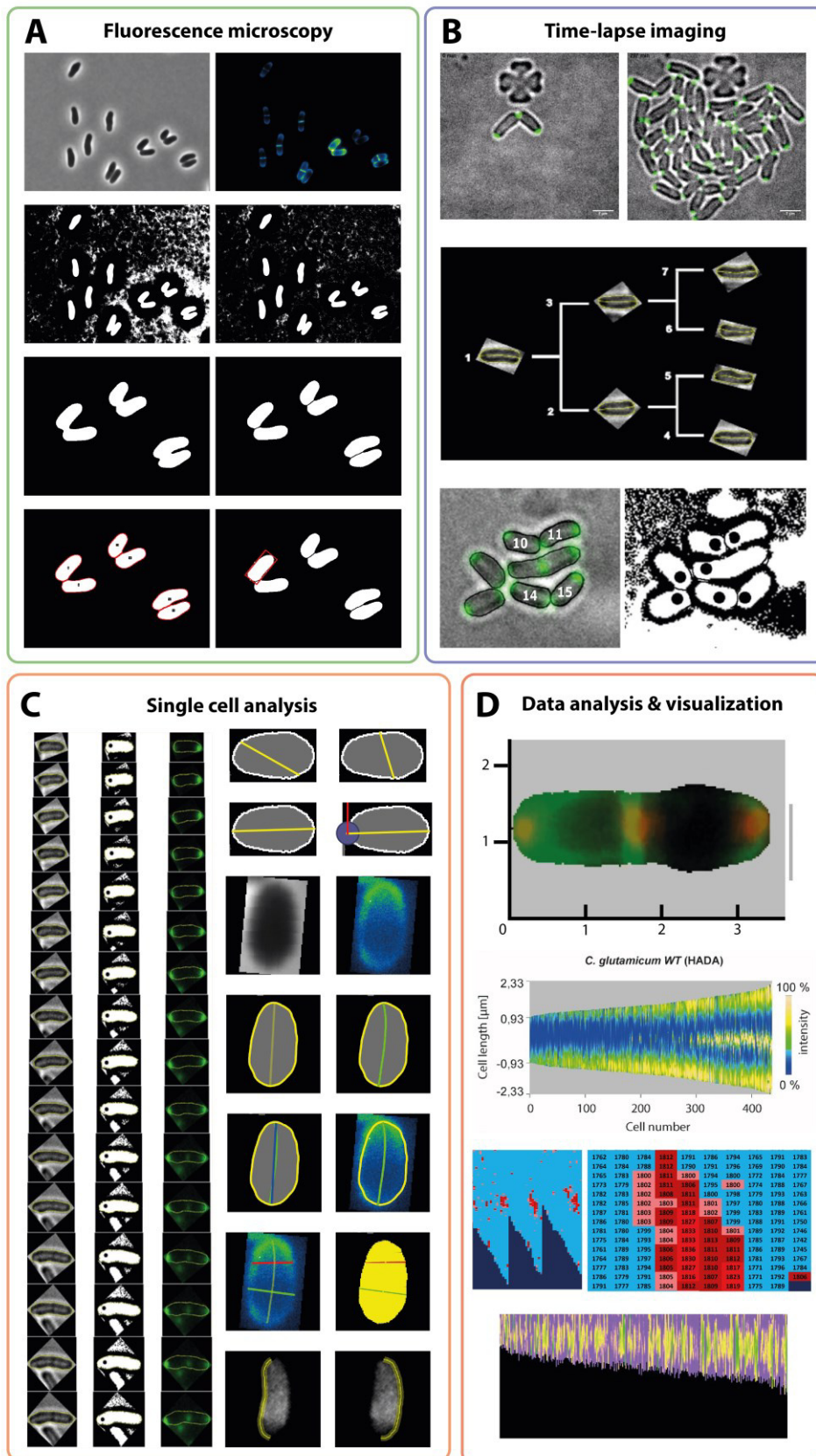
Figure 10: Basic steps of the developed workflow. (A) Binaries from phase contrast micrographs are used to extract single cells from larger images including the potential fluorescence information. **(B)** The method can be applied to static and time-lapse images. **(C)** Single cells get analyzed independent from their morphology. **(D)** The logic of data storage allows for further sorting, analyses, and visualizations.

1.4.3 Time-lapse analysis

In nearly all biological disciplines, time-lapse imaging is a common method for obtaining information about protein localization in a spatio-temporal context. Therefore, an adaptation for time-lapse acquisitions of growing micro-colonies was realized. For that, the process of cell gathering was modified and supplemented with information about lineage, age and orientation of the cell pole, and the respective frame in the time-stack. A usual format for such an analysis would be a cut-out from a larger scene that shows a single cell in the beginning. Over about 100 frames (with an interval of 2 min) the development of the microcolony is captured in phase contrast and fluorescence (Fig. 10).

The information about the genealogy of the population is determined prior to the analysis. Starting with a single cell with the name n (001), the progeny now is named (002) and (003) respectively. According to this rationale, the offspring of each cell is named dependent on the number of the parent. For (003), based on 2n and 2n+1, this defines (006) and (007) as names of the descendants. Practically, this can only be realized by keeping track of the individual cell poles. For that, the binary mask of the scene is used to specify the new pole of each cell with a black dot, starting with the first division. This dot gets automatically recognized in a later step and guarantees the correct orientation of the image-duplicate during the reconstruction of the cell cycle. The most significant information is hidden in the filename, since it connects the present image with the genealogical context of the individual cell and the frame-number of the scene.

1.4.4 Single cell analysis

The basic output format of the previous algorithm consists of a minimum of three channels: a binary image, a phase contrast-, and one fluorescence channel. Each of the single cell image serves as input for the actual cell analysis, step by step. The process uses the folder that was used for saving before. Each processed imaged is moved to a different folder, the program ends with the last element (Fig. 10).

The cut-out is usually orientated in an random angle. In a first step, this orientation is determined, and the cell is turned in an vertical position. This is necessary since the

construction of the adaptive central line depends on a growing value for the y-axis. An adaptation of the procedure for different angles becomes unnecessary if the cells are roughly in the same orientation. The measurement of the orientation is realized via the outline of the cell. Since the coordinates are present as a list, the pairwise connection of all points gives a list of distances. This list is now sorted by length and gives a rough estimate of the cell poles. According to the angle between this line and the x-axis, the whole cut-out is rotated respectively and sized up by the factor of 2.5x. This ensures a virtual subpixel resolution and thus enables for a more precise construction of diverse morphologic features. During scaling and rotation, basic interpolation is applied. By this, only minor systematic errors are introduced.

The vertical oriented cut-out is saved, and the poles (point 1,2) and angle (A) are determined again. Now the iterative construction of the adaptive central line follows. The upper pole (1) and the first 5 pixels of the connecting line define a new point (3). From this point and perpendicular to A, rather horizontal lines towards the black edge are constructed and define the points 4 and 5. The center of this 'slice' is usually different from 3 and defines the first point of the line L1. By connecting now 1 and L1 a new angle B is defined. The calculated elements L1 and B are then used to substitute 3 and A in the process. By this, the line adapts to the shape until a proximity with 2 is reached. Since there are possible artifacts generated in the beginning of the process, the process feeds back towards 1 and finally defines the cell poles and the central line precisely.

The center of the central line and the poles define a further angle (C). This value can be interpreted as a proxy for the cell curvature. This becomes important for bent cell morphologies like in *Vibrio cholerae* or *Rhodospirillum rubrum* (Peschek et al., 2020; Poehl et al., n.d.). Based on the intersect of the poles and the outline, the outline can be divided into a left and right half. Since vertically corrected images are either bent to the left or the right, the algebraic sign of C helps to correct for the orientation. By this the inner and outer curvature can be measured in a distinct and continuous line scan for comparison.

Each of these constructed elements is saved as a set of ROIs and used as base for measurements of lengths and fluorescence profiles. For this, line-scans of variable

widths are applied, and result in numeric vectors that reflect the signal. For images from a time-lapse dataset, the position of the black dot along the centerline is used normalize the orientation. An integrated fail-save ability enables for the manual exclusion of undesired, traceable, single elements. The results are stored systematically, in a format that grants the further access for analysis and/or visualization procedures.

1.4.5 Data analysis and visualization

The potential comprehensive numeric output of the single cell analysis enables for various kind of explorative data analyses. For basic evaluation of the data, Microsoft excel was used. Further, and depending on the task, the statistical software R was applied together with the package ggPlot2 (R Development Core Team, 2003; Wickham, 2011). From still images, basic geometric parameters, as the distributions of cell lengths, the mean widths or areas can be displayed as histograms or violin plots and statistically compared. For time-lapse analyses these parameters were placed into a genealogical context and thus create the element 'cell cycle'. These can be further analyzed and compared (Fig. 10).

The fluorescence scans of the central lines are commonly depicted as demographs. The procedure in the algorithm is usually defined per channel, but, if available, combinations of all existing channels are possible. Demographs result as the color-coded display of line-scans that are combined to a matrix and sorted by length. An optional step of sorting would be the adjustment of the pole orientation. This is only possible if a unequal polar marker is present in the dataset, as in the case of a HADA-staining in *C. glutamicum* (Meyer et al., 2023; Schubert et al., 2017). By this sorting, all simultaneously recorded channels can be sorted as well, even if no polar marker is present for them. The principle of the demographs was expanded by further center of reference. By displaying a pair of line scans from the two cell halves, membrane and cell wall related process can be distinctively depicted.

The scans perpendicular to the central line can be combined to a graphical reconstruction of the cell that shows morphological details and fluorescence pattern, but this is rather uncommon. This serves more to illustrate the extent of the obtained data. MS excel turned out to possess a simple, native function for the illustration of such

datasets. By the application of conditional formatting, the (excel)cells can be color-coded according to numeric values. By this, and a maximum zoom-out, the obtained results of still image- or time-lapse experiments can be easily visualized.

Danksagung

Zuallererst, danke Marc. Danke für den Freiraum, und danke für die Leitplanken.

Über die Jahre durfte ich in der Arbeitsgruppe einer bunten Mischung aus verschiedensten Charakteren begegnen, die den Alltag stets am Laufen gehalten haben und das bis heute tun.

Ein besonderer Dank für die Zeit in München geht an dieser Stelle an Karin. Gerne denke ich auch zurück an Cat, Lijun, Prachi, Boris, Tom und Juri. Danke auch an Gustavo, Derk, Fiona und Richard.

Der Umzug nach Kiel war eine besondere Erfahrung, die ich mit ein paar meiner Münchner Kollegen teilen durfte. Der gemeinsame Aufbau des Labors war spannend und abwechslungsreich. Danke an dieser Stelle an Manuela, Abbi, Giacomo und Helge. Ebenso wichtig für den reibungslosen Aufbau, war die tatkräftige Unterstützung unserer neuen Kollegen aus dem Kieler ‚Bestand', allen voran Holger, Ulrike J., Dagmar und Astrid. Danke auch an Marius und Andreas. Da bekanntlich alles fließt gibt es mittlerweile auch eine neue Generation an Kieler Studenten. Für die bisherige gute Zusammenarbeit danke an Kartikeyan, Sarah und Samia. Und danke Katya für die Mithilfe am BTZ-Paper und den Forschergeist beim PldP-Projekt.

Durch die Begleitung der Neuausrichtung der zentralen Mikroskopie haben sich mir viele ungeahnte Details offenbart, vor allem wissenschaftlich. Vielen Dank Urska, und danke Ulrike V. und Tanja.

Speziell bedanken möchte ich mich auch bei allen Kollegen, mit denen ich eine Veröffentlichung auf den Weg bringen konnte. Kollaboratives Verhalten führt häufig zu Synergieeffekten. Oft ist das Resultat dann mehr als nur die Summe seiner Teile. Danke Chase und Joris. Danke Karin und Boris. Danke Kati. Danke Urska. Danke Katya. Danke Cat, Gustavo und Manu. Danke Giacomo, Helge, Peter und Benni. Danke Feng. Danke Diego, Adrian und Petra. Danke Nikolai, Roman, Kai und Kathrin. Danke Basti und Martin. Danke Prof. Wanner. Und danke Prof. Bramkamp.

Das Ganze wäre nicht möglich gewesen ohne ein solides Fundament. Deshalb, ein ganz herzliches Dankeschön (!!!) an meine Familie, meine Eltern Anne und Ralph, meinen Bruder Dominik und dessen Freundin Mira. Danke für das Vertrauen und die Geduld. Allen anderen die mir die Daumen gedrückt haben sei an der Stelle auch nochmal gedankt: danke Marion, Robert und Andrea, Birgit und Danino und danke Onkel Schorsch.

Manchmal entwickeln sich Freundschaften über Jahrzehnte, manchmal spielen dabei Raum und Zeit nur eine Nebenrolle. Merci Leute für's mitfiebern! Allen voran gilt das für den harten Kern aus dem Münchner Westen: Matze, Hannes, Chris, Flori, Max, Norbert und Dan, und natürlich den jeweils besseren Hälften. Vielen Dank Alma. Vielen Dank Basti und Elsa. Vielen Dank Lyni und Gigi. Vielen Dank Jan und Anna. Vielen Dank Conny. Vielen Dank Thorsten. Vielen Dank Tom. Vielen Dank Livia. Vielen Dank Moritz. Vielen Dank Benni. Vielen Dank Friedi. Vielen Dank Nina. Vielen Dank Bettina. Vielen Dank Michaela und Thomas. Vielen Dank Ruth. Vielen Dank Véro. Vielen Dank Ingrid.

Curriculum vitae

Fabian Mark Meyer

Publications and contributions

First and shared first author publications:

Meyer, F. M., Repnik, U., Karnaukhova, E., Schubert, K., & Bramkamp, M. (2023). Effects of benzothiazinone and ethambutol on the integrity of the corynebacterial cell envelope. *The Cell Surface*, 100116.

Messelink J.J.*, **Meyer F.***, Bramkamp M., Broedersz C.P. (2021) Single-cell growth inference of *Corynebacterium glutamicum* reveals asymptotically linear growth. *Elife*, 10:e70106.
doi: 10.7554/eLife.70106. https://doi.org/10.7554/elife.70106

Schubert K.*, Sieger B.*, **Meyer F.***, Giacomelli G., Böhm K., Rieblinger A., Lindenthal L., Sachs N., Wanner G., Bramkamp M. (2017) The antituberculosis drug ethambutol selectively bocks apical growth in CMN group bacteria. *MBio*, 8(1):e02213-16. https://doi.org/10.1128/mbio.02213-16

Co-author publications:

Peng, F., Giacomelli, G., **Meyer, F. M.**, Linder, M., Haak, M., Rueckert-Reed, C., ... & Bramkamp, M. (2023). Deletion of SMC renders FtsK essential in *Corynebacterium glutamicum*. *bioRxiv*, 2023-10.

Böhm K., **Meyer F.**, Rhomberg A., Kalinowsk J., Donovan C. & Bramkamp M. (2017) Novel chromosome organization pattern in Actinomycetales —Overlapping replication cycles combined with diploidy. *MBio*, 8(3), e00511-17. https://doi.org/10.1128/mbio.00511-17

Giacomelli G*., Feddersen H*., Peng F., Martins G.B., Grafemeyer M., **Meyer F.**, Mayer B., Graumann P.L., Bramkamp M. (2022) Subcellular Dynamics of a conserved bacterial polar scaffold protein. *Genes*, 13(2):278. https://doi.org/10.3390/genes13020278

Ramirez-Diaz D.A., Merino-Salomón A., **Meyer F.**, Heymann M., Rivas G., Bramkamp M., Schwille P. (2021) FtsZ induces membrane deformations via torsional stress upon GTP hydrolysis. *Nat Commun*, 12(1):3310. https://doi.org/10.1038/s41467-021-23387-3

Peschek N., Herzog R., Singh P.K., Sprenger M., **Meyer F.**, Fröhlich K.S., Schröger L., Bramkamp M. & Papenfort K. (2020) RNA-mediated control of cell shape modulates antibiotic resistance in Vibrio cholerae. *Nature communications*, 11(1), 1-11. https://doi.org/10.1038/s41467-020-19890-8

Böhm K., Giacomelli G., **Meyer F.**, Bramkamp M. (2020) Chromosome Organization and Cell Growth of Corynebacterium glutamicum. In: Inui M., Toyoda K. (eds) *Corynebacterium glutamicum*. Microbiology Monographs, vol 23., Springer, Cham. https://doi.org/10.1007/978-3-030-39267-3_1.

Briciu, V. T., Flonta, M., Ţăţulescu, D. F., **Meyer, F.**, Sebah, D., Cârstina, D., ... & Lupşe, M. (2017). Clinical and serological one-year follow-up of patients after the bite of *Ixodes ricinus* ticks infected with *Borrelia burgdorferi* sensu lato. *Infectious Diseases*, *49*(4), 277-285.

Briciu VT, Sebah D, Coroiu G, Lupşe M, Cârstina D, Ţăţulescu DF, Mihalca AD, Gherman CM, Leucuţa D, **Meyer F**, Hizo-Teufel C, Fingerle V, Huber I. (2016). Immunohistochemistry and real-time PCR as diagnostic tools for detection of *Borrelia burgdorferi* sensu lato in ticks collected from humans. *Experimental and Applied Acarology*, *69*, 49-60. https://doi.org/10.1007/s10493-016-0012-y

Briciu, V. T., **Meyer, F.**, Sebah, D., Ţăţulescu, D. F., Coroiu, G., Lupşe, M., ... & Fingerle, V. (2014). Real-time PCR-based identification of *Borrelia burgdorferi* sensu lato species in ticks collected from humans in Romania. *Ticks and Tick-borne Diseases*, *5*(5), 575-581.